Dear Professor Catherine Jeandel,

It is my pleasure to provide the revised manuscript (with and without tracked changes). Please find also attached the detailed answer (in bold) to reviewers' comments (in italics). The latter file indicates the changes made in the revised manuscript with page and line numbering corresponding to the 'track changes' version.

Both reviewers agreed with the major scientific outcomes and with the interpretation of the data. Yet, some changes were suggested, both of more general and specific character. As requested, we have addressed them all. This resulted into a new version of the manuscript, in which new sections have been incorporated and others have been rewritten. Please, see these changes and the response to reviewers in the attached documents.

We hope that after addressing the comments of both reviewers, you will find the manuscript suitable for publication in the GEOVIDE special issue in Biogeosciences.

Maxi Castrillejo, on behalf of all co-authors.
maxic@phys.ethz.ch

Detailed answer to reviewers 1 and 2 and corresponding changes made on the revised manuscript entitled: 'Tracing water masses with ^{129}I and ^{236}U in the subpolar North Atlantic along the GEOTRACES GA01 section' by Castrillejo et al.

Reviewer 1

We are grateful for the thorough review and the constructive comments from the reviewer.

We have addressed most of the changes suggested by the reviewer. Special emphasis has been placed on providing a more detailed introduction on sources/levels of the tracers and their transport and distribution, the ocean circulation of the study area, and also highlighting the objectives. The 'results and discussion' section includes a first, new subsection with a full description of the water mass structure. The overall discussion has been revised to clarify what is new information obtained from these tracers during the GEOVIDE cruise and what are confirmations of earlier tracer/physical studies. All specific comments have also been addressed, as shown in the point by point answer (in bold) to the comments made by the reviewer (in italics).

On behalf of all coauthors,

Maxi Castrillejo

Detailed point by point answers to Reviewer 1.

This manuscript focus on the distribution of ^{129}I and ^{236}U along the GEOVIDE section (transect GEOTRACES GA01) in spring 2014. GEOVIDE cruise covered the subpolar North Atlantic Ocean and the Labrador Sea. This manuscript represents an important updated dataset and the authors successfully use ^{129}I and $^{236}/^{238}U$ and $^{236}U/^{129}I$ atom ratios to describe water masses. The authors confirm with this study the major potential of the combination of ^{129}I and ^{236}U as circulation tracers, especially in the area of study and the Arctic Seas and I really enjoyed reading it. However, I think that given that the combined use of ^{129}I and ^{236}U provide such rich information, some of the results provided could be discussed in more depth. My impression is that the description and overall use of some the data still require a bit of discussion.

If I am not mistaken, the paper have three main objectives that should be emphasized and clarified in the abstract and the introduction.

1. Update and improve the database of ^{129}I and ^{236}, to be used for future studies and/or modelisation of the ocean circulation in the North Atlantic

2. Present new evidences of the advantages of using both radionuclides as dual tracers in the ocean. In this case, what I miss in the text is a more detailed explanation/introduction of why and how ^{236}U, ^{129}I and $^{236}/^{129}I$ combined provide different and complementary information.

The authors reference previous works but should provide the reader with a bit of context and additional information about how these tracers/methodology work.

3. Use the tracers to understand ocean circulation in the area. This seems to be the main objective of the paper, however the conclusions from this part are mixed with the other two objectives, together with what is already known and what is novel in this paper. e.g. the final conclusion in the Abstract "Data of ^{129}I and ^{236}U from 2014 and the ^{129}I time series in the Labrador Sea agrees with the hypothesis that Atlantic Waters follow at least two circulation loops from their source region […] recirculation in the Arctic Eurasian Basin" is not new was already stated by Orre et al. (2010) with ^{129}I and partially by Povinec et al., (2003) using other radioactive tracers such as ^{137}Cs. But there is missing information in the abstract to emphasize that the other conclusions are indeed novel, i.e contribution of ISOW to eastern SPNA is quite recent.
The objectives of the paper are now clearly presented in both the abstract and the introduction.

Abstract (page 2, lines 1-7): 'Pathways and time scales of water mass transport in the Subpolar North Atlantic Ocean (SPNA) <u>have been investigated</u> by many studies <u>due to their importance for</u> Meridional Overturning Circulation and thus for the global ocean. <u>In this sense,</u> observational data on <u>geochemical tracers provide complementary information to improve the current understanding of the circulation in the SPNA</u>. <u>To this end,</u> we present the first simultaneous distribution of artificial ^{129}I and ^{236}U in 14 depth profiles and in surface waters along the GEOVIDE section covering a zonal transect through the SPNA in spring 2014.'.

Introduction (page 7, lines 1-15): '<u>In this study, we aim at</u> using artificial ^{129}I and ^{236}U to investigate the transport pathways and time scales of water mass circulation in the SPNA. <u>To this end</u>, we present the first simultaneous distribution of ^{129}I and ^{236}U along the GEOVIDE cruise track in spring 2014 (Figure 1). <u>The study pursues three specific objectives</u>. <u>Firstly,</u> we study the zonal distribution of ^{129}I and ^{236}U and their relationship with the water mass structure. Although the distribution of ^{129}I in the Irminger and Labrador Seas has been well studied in the last 30 years, there is a significant data gap east of the Reykjanes Ridge for ^{129}I, and for most of the section for ^{236}U. <u>Secondly</u>, we use the dual ^{129}I/^{236}U - ^{236}U/^{238}U tracer approach to distinguish the sources contributing to the presence of ^{129}I and ^{236}U in the SPNA. This information is then valuable to study the origin, mixing and spreading pathways of water masses participating in the AMOC. The combined use of ^{129}I and ^{236}U allows tracing circulation features that received significant attention in earlier modelling, tracer and physical studies, and helps validating recent interpretations on the ventilation of the North Atlantic by overflow waters. <u>Thirdly,</u> tracer data from 2014 are combined with the extensive ^{129}I time series in the central Labrador Sea to further investigate the circulation time scales of AWs downstream of European NRPs.'.

A general comment on the paper is that it presents an impressive dataset and it would be desirable to make more clear which of the conclusions are confirmations of previous hypotheses/results. In the text it is indeed explained, however I think that the novel results, found mainly from the dual use of these radiotracers, are mixed with results that are confirmation of known facts and its relevance it is not explicitly enhanced, which is a shame.

Section 3.4 is basically where the novel features of these tracers are presented, in contrast with previous sections that basically use previous data and hypotheses and verify that the new ^{129}I and ^{236}U data are in agreement. However, this distinction is, in my opinion, not totally clear especially when presenting section 3.3. Novel and/or on discussion hypotheses reinforced by these dataset should be highlighted. I would also emphasize conclusions obtained by the use of ^{236}U and $^{129}I/^{236}U$, since they are novel tracers and the first time that they are measured simultaneously in the area. However, in this sense I find the Conclusion section very well structured.

The discussion has been modified (as shown in specific comments below) in order to clarify which are the novel results and which confirm the hypotheses/results reported in the literature. Special care has been taken to revise section 3.3.

Finally, it is assumed in the text that the reader knows well about the ocean circulation in the North Atlantic and Arctic Oceans and about ^{129}I and ^{236}U, if this is the case, the paper is quite straightforward to read. But in my opinion one can get easily lost if that is not the case, I have add a few examples of this in the specific comments below.

To provide a general background to better understand the discussion of the results I suggest something like:

1. Presenting first a brief introduction to ocean circulation and water masses involved with the data.

In this revised version, we include a brief introduction to the ocean circulation and water masses involved in the tracer transport. For example:

Page 5, lines 2-17: '<u>The schematic transport of NRP effluents and water masses in the SPNA-Artic Ocean region is displayed in Figure 1.</u> NRP-labelled AWs are first transported by surface currents into the North Sea and then carried poleward by the Norwegian Coastal Current (NCC) into the Nordic Seas (Edmonds et al., 1998; Raisbeck and Yiou, 2002) while mixing with the Norwegian Atlantic Current (NwAC) (Gascard et al., 2004; Kershaw and Baxter, 1995). The current splits in two branches north of Norway, one branch entering the Barents Sea as Barents Sea Branch Water (BSBW) and the other branch approaching the Fram Strait west of Spitsbergen where it bifurcates again. One branch joins the East Greenland Current (EGC) and recirculates southwards as Return Atlantic Water (RAW) (Fogelqvist et al., 2003) mixing with IrSPMW and PIW (modified AW that has recirculated in the Arctic Ocean; Rudels et al., 1999b). The other branch, the West Spitsbergen Current (WSC), transports the remaining AWs at shallow to intermediate depths into the Arctic Ocean via the Fram Strait Branch Water (FSBW), where they recirculate in the Arctic Eurasian Basin before outflowing back through the Fram Strait and continuing southwards carried by the EGC (Rudels, 2015). The NRP signal also penetrates deep in the water column due to the formation of dense water north of the Greenland-Iceland and Iceland-Scotland passages, providing means of tracing the deep overflows that ventilate the deep North Atlantic Ocean (e.g. Smith et al., 2005).'.

2. Explain in more detail the role of ^{129}I, ^{236}U and $^{236}U/^{129}I$ as ocean tracers of the SPNA, making clear what we have learn so far using them i.e. provide context.

In the revised manuscript we provide more detail on sources which is necessary to understand the values of ^{129}I, ^{236}U and $^{236}U/^{129}I$. We also explain why the combination of both tracers is important. For example:

Page 5, lines 26-28; and page 6, lines 1-3:'the presence of ^{129}I in those regions is dominated by the liquid discharge from European NRPs, which has a well-documented release history (> 5700 kg; He et al., 2013a; Raisbeck et al., 1995), while the contribution from GF is comparably negligible (~ 90 kg worldwide release; Hou, 2004; Raisbeck and Yiou, 1999; Wagner et al., 1996). Consequently, the seawater affected by NRPs may present ^{129}I concentrations 1 – 4 orders of magnitude above the background due to GF (~ 2.5×10^{7} at/kg; Edmonds et al., 1998).'.

Page 6, lines 15-22: 'Surface seawaters of the northern hemisphere present $^{236}U/^{238}U$ atom ratios of about 1000×10^{-12} (e.g. Christl et al., 2012) in the <u>unique presence of GF (about 900 kg released worldwide;</u> Sakaguchi et al., 2009). <u>However, the $^{236}U/^{238}U$ ratios can be significantly higher</u> in the Arctic and North Atlantic Oceans due to the liquid discharge of ^{236}U from European NRPs (about 100 kg, Christl et al., 2015a). T<u>his has allowed tracing the waters carrying NRP-^{236}U</u> with $^{236}U/^{238}U$ ratios up to 3800×10^{-12} in the Arctic Ocean in 2011 – 2012 (Casacuberta et al., 2016), and up to 1400×10^{-12} in LSW and DSOW in the western SPNA in 2010 (Casacuberta et al., 2014).'.

Page 6, lines 23-26: In addition, both ^{236}U and ^{129}I can be combined as the dual tracer, $^{129}I/^{236}U$ - $^{236}U/^{238}U$, to identify the radionuclide source(s) present in a given water mass (Casacuberta et al., 2016; Christl et al., 2015b). This is possible because the GF and the European NRPs introduced different amounts of ^{236}U and ^{129}I (see above) to the environment and tagged the waters with characteristic $^{129}I/^{236}U$ and $^{236}U/^{238}U$ atom ratios depending on the proximity from the source(s).

It would be also good to better explain how to read and understand Figure 3. Which is extremely useful and provides a lot of information.

We have modified the structure of section 3.3 to include a paragraph that facilitates the interpretation of Figure 4 (former Figure 3). This is achieved by including the expected values of $^{129}I/^{236}U$ and $^{236}U/^{238}U$ atom ratios in the subpolar North Atlantic water (page 14, lines 8-15): 'As done in earlier studies (Casacuberta et al., 2016), we can estimate the contribution to our samples from the LB, GF and NRP by combining the $^{129}I/^{236}U$ and $^{236}U/^{238}U$ on a dual tracer approach (Figure 4). <u>This is possible because the atom ratios of $^{129}I/^{236}U$ and $^{236}U/^{238}U$ display a wide range of values due to the different input of ^{129}I and ^{236}U from the three source</u>s. <u>For example,</u> the <u>GF</u> introduced about 10 times more ^{236}U than ^{129}I, thus this endmember is characterized by <u>$^{129}I/^{236}U < 1$ and $^{236}U/^{238}U$ surface ratios in the $(1000–2000) \times 10^{-12}$ range</u>. <u>On the contrary</u>, the total amount of ^{236}U introduced from European NRPs was much smaller than for ^{129}I. Therefore, a water mass with the additional influence from the European NRP may present <u>$^{129}I/^{236}U$ on the 1–350 range and $^{236}U/^{238}U$ above the GF</u>.'.

We also explain with an example what it means to fall in one part or the other of the chart (page 14, lines 22- 23): 'For instance, a sample falling in the 1 % value on the GF-NRP

binary mixing line would be composed of waters carrying largely GF and about 1 % of the NRPs signal.'.

ABSTRACT

1) I think that these lines "Results show that part of the effluents discharged from Sellafield and La Hague apparently enter the eastern SPNA directly through the Iceland-Scotland passage or the English Channel/Irish Sea, as it is shown by elevated ^{129}I concentrations and $^{129}I/^{236}U$ ratios in shallow central waters flowing in the West European Basin (WEB)" are saying the same than these ones "The Iceland-Scotland Overflow Water spreading pathways into the eastern SPNA have been confirmed by the unequivocal transport of reprocessing ^{129}I into the deep WEB".

The abstract has been re-written to clarify, among other things, that the signals from the reprocessing plant may follow alternative pathways, not only through overflow waters, but also on the surface through the Iceland-Scotland passage. For example (page 2, lines 15-17): 'Nevertheless, our results show that the effluents from NRPs may also directly enter the surface eastern SPNA through the Iceland-Scotland passage or the English Channel/Irish Sea.'.

2) When it is said "The Iceland-Scotland Overflow Water spreading pathways into the eastern SPNA have been confirmed by the unequivocal transport of reprocessing ^{129}I into the deep WEB", it should be briefly explained why we find this transport unequivocal.

It has been briefly explained in the abstract (page 2, lines 24-27): 'Several depth profiles also show an increase in ^{129}I concentrations in near bottom waters in the Iceland and the West European Basins that are very likely associated to the transport of the NRP signal by the Iceland-Scotland Overflow Water (ISOW). This novel result would support current modelling studies indicating the transport of ISOW into the eastern SPNA.'.

INTRODUCTION

3) When one reads from lines 15 (Page 3) to line 23 (Page 4) gets a very general idea about how ^{129}I and ^{236}U are distributed in the North Atlantic, but do not get a precise picture of what are the paths followed by the radionuclides when released by the RP. That information is given later in the text, the problem is that it is scattered in different sections of the manuscript.

In the revised version, we explain the precise path(s) followed by the radionuclides when released by the RP (page 5, lines 2-17): '<u>The schematic transport of NRP effluents and water masses in the SPNA-Artic Ocean region is displayed in Figure 1.</u> NRP-labelled AWs are first transported by surface currents into the North Sea and then carried poleward by the Norwegian Coastal Current (NCC) into the Nordic Seas (Edmonds et al., 1998; Raisbeck and Yiou, 2002) while mixing with the Norwegian Atlantic Current (NwAC) (Gascard et al., 2004; Kershaw and Baxter, 1995). The current splits in two branches north of Norway, one branch entering the Barents Sea as Barents Sea Branch Water (BSBW) and the other branch approaching the Fram Strait west of Spitsbergen where it bifurcates again. One branch joins the East Greenland Current (EGC) and recirculates southwards as Return Atlantic Water (RAW) (Fogelqvist et al., 2003) mixing with IrSPMW and PIW (modified AW that has recirculated in the Arctic Ocean; Rudels et al., 1999b). The other branch, the West Spitsbergen Current (WSC), transports the remaining AWs at shallow to intermediate depths into the Arctic Ocean via the Fram Strait Branch Water (FSBW), where they

recirculate in the Arctic Eurasian Basin before outflowing back through the Fram Strait and continuing southwards carried by the EGC (Rudels, 2015). The NRP signal also penetrates deep in the water column due to the formation of dense water north of the Greenland-Iceland and Iceland-Scotland passages, providing means of tracing the deep overflows that ventilate the deep North Atlantic Ocean (e.g. Smith et al., 2005).'.

4) Furthermore, lines 15 to 20 (Page 4) provides some information about previous results of $^{236}U/^{129}I$ however it does not explain what these numbers represent or why and how they change geographically or in time. For example, it is not explained why "Yet, LSW and DSOW were clearly identified by $^{236}U/^{238}U$ >1000 x 10^{-12}"; or why the atom ratio varies from "$^{129}I/^{238}U$ < 1 for GF to about 1 - 350 for European NRPs".
This is now better explained by providing more information on sources, oceanic levels and the usefulness of using these tracers alone and in combination. For example:

Page 5, lines 26-28; and page 6, lines 1-3:'the presence of ^{129}I in those regions is dominated by the liquid discharge from European NRPs, which has a well-documented release history (> 5700 kg; He et al., 2013a; Raisbeck et al., 1995), while the contribution from GF is comparably negligible (~ 90 kg worldwide release; Hou, 2004; Raisbeck and Yiou, 1999; Wagner et al., 1996). Consequently, the seawater affected by NRPs may present ^{129}I concentrations 1 – 4 orders of magnitude above the background due to GF (~ 2.5×10^{7} at/kg; Edmonds et al., 1998).'.

Page 6, lines 15-22: 'Surface seawaters of the northern hemisphere present $^{236}U/^{238}U$ atom ratios of about 1000×10^{-12} (e.g. Christl et al., 2012) in the <u>unique presence of GF (about 900 kg released worldwide;</u> Sakaguchi et al., 2009). <u>However, the $^{236}U/^{238}U$ ratios can be significantly higher</u> in the Arctic and North Atlantic Oceans due to the liquid discharge of ^{236}U from European NRPs (about 100 kg, Christl et al., 2015a). T<u>his has allowed tracing the waters carrying NRP-^{236}U</u> with $^{236}U/^{238}U$ ratios up to 3800×10^{-12} in the Arctic Ocean in 2011 – 2012 (Casacuberta et al., 2016), and up to 1400×10^{-12} in LSW and DSOW in the western SPNA in 2010 (Casacuberta et al., 2014).'.

Page 6, lines 23-26: In addition, <u>both ^{236}U and ^{129}I can be combined as the dual tracer</u>, $^{129}I/^{236}U$ - $^{236}U/^{238}U$, to identify the radionuclide source(s) present in a given water mass (Casacuberta et al., 2016; Christl et al., 2015b). <u>This is possible because the GF and the European NRPs introduced different amounts of ^{236}U and ^{129}I</u> (see above) to the environment and tagged the waters with characteristic $^{129}I/^{236}U$ and $^{236}U/^{238}U$ atom ratios depending on the proximity from the source(s).

5) Lines 10-15 (Page 4). Why reference data are given here and not for ^{129}I?
In the revised version we provide reference data also for I-129. For example;

Page 6, lines 1-3: 'the seawater affected by NRPs may present ^{129}I concentrations 1 – 4 orders of magnitude above the background due to GF (~ 2.5×10^{7} at/kg; Edmonds et al., 1998).'.

6) Line 18 (Page 5). No mention to deep water formation at the Greenland Sea? And ISOW formation? ISOW is later described (Line 7, Page 8), but it would be easier to follow the manuscript having the whole picture since the beginning.
This is now described in the text of the introduction (page 5, lines 14-17): 'The NRP signal also penetrates deep in the water column due to the formation of dense water north of the Greenland-Iceland and Iceland-Scotland passages, providing means of tracing the deep overflows that ventilate the deep North Atlantic Ocean (e.g. Smith et al., 2005).'.

SECTION 3.1. **(Now section 3.2)**
7) Line 5 (Page 7). A brief introduction to $^{129}I/^{236}U$ ratios is missing to understand their values and the further discussions.
The revised introduction includes more detailed information on sources and oceanic levels of these tracers, which then used to introduce that ratio:'

Page 5, lines 26-28; and page 6, lines 1-3: 'the presence of ^{129}I in those regions is dominated by the liquid discharge from European NRPs, which has a well-documented release history (> 5700 kg; He et al., 2013a; Raisbeck et al., 1995), while the contribution from GF is comparably negligible (~ 90 kg worldwide release; Hou, 2004; Raisbeck and Yiou, 1999; Wagner et al., 1996). Consequently, the seawater affected by NRPs may present ^{129}I concentrations 1 – 4 orders of magnitude above the background due to GF (~ 2.5×10^{7} at/kg; Edmonds et al., 1998).'

Page 6, lines 15-22: 'Surface seawaters of the northern hemisphere present $^{236}U/^{238}U$ atom ratios of about 1000×10^{-12} (e.g. Christl et al., 2012) in the <u>unique presence of GF (about 900 kg released worldwide;</u> Sakaguchi et al., 2009). <u>However, the $^{236}U/^{238}U$ ratios can be significantly higher</u> in the Arctic and North Atlantic Oceans due to the liquid discharge of ^{236}U from European NRPs (about 100 kg, Christl et al., 2015a). T<u>his has allowed tracing the waters carrying NRP-^{236}U</u> with $^{236}U/^{238}U$ ratios up to 3800×10^{-12} in the Arctic Ocean in 2011 – 2012 (Casacuberta et al., 2016), and up to 1400×10^{-12} in LSW and DSOW in the western SPNA in 2010 (Casacuberta et al., 2014).'.

Page 6, lines 23-26: 'In addition, <u>both ^{236}U and ^{129}I can be combined as the dual tracer</u>, $^{129}I/^{236}U$ - $^{236}U/^{238}U$, to identify the radionuclide source(s) present in a given water mass (Casacuberta et al., 2016; Christl et al., 2015b). <u>This is possible because the GF and the European NRPs introduced different amounts of ^{236}U and ^{129}I</u> (see above) to the environment and tagged the waters with characteristic $^{129}I/^{236}U$ and $^{236}U/^{238}U$ atom ratios depending on the proximity from the source(s).'.

In addition, we have modified the structure of section 3.3 to include a paragraph that facilitates the interpretation of Figure 4 (former Figure 3). This is achieved by including the expected values of $^{129}I/^{236}U$ and $^{236}U/^{238}U$ atom ratios in the subpolar North Atlantic water (page 14, lines 8-15): 'As done in earlier studies (Casacuberta et al., 2016), we can estimate the contribution to our samples from the LB, GF and NRP by combining the $^{129}I/^{236}U$ and $^{236}U/^{238}U$ on a dual tracer approach (Figure 4). <u>This is possible because the atom ratios of $^{129}I/^{236}U$ and $^{236}U/^{238}U$ display a wide range of values due to the different input of ^{129}I and ^{236}U from the three source</u>s. <u>For example,</u> the <u>GF</u> introduced about 10 times more ^{236}U than ^{129}I, thus this endmember is characterized by <u>$^{129}I/^{236}U < 1$ and</u>

$^{236}U/^{238}U$ surface ratios in the (1000–2000) × 10^{-12} range. On the contrary, the total amount of ^{236}U introduced from European NRPs was much smaller than for ^{129}I. Therefore, a water mass with the additional influence from the European NRP may present $^{129}I/^{236}U$ on the 1–350 range and $^{236}U/^{238}U$ above the GF.'.

8) Line 10-30 (Page 7). I also miss a complete introduction to water mass structure. It will be easier to follow the discussion if first we understand water mass structure and then 129I and 236U/238U are given.

This way, ISOW description (Lines 7 -11, Page 8) should be move to that introduction, and merge with description in Page 5.
The discussion now begins with a new section 3.1 (pages 10 and 11), which describes the structure of water masses:

'3.1 Water mass structure in 2014

The water mass structure in spring 2014 is described using the zonal sections for salinity, potential temperature and dissolved oxygen concentrations (Figure 2) to facilitate the understanding of ^{129}I and ^{236}U distributions in section 3.2. The assessment of the water mass structure from GEOVIDE was performed using an extended Optimum Multi-Parameter analysis (OMP) (further details are found in García-Ibáñez et al. 2018).

In the upper water column (< 500 m), warm and saline Central Waters dominate the eastern part of the section between the coast off Portugal and station 26 (Figures 2A and 2B). Central waters (or East North Atlantic Central Water, ENACW) are characterized by the highest potential temperatures and relatively high salinities as they have been transported from subtropical latitudes into the eastern part of the section by the northeast-flowing branches of the NAC. Part of ENACW recirculates into the Iceland Basin and the Irminger Sea, where air-sea fluxes transform them into colder and fresher SPMWs (McCartney and Talley, 1982) that occupy equivalent depths between the Subarctic Front (SAF; roughly at 22.5 °W, station 26) and Greenland (Figure 2A and 2B). The upper water column on the continental shelves and slopes of Greenland and Canada is occupied by PIW, which presents very low salinities (< 34) and potential temperatures usually < 0 ºC (Figures 2A and 2B). PIW originates from the Arctic Ocean, enters through the Fram (PIW-Atlantic) and Nares Straits (PIW-Canada), and joins the shallow western boundary transport in the EGC and LC (Figure 1).

At intermediate depths, LSW is the most abundant water mass and fills the whole section from the upper water-levels to about 2000 m depth (Figure 2). LSW is formed in the Labrador Sea and, to less extent, in the Irminger Sea by transformation of SPMWs via winter convection (e.g., Jong and Steur, 2016). Then, it flows south as part of the DBWC (e.g. Bersch et al., 2007) or east into the Irminger, Iceland and West European Basins (Figure 1). LSW is characterized by a relative minimum in salinity (< 34.9) and in temperature (~ 3 ºC) at its formation region, and warmer and saltier values as it mixes with surrounding waters along its equatorward and eastward transport (Figures 2A and 2B). Station 26 is also affected by the Subarctic Intermediate Water (SAIW), which presents lower salinities (~ 34.9) and potential temperatures (4 – 7 ºC) than the other

water masses surrounding it at similar depths, i.e. ENACW and SPMW from the Iceland Basin (IcSPMW), respectively (Figures 2A and 2B). SAIW forms in the western boundary of the SPNA (i.e. the LC) by mixing between LSW and subtropical waters carried by the NAC (Arhan, 1990; Read, 2000), before subducting at about 400 m depth and being advected within the northern branch of NAC (Figure 2). Depths around 1000 m in the WEB (stations 1 and 13) are also influenced by the northward-flowing Mediterranean Water (MW) (Figure 1) that is characterized by a maximum in salinity (> 36) and minimum in oxygen (~ 180 μmol/kg) (Figures 2A and 2C).

In the deep-water column (> 2000 m), the lower North East Atlantic Deep Water ($NEADW_L$) dominates the section in the WEB (east of 20 ºW), while in the western part, dense overflow waters are the most abundant water masses. $NEADW_L$ is generally saltier, colder and older than the overlying LSW due to the major contribution of the northward flowing Antarctic Bottom Water (AABW) (Figures 2A – 2C). Dense overflow waters dominate bottom depths at both sides of the Reykjanes Ridge and in the Irminger and Labrador Seas (Figure 1). ISOW is best identified thanks to its local salinity maximum (~ 34.92) on the flanks of the Reykjanes Ridge and between the LSW and DSOW in the Irminger and Labrador Seas (Figure 2A). This water mass is produced by mixing of old Norwegian Sea waters that overflow the Iceland–Scotland Sill and entrain SPMW and LSW in the SPNA (e.g., van Aken and De Boer, 1995). ISOW mainly flows along the eastern flank of the Reykjanes Ridge into the Irminger and Labrador Seas (Figure 1), yet increasing studies point towards the eastward return flow of this water mass through passages in the Mid Atlantic Ridge (Xu et al., 2018) or directly along the flanks of the Rockall Through into the eastern part of the GEOVIDE section (e.g. Zou et al., 2017) (Figure 1). Finally, DSOW is present between ISOW and the seafloor in the Irminger and Labrador Seas (notably stations 44 and 69). This overflow water can be distinguished from ISOW by its lower salinities (< 34.90), potential temperatures (< 2 ºC) and higher oxygen concentration (> 290 μmol/kg) (Figures 2A – 2C) that result from the more recent ventilation and rapid advective flow from the DSOW formation region north of the Denmark Strait in to the GEOVIDE section (e.g. Read, 2000) (Figure 1). '.

This section is supported by a new figure (Figure 3 in page 38) presenting the distribution of hydrographic properties:

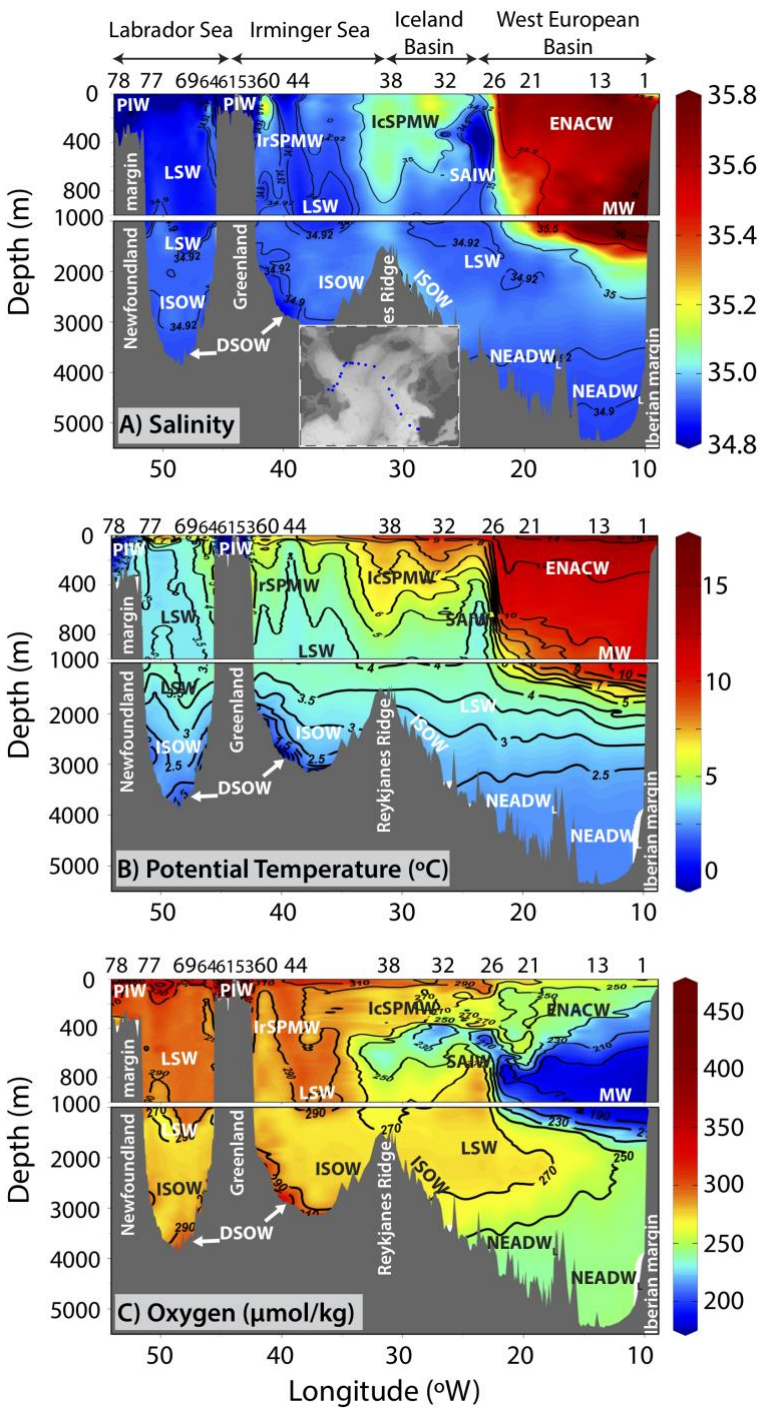

Figure 2. Vertical distribution of (A) salinity, (B) potential temperature and (C) dissolved oxygen along the GEOVIDE section in spring 2014. Water mass acronyms are defined in Table 1.'

9) Line 26 (Page 7). "SAIW probably incorporates ^{129}I from precursor water masses (e.g., waters carried by LC and/or LSW) while forming in the western SPNA". Why is that? Some of the statements, like this one, are properly given but not explained in terms of ^{129}I (or $^{236}U/^{238}U$) values.

In the revised manuscript we explain better that LC carries a large NRP signal, that SAIW forms in the LC and then is transported into the GEOVIDE transect, resulting in a large tracer signal due to the influence from NRPs. For example:

Page 12, lines 15-18: 'The highest ^{129}I concentrations (~ 250 × 10^7 at/kg) and ^{236}U/^{238}U ratios (~ 2300 × 10^{-12}) are present in PIW and RAW carried by the EGC and LC over the shelves and slopes of Greenland and Canada. This water admixture, largely influenced by NRPs (e.g. Alfimov, 2004), …'.

Page 11, lines 3-6: 'SAIW forms in the western boundary of the SPNA (i.e. the LC) by mixing between LSW and subtropical waters carried by the NAC (Arhan, 1990; Read, 2000), before subducting at about 400 m depth and being advected within the northern branch of NAC (Figure 2).'.

Page 13, lines 2-3: 'SAIW also presents relatively high ^{129}I concentrations (~ 20 × 10^7 at/kg) at stations 26 and 32, probably because of the influence of waters carried by the LC.'.

10) Line 5 (Page 8). "Thus, 2014 data probably reflects the dilution with old LSW and SPMW carrying less ^{129}I and ^{236}U than MW". How is it that waters from LSW and SPMW, both affected by NFRP, carry less ^{129}I and ^{236}U/^{238}U than MW, also mainly affected by GF? Is it the influence of Marcule?

Yes. The ^{129}I concentrations and ^{236}U/^{238}U atom ratios are higher than expected from the GF in the Mediterranean Sea. Recent work showed that this is very likely due to the discharge of ^{129}I and ^{236}U from the Marcoule reprocessing plant (see Castrillejo et al., 2017, Science of the Total Environment). The sentence now reads (page 13, lines 6-11): 'Similar depths are also influenced by MW (stations 1 and 13), yet, its ^{129}I concentrations (~ 3 × 10^7 at/kg) and ^{236}U/^{238}U ratios (~ 1000 × 10^{-12}) in 2014 were significantly lower than average ^{129}I concentrations (9 × 10^7 at/kg) and ^{236}U/^{238}U ratios (1600 × 10^{-12}) reported in the outflow region of MW at the Strait of Gibraltar in 2013 (Castrillejo et al., 2017). Thus, 2014 data probably reflects the dilution of MW, which is largely affected by inputs from the Marcoule nuclear facility (Castrillejo et al., 2017), with old LSW and SPMW carrying a diluted NRP signal.'.

11) Lines 1-13 (Page 8). This is clearly explained, but it will be even easier to follow if the name of stations and references to Table 2 are given.

The reader is referred to Table 2 and station numbers throughout section 3.2 (pages 12 and 13).

12) Lines 14 -18. As already said, previous brief introduction to the use of ^{129}I/^{236}U as tracer should be included to make these lines easier to follow. This way it said "The highest ^{129}I/^{236}U ratios (> 100) are present in waters transported by the shallow EGC and LC. Overflow waters are also distinguishable by their relatively high ^{129}I/^{236}U ratios (60 to 110 for DSOW, 15 to 40 for ISOW)" Why is that?

That is because they have a greater contribution from the European nuclear fuel reprocessing plants than other waters that are only affected by global radioactive fallout.

This kind of sentences are now easier to follow, since a more detailed information on sources and transport of the tracers and their use is provided in the Introduction section.

SECTION 3.2.
13) Line 25- 30 (Page 8). I really like Figure 3. I contains lots of information, may be it could be further explained in the mentioned intro introducing the $^{129}I/^{236}U$ tracer?
As previously stated, in the revised version we include further explanation on the sources which helps better understanding the values found for the $^{129}I/^{236}U$ ratio.

We have also modified the structure of section 3.3 to include a paragraph that facilitates the interpretation of Figure 4 (former Figure 3). This is achieved by including the expected values of $^{129}I/^{236}U$ and $^{236}U/^{238}U$ atom ratios in the subpolar North Atlantic water (page 14, lines 8-15): 'As done in earlier studies (Casacuberta et al., 2016), we can estimate the contribution to our samples from the LB, GF and NRP by combining the $^{129}I/^{236}U$ and $^{236}U/^{238}U$ on a dual tracer approach (Figure 4). <u>This is possible because the atom ratios of $^{129}I/^{236}U$ and $^{236}U/^{238}U$ display a wide range of values due to the different input of ^{129}I and ^{236}U from the three sources</u>. <u>For example,</u> the <u>GF</u> introduced about 10 times more ^{236}U than ^{129}I, thus this endmember is characterized by <u>$^{129}I/^{236}U < 1$ and $^{236}U/^{238}U$ surface ratios in the (1000–2000) $\times 10^{-12}$ range</u>. <u>On the contrary</u>, the total amount of ^{236}U introduced from European NRPs was much smaller than for ^{129}I. Therefore, a water mass with the additional influence from the European NRP may present <u>$^{129}I/^{236}U$ on the 1–350 range and $^{236}U/^{238}U$ above the GF</u>.'.

SECTION 3.3.
14) Line 14 (Page 9). "^{129}I discharge rate from European NRPs was observed in the whole water column, being more pronounced (about 10 times increase) in overflow waters". This actually an previously observed fact but an explanation should be given here.
Some parts of this section 3.4 (former section 3.3) have been rewritten to emphasize that data from the GEOVIDE cruise in 2014 is compared to the literature (e.g., page 15, lines 13-14):' In this section we compare radionuclide concentrations reported in the literature with those measured at nearby stations during GEOVIDE (Figure 5).'.

In addition, the section about I-129 begins with a summary of previous findings (e.g., page 15, lines 16-22): 'In the case of ^{129}I, the existing time series for the central Labrador Sea (1993–2013, Figure 5A) demonstrated that most of the tracer transport was carried by overflow waters (e.g. DSOW) and that the temporal evolution of ^{129}I concentrations in those waters could be associated with the tracer release from the European NRPs some years earlier (Edmonds et al., 2001; Orre et al., 2010; Smith et al., 2005, 2016). For instance, the literature on ^{129}I shows a rise in tracer concentrations due to the increased ^{129}I discharge rate from European NRPs in the whole water column, being more pronounced (about 10 times increase) in overflow waters (Figure 5A).'.

15) Figure 4A. Indicate in the caption that Smith 2016 corresponds to 2012 and 2013 profiles. "The depth distribution of ^{129}I concentrations in the Labrador Sea in 2014 (station 69), displays ^{129}I concentrations in DSOW about 15 % lower than in 2012 – 2013 (Smith et al., 2016)". Is this because samples from 2012-2013 are measuring the peak in the NFRP

releases? If this is the case, please mention that the explanation for that decrease will be given in Section 3.5.
The figure caption has been amended to reflect the source of the data (page 41, lines 1-10).

Yes, the interpretation is that the 2014 data suggests that the peak occurred in 2013. As suggested by the reviewer, we refer to this in the text (page 15, lines 23-24): 'The depth distribution of ^{129}I concentrations in the Labrador Sea in 2014 (station 69) displays ^{129}I concentrations in DSOW about 15 % lower (see section 3.5.4) than in 2012 – 2013 (Smith et al., 2016),'.

We give the explanation in page 20, lines 22-24: 'Thus, 2014 data reported in this study supports the current interpretation on the 'Arctic loop' (e.g. Smith et al., 2016) and suggests that the second ^{129}I front probably peaked before the GEOVIDE cruise.'.

16) As I said, it is a well-known fact DSOW present an increase in ^{129}I concentrations for all years. This is already approached by previous works, but a brief discussion could be also given here.
Please see answer to comment 14.

17) Line 18 (Page 9). "The main difference between the ^{129}I depth profiles in the Irminger Sea (station 44) and central Labrador Sea (station 69) in 2014 is the surface ^{129}I peak in the latter one (Figure 4A). Which is probably caused by waters that split off from the boundary currents, either the West Greenland Current or the LC". I don't quite understand this. Splitting won't change ^{129}I concentrations.
The EGC and the LC are characterised by particularly high ^{129}I and ^{236}U concentrations, respectively. We propose that the surface waters in the central Labrador Sea may have been influenced by waters that separated from the mainstream of the WGC/LC. Indeed, such surface peak is also observed in the profile of U-236 concentrations represented in Figure S1. The sentence has been changed to clarify the interpretation (page 15, lines 27 and page 16, lines 1-4): 'Considering the 30 m deep freshwater surface layer observed between station 69 and Greenland (not shown here), we suggest that waters carried by the West Greenland Current (continuation of the EGC) may have separated from the main western boundary transport and entered the Central Labrador Sea (Cuny and Rhines, 2002). This can also explain the peak in ^{236}U/^{238}U ratios observed at the same location (Figure S1).'

18) Line 26 (Page 9). "This similarity suggests little time variation and similar water mass composition for that region, although PAP might present slightly larger ^{129}I concentrations because of its proximity to Sellafield and La Hague". And will support the later mentioned hypothesis of direct contribution of NFRP to SPNA without previous recirculation (Line 10, Page 10).
Indeed, this is probably the case. We have added the reviewers' point in the revised text (page 15, lines 15-18): 'These results suggest a similar water mass composition for that region, yet the offset in deep ^{129}I concentrations would support the hypothesis that effluents from the nearby Sellafield and/or La Hague NRPs may enter directly into the SPNA without previous circulation in the Nordic Seas (see section 3.5.1).'.

SECTION 3.4. **(now section 3.5.1)**
19) Line 17 (Page 10). "twice" instead of "two times"
This has been changed (page 17, line 17).

20) Line 16 -17 (Page 10). "near-surface transport of ^{129}I from European NRPs also across Iceland-Scotland into the eastern SPNA" is also clearly seen in Table 2. That shows that profiles 1, 13 and 21 strongly contrast from profiles 26 and 32. Not only due to ISOW (IcSPMW) contribution in intermediate depths but also at shallower depths.
The station numbers and Table 2 have been referenced (page 17, lines 19-20): 'Consequently, ^{129}I concentrations in shallow waters at stations 1, 13 and 21 strongly contrast with those at stations 26 and 32 located west of the SAF (Table 2)'.

21) Line 27 (Page 10). allowing to identify key circulation features such as the EGC/LC and the DWBC in the Labrador and Irminger Seas. Explain in terms of radioactive tracers.
This comment and the following ones (22 and 23) have been addressed by: i) adding a brief introduction to the section on the circulation of the EGC and LC and the subsequent supply of waters of Atlantic and Canada origin; and ii) discussing their different tracer levels (page 18, lines 2-17): 'It is well known that the eastern coast of Greenland receives RAW and PIW-Atlantic injected in the EGC (Figure 1). Similarly, the shelf of Newfoundland is bathed by the LC, which carries EGC waters and PIW-Canada, this last one being supplied through the Nares Strait (Curry et al., 2014). The tracer levels are particularly high in such waters residing on the shelves, slopes and very deep waters around Greenland and Newfoundland (Figure 3). Further, the tracer content differs between Arctic waters of Atlantic and Canadian origin enriched in ^{129}I and ^{236}U, respectively. Thus, one may use them to distinguish key circulation features such as the EGC/LC and the DWBC in the Labrador and Irminger Seas (Figure 1). For example, at shallow depths, the EGC (stations 53 to 64) presents remarkably high ^{129}I concentrations (up to $\sim 250 \times 10^7$ at/kg) and $^{129}I/^{236}U$ ratios (up to 200), while both values are significantly lower in the LC (station 78) which is characterized by comparably higher $^{236}U/^{238}U$ ratios (up to 2350×10^{-12}) (Figure 3). Such differences on the ^{129}I and ^{236}U composition of the two shallow boundary currents are likely due to the fact that waters of Atlantic origin (PIW-Atlantic and RAW) have been largely influenced by NRP effluents (high ^{129}I). On the contrary, the LC records lower ^{129}I concentrations due to the influence of PIW-Canada waters with mainly GF signal (Ellis and Smith, 1999; Smith et al., 1998), and a large ^{236}U content ($^{236}U/^{238}U$ ratios are likely > 2000×10^{-12}) from both the GF and unconstrained Arctic rivers inputs (Casacuberta et al., 2016).'.

22) Line 30 -30. Differences of ^{129}I and ^{236}U in boundary currents are mentioned but not explained. It should be further discussed in terms of radioactive tracers.
Please see answer to comment 21.

23) Line 1-2 (Page 11). "EGC shows particularly high ^{129}I concentrations and $^{129}I/^{236}U$ ratios because it is carrying Arctic water of Atlantic origin (PIW-Atlantic) and RAW that have been largely influenced by NRP effluents". I assume the authors do not explain this further because this is well known from previous works. Nevertheless, a brief description should be given, may be in the previously mentioned introduction?

Please see answer to comment 21.

24) Line 5-6 (Page 11). "while its $^{236}U/^{238}U$ ratios are likely > 2000 10^{-12} due to GF and unconstrained Arctic rivers inputs". Influencing how? In ^{236}U, ^{129}I or both?
Previous studies showed that the Arctic-Canada water arriving to the Labrador Sea carry low concentrations of ^{129}I (Ellis and Smith, 1999), while the $^{236}U/^{238}U$ atom ratios are unexpectedly high for those waters (Casacuberta et al., 2014). Although that source is not well constrained yet, it would appear that Arctic rivers might be a source, especially for ^{236}U.

This is now explained in page 22, lines 1-4: 'For example, the LC presents mainly the GF signal and unconstrained <u>Arctic river inputs (more ^{236}U relative to ^{129}I)</u> indicating the contribution from PIW-Canada through the Canadian Archipelago, while the EGC, largely influenced by the <u>NRPs (more ^{129}I relative to ^{236}U),</u> indicates the contribution of RAW and PIW-Atlantic.'.

25) Line 12 (Page 11). "rise of ^{129}I concentrations at certain depths on the Greenland slope (e.g., station 60; Figure 2 and Figure S1), and particularly in bottom waters of the Irminger Sea (station 44), which are probably related to the cascading of ^{129}I-rich waters from the Greenland Shelf". And why not an increase in ^{236}U?
Our interpretation is that waters carried by the EGC may cascade from the continental shelf (station 53 and 61) over the slopes in the eastern (station 60) and western (station 64) sides of the southern tip of Greenland. The EGC transports about 10 times more ^{129}I (the core presents about 250 x 10^7 at kg^{-1}, station 53 and 61, Table 2) than in surrounding offshore waters (about 20-25 x 10^7 at kg^{-1}, e.g. station 60 and 64). In contrast, ^{236}U concentrations in the EGC (about 15 x 10^6 at kg^{-1}) are only 50% higher than in the mentioned offshore waters. Thus, while the spike of ^{129}I is easily observed near the bottom on the western and eastern slopes of Greenland (stations 60 and 64, Figure 2 and vertical profiles in the supplemental material), such increase is not distinguishable for ^{236}U.

26) Line 22-23 (Page 11). "The ISOW is best distinguished by its relative ^{129}I concentration maxima". Explain origin of this maximum.
The origin of the maximum has been explained in page 19, lines 8-9: 'The ISOW is best distinguished by its relative ^{129}I concentration maxima and $^{129}I/^{236}U$ ratios of 15 – 40 <u>due to NRPs</u>,'.

27) Line 24 (Page 11). The differences can be more clearly seen in Table 2.
Table 2 has been referenced (page 19, line 11).

28) Line 24-25(Page 11). "Further, in the next years one can expect a stronger ^{129}I signal associated with ISOW in the SPNA due to the releases from the NRPs". Explain this further.
A better explanation is now provided (page 19, lines 14-17): 'In the comming years, one can expect a stronger ^{129}I signal carried by ISOW because tracer concentrations in ISOW precursor waters have increased from 7 × 10^7 at/kg to 63 × 10^7 at/kg at the Iceland–

Scotland Sill from 1993 to 2012 in response to releases from the NRPs (Alfimov et al., 2004; Edmonds et al., 2001; Vivo-Vilches et al., 2018).'.

29) Line 3 (Page 12). "The evolution of ^{129}I (and ^{236}U) in the SPNA is closely related to the effluents discharged from the two European NRPs". It sounds weird to mention this at the end of the paper.
This is now mentioned in the Introduction and particularly when the temporal evolution of I-129 is discussed in section 3.4 (e.g. page 15, lines 16-20): 'In the case of ^{129}I, the existing time series for the central Labrador Sea (1993–2013, Figure 5A) demonstrated that most of the tracer transport was carried by overflow waters (e.g. DSOW) and that the temporal evolution of ^{129}I concentrations in those waters could be associated with the tracer release from the European NRPs few years earlier (Edmonds et al., 2001; Orre et al., 2010; Smith et al., 2005, 2016).'.

30) Line 18 (Page 12). "Data reported in this study (2014) supports this 'Arctic loop' and suggests that the second 129I front probably peaked before the GEOVIDE cruise". Could Vivo et al. values be also used to support this "Arctic loop"?
It is difficult to do so, given the different locations and sampling times of the two studies. We think that the comparison should be kept to nearby stations measured repeatedly over time to avoid uncertainties related to transit times and mixing of water mass. For instance, the DSOW dilutes 1 - 2 times during the 0.3 – 2.0 years of transport from the Denmark Strait to the Central Labrador Sea (Smith et al., 2005).

<u>Reviewer 2</u>,
In general, this article presents new information about two circulation loops of Atlantic Waters which are tagged with nuclear reprocessing plant effluents from their source region based on the observations at stations from Lisbon (Portugal) to the southern tip of Greenland (Cape Farewell), and from Cape Farewell to St. John's (Newfoundland, Canada). The reviewer thinks that this article should be published in Biogeoscience, but there are several points should be revised before publication.

<u>Major points:</u>
1) Page 8 line 25 The authors used a binary mixing model of which three end members are LB, GF and NRP. But, as the authors recognized and stated in the text, most of the samples can be explained by simple two end members model except 6 samples collected in the deeper layers (page 9, line 2) which towards the lithogenic background, LB. This means that in the surface to mid depths in this region, to discuss sources of ^{129}I and ^{236}U in the SPNA, the reviewer thinks that it is enough to use simple two end members mixing model and the authors can revise the discuss here.
We acknowledge that using a two end-member model could render similar results in most instances. Yet, the reason for including the lithogenic background is that, despite its small contribution (by mass of radionuclide), it has a very distinct $^{129}I/^{236}U$ and $^{236}U/^{238}U$ atom ratio that makes this source clearly distinguishable from the two artificial radionuclide sources (NRP and the GF). Therefore, the third (natural) source (i.e. Lithogenic background) allows identifying waters that have a very small anthropogenic impact. This is the case of $NEADW_L$, a water mass that has a large presence in the eastern part of the

section. Therefore, we prefer to keep the lithogenic background in the binary mixing model.

2) Page12 Line 1 -27 The discussion about transit times and dilution factors in the paragraph is poor and difficult to understand how the authors calculate time scales of 8-10 years for shorter loop and 8-18 years for longer loop.
This section 3.5.4 (pages 19-21) has been rewritten to better explain: i) what was known prior to this study about the circulation loops of Atlantic Waters and their time scales, ii) what are the calculations we have made and how they are done, and, iii) the reasons for possible inconsistencies. We also improved the caption of Figure 6 (former figure 5) to facilitate understanding the interpretation of the data. We believe that the discussion in now clearer for the reader.

3) This 8-18 years statement is also inconsistent the numbers stated "between the maximum 16-8 years (page 13 line 19)" in the conclusion.
We thank the reviewer for noting such inconsistency. The correct time scales are now stated in page 22, lines 13-15: ' This study supports the current interpretations on the circulation of AWs, which apparently follow a short loop trough the Nordic Seas (8 – 10 years in this study) and a longer loop including the recirculation in the Arctic Eurasian Basin (16 – 18 years in this study).'.

4) The authors used ^{129}I input function at 60 N deg. By Christl 2015 and compared observational peak. But the input function already includes several assumptions and based on the figure caption, no explanation in the main text, the authors expanded the function to fit the measurement. But as shown in Figures 4A and 4B, the reviewer observes inconsistency between input functions and observations for both ^{129}I and ^{236}U.
We provide the assumptions made by Christl et al. (2015) which followed previous modelling studies using tracer inputs from the European NRPs. For example (page 20, lines): 'we took the ^{129}I input function at 60 °N for the northern North Sea (Figure 6A, green dashed line) used in earlier studies (e.g. Christl et al., 2015b; Orre et al., 2010; Smith et al., 2005). <u>This input function is estimated assuming</u> that the signal of both NRPs mixes in the North Sea and then is advected to 60 °N in 2 years from La Hague and in 4 years from Sellafield.'.

The inconsistencies between measured and estimated U-236 concentrations are are briefly mentioned in page 21, lines 5–10: 'Although the ^{236}U data would agree with the hypothesis of a second delayed ^{129}I pulse arriving from the Arctic Ocean, there are significant inconsistencies between the simulated and measured concentrations. These might be attributed to, among other factors, the large uncertainty of the used ^{236}U data point for 2014, uncertainties on the amount released by the Sellafield NRP (Christl et al., 2015), missing information on other sources, or unaccounted features on the water mass circulation downstream NRP.'.

5) Therefore, the reviewer suggests that the authors can and should collaborate with numerical modeling guys to get modeling results and compared with authors observation.
The reviewer is certainly right that model simulations are desirable to better understand the observed tracer levels and their distribution. Indeed, we initiated collaborations with

ocean circulation modellers to understand better the release and transport of ^{129}I and ^{236}U in the subpolar North Atlantic. Yet, such modelling studies are highly complex and the results not at the stage of being ready for publication. Furthermore, the focus of this manuscript is the presentation and interpretation of the measured data. A model vs data study would certainly be out of the scope of this manuscript. The two main reasons are that the experimental data already provide a very rich information for one manuscript, and that finding a suitable model which can fit the tracer input in a well resolved ocean circulation for the subpolar North Atlantic is apparently not trivial.

Minor points:

6) page 2 line 25-29 The authors should add about ^{238}U data in their study.

Now, we provide the ^{238}U in a supplemental table.

7) Page 5 line 25 and 24 12L Niskin bottles.! and 24 of 12L Niskin bottles.?

The sentence has been clarified (page 8, line 1): ' 24 Niskin bottles of 12L each'.

*8) Page 7 line 8 The authors used data marked * , but the uncertainties are so large for $^{236}U/^{238}U$ ratio $^{129}I/^{236}U$ ratio as 2350+- 370 and 200+-60, respectively. These numbers should be in the blanket ( ), and 2090+-140 and 140+-30 should be used. Due to larger uncertainty, 2350+-370 and 2090+-140 mean within the same and 200+-60 and 140+-30 locate are also within the same.*

We think the symbols '(' and ')' are used correctly in the original manuscript (now page 12, lines 1-7). A small part of the dataset has large uncertainties for U-236. This is because additional corrections had to be made to address limited contamination issues in those samples. We are confident that these data are valid and well represented as long as they are reported with the appropriate uncertainty.

9) Page 8 line 3 andc1600 x . The reviewer can not understand the meaning of this part. Please clarifiy the meaning of this part.

The error has been corrected in page 13, line 8: 'average ^{129}I concentrations (9×10^{7} at/kg) and $^{236}U/^{238}U$ ratios (1600×10^{-12}) reported in'.

10) Page 27 Figure4 Caption of Figure 4 is not enough and color coordinations for previous and current date are not good, eg. think open green circle in Fig.4B was hard to find in Fig.4D.

We have improved the Figure by: i) enlarging symbols in Figure 5D; ii) changing the colours in Figure 5A, iii) adding sampling years in Figures A, B and C; and iv) by further explaining the figure caption (page 41, lines 2-10): 'Figure 5. Vertical profiles of ^{129}I concentrations at locations shown in (D) of selected GEOVIDE stations and of those reported in nearby locations by earlier studies. (A) ^{129}In the Labrador and Irminger Seas, red profiles represent data from this work (2014). Data from 1993 was reported southwest of GEOVIDE station 69 by Edmonds et al. (2001). Data from 1997 to 2013 were reported at Station 17 of the AR7W line: for 1997, 1999 and 2001 by Smith et al. (2005); for 2003, 2005 and 2009 by Orre et al. (2010); and for 2012 and 2013 by Smith et al. (2016). (B) In the Icelandic Basin, green profiles show data from GEOVIDE stations 32 and 38 in 2014, while black profiles represent data from 1993 reported by Edmonds et al. (2001). (C) In the West European Basin, blue profiles represent data from GEOVIDE

stations 1 to 26, while data from 2012 in the Porcupine Abyssal Plain (PAP) was reported by Vivo-Vilches et al. (2018). Water masses found during GEOVIDE cruise have been summarized and represented in same colour as the ^{129}I concentration profiles. Acronyms are defined in Table 1.'.

We hope the interpretation of Figure 5 (former figure 4) is now clear.

11) Time series data in Fig.4A is also not good to undestand temporal changed of ^{129}I concentration.
Please see answer to comment 10.

12) In general, all figure captions did not contain enough information about meaning of each color and each mark. Please state more precisely.
All the figure captions have been revised and completed to make figure interpretation more straightforward in pages 38-42.

End of comments.

Tracing water masses with ^{129}I and ^{236}U in the subpolar North Atlantic along the GEOTRACES GA01 section

Maxi Castrillejo[1,2], Núria Casacuberta[1,3], Marcus Christl[1], Christof Vockenhuber[1], Hans-Arno Synal[1], Maribel I. García-Ibáñez[4,5], Pascale Lherminier[6], Géraldine Sarthou[7], Jordi Garcia-Orellana[2,8] and Pere Masqué[2,8,9]

[1]Laboratory of Ion Beam Physics, ETH-Zurich, Otto Stern Weg 5, Zurich, 8093, Switzerland

[2]Institut de Ciència i Tecnologia Ambientals, Universitat Autònoma de Barcelona, Bellaterra, 08193, Spain

[3]Institute of Biogeochemistry and Pollutant Dynamics, Environmental Physics, ETH-Zurich, Universitätstrasse 16, Zurich, 8092, Switzerland

[4]Uni Research Climate, Bjerknes Centre for Climate Research, Bergen 5008, Norway

[5]Instituto de Investigaciones Marinas (IIM-CSIC), Eduardo Cabello 6, 36208 Vigo, Spain

[6]Ifremer, Univ. Brest, CNRS, IRD, Laboratoire d' Océanographie Physique et Spatiale, IUEM, Plouzané, France

[7]Laboratoire des Sciences de l'Environnement Marin (LEMAR), UMR 6539, IUEM, Technopôle Brest Iroise, 29280 Plouzané, France

[8]Departament de Fisica, Universitat Autònoma de Barcelona, Bellaterra, 08193, Spain

[9]School of Science, Centre for Marine Ecosystems Research, Edith Cowan University, Joondalup, WA 6027, Australia

Correspondence to: Maxi Castrillejo (maxic@phys.ethz.ch)

Marcus Christl 15/8/2018 11:12
Con formato: Alemán (Suiza)

Microsoft Office User 24/8/2018 8:09
Eliminado: & Departament de Física

Microsoft Office User 24/8/2018 8:10
Eliminado: France

Microsoft Office User 24/8/2018 8:10
Eliminado:

Microsoft Office User 24/8/2018 8:10
Eliminado: 8

Microsoft Office User 21/8/2018 11:08
Eliminado: ... [1]

Núria Casacuberta 14/8/2018 9:23
Eliminado: ... [2]

Microsoft Office User 9/8/2018 10:26
Eliminado: ... [3]

Núria Casacuberta 14/8/2018 9:23
Con formato: Correspondence

Abstract.

Pathways and time scales of water mass transport in the Subpolar North Atlantic Ocean (SPNA) have been investigated by many studies due to their importance for the Meridional Overturning Circulation and thus for the global ocean. In this sense, observational data on geochemical tracers provide complementary information to improve the current understanding of the circulation in the SPNA. To this end, we present the first simultaneous distribution of artificial ^{129}I and ^{236}U in 14 depth profiles and in surface waters along the GEOVIDE section covering a zonal transect through the SPNA in spring 2014. Our results show that the two tracers are distributed following the water mass structure and that their presence is largely influenced by the global fallout (GF) and liquid effluents discharged to north western European coastal waters by the Sellafield and La Hague nuclear reprocessing plants (NRPs). As a result, ^{129}I concentrations and ^{236}U/^{238}U atom ratios and ^{129}I/^{236}U atom ratios display a wide range of values: (0.2 – 256) × 10^{7} at/kg, (40 – 2350) × 10^{-12} and 0.5 – 200, respectively. The signal from NRPs, that is characterized by higher ^{129}I concentrations and ^{129}I/^{236}U atom ratios compared to GF, is transported by Atlantic Waters (AWs) into the SPNA, notably by the East Greenland Current (EGC)/Labrador Current (LC) at the surface and by waters overflowing the Greenland-Scotland passage at greater depths. Nevertheless, our results show that the effluents from NRPs may also directly enter the surface eastern SPNA through the Iceland-Scotland passage or the English Channel/Irish Sea. The use of the ^{236}U/^{238}U and ^{129}I/^{236}U dual tracer approach further serves to discern Polar Intermediate Water (PIW) of Canadian origin from that of Atlantic origin which carries comparably higher tracer levels due to NRPs (particularly ^{129}I). The cascading of these waters appears to modify the water mass composition in the bottom of the Irminger and Labrador Seas, which are dominated by Denmark Strait Overflow Water (DSOW). Indeed, PIW-Atlantic which has a high level of ^{129}I compared to ^{236}U appears to contribute to the deep Irminger Sea rising the ^{129}I concentrations in the realm of DSOW. A similar observation can be made for ^{236}U for PIW entering through the Canadian archipelago into the Labrador Sea. Several depth profiles also show an increase in ^{129}I concentrations in near bottom waters in the Iceland and the West European Basins that are very likely associated to the transport of the NRP signal by the Iceland-Scotland Overflow Water (ISOW). This novel result would support current

Movido (inserción) [13] ... [5]
Marcus Christl 15/8/2018 11:13
Eliminado: The transport p…athways and ... [4]
Marcus Christl 15/8/2018 11:14
Eliminado: implication in …eridional Over ... [6]
Microsoft Office User 9/8/2018 13:18
Eliminado: . T…irst simultaneoushe…distr ... [7]
Marcus Christl 15/8/2018 11:20
Eliminado: that …overinged ... [8]
Microsoft Office User 9/8/2018 13:46
Eliminado: subpolar North Atlantic ... [9]
Marcus Christl 15/8/2018 11:53
Eliminado: se
María Isabel García Ib…, 13/8/2018 18:30
Eliminado: , respectively, …a wide range ... [10]
Microsoft Office User 20/8/2018 10:37
Eliminado: $^{-1}$
María Isabel García Ib…, 13/8/2018 18:31
Eliminado: - …350) × 10^{-12} and 0.5 – - ... [11]
Marcus Christl 15/8/2018 11:55
Eliminado: these …RPs, that is characteri ... [12]
María Isabel García Ib…, 13/8/2018 18:31
Eliminado: for
Marcus Christl 15/8/2018 11:56
Eliminado:
Microsoft Office User 20/8/2018 10:38
Eliminado: northwards
María Isabel García Ib…, 13/8/2018 18:31
Eliminado: –
Microsoft Office User 9/8/2018 11:42
Subido [13]: This work investigates the u ... [13]
Microsoft Office User 9/8/2018 14:09
Eliminado: This work investigates the use ... [14]
María Isabel García Ib…, 13/8/2018 18:31
Eliminado: effluents
Marcus Christl 15/8/2018 12:00
Eliminado: also …irectly enter the surface ... [15]
María Isabel García Ib…, 13/8/2018 18:32
Eliminado: t
Microsoft Office User 9/8/2018 13:32
Eliminado: The highest tracer levels were ... [16]
Marcus Christl 15/8/2018 12:01
Eliminado: , as shown by relatively high ^{129} ... [17]
Microsoft Office User 9/8/2018 13:55
Eliminado: , as it is shown by elevated ^{129} ... [18]
María Isabel García Ib…, 13/8/2018 18:32
Eliminado: ^{68}
Microsoft Office User 9/8/2018 11:47
Eliminado: ^{8}
Marcus Christl 15/8/2018 12:07
Eliminado: also
Microsoft Office User 20/8/2018 10:02
... [19]
Marcus Christl 15/8/2018 12:04
... [20]
Microsoft Office User 21/8/2018 11:35
... [21]
Microsoft Office User 9/8/2018 14:16

modelling studies indicating the transport of ISOW into the eastern SPNA. Finally, our tracer data from 2014 is combined with published ^{129}I data for the deep central Labrador Sea between 1993 and 2013. The results obtained from comparing simulated and measured ^{129}I concentrations support the previously suggested two major transport pathways for the AWs in the SPNA, i.e. a short loop through the Nordic Seas into the SPNA and a longer loop which includes recirculation of the AWs in the Arctic Ocean before entering the western SPNA.

Microsoft Office User 9/8/2018 14:18
Eliminado: spreading pathways into the eastern SPNA have been confirmed by the unequivocal transport of reprocessing ^{129}I into the deep WEB.

Microsoft Office User 9/8/2018 12:31
Eliminado: D

Microsoft Office User 9/8/2018 12:31
Eliminado: of ^{129}I and ^{236}U

Marcus Christl 15/8/2018 12:11
Eliminado: are coupled

Microsoft Office User 9/8/2018 12:31
Eliminado: and

Microsoft Office User 9/8/2018 14:20
Eliminado: the

Microsoft Office User 9/8/2018 14:19
Eliminado: time

María Isabel García Ib..., 13/8/2018 18:34
Eliminado: seriesconcentration

Marcus Christl 15/8/2018 12:11
Eliminado: reported in the literature

Microsoft Office User 20/8/2018 10:07
Eliminado: results ing

Microsoft Office User 9/8/2018 14:35
Eliminado: in the Labrador Sea agrees with the hypothesis that Atlantic Waters (tagged with nuclear reprocessing plant effluents) follow at least two circulation loops from their source region: one short loop through the Nordic Seas into the SPNA of about 8 - 10 years, and a second, long loop, which adds about 8 years more of

Microsoft Office User 9/8/2018 14:44
Eliminado: Eurasian Basin

Microsoft Office User 9/8/2018 14:35
Eliminado: .

Microsoft Office User 20/8/2018 11:06
Eliminado:

1 Introduction

The subpolar North Atlantic (SPNA) is a key region for the global ocean circulation (see all acronyms in Table 1). The North Atlantic Current (NAC) carries warm subtropical waters northwards to the SPNA, where they are transformed into cold Subpolar Mode Water (SPMW) and ultimately into Labrador Sea Water (LSW), which circulates southwards along with the overflow waters from the Nordic Seas (Figure 1). These water mass formation processes constitute the starting point of the Atlantic Meridional Overturning Circulation (AMOC). Among other studies, the repeated hydrographic cruises along the Greenland-Portugal OVIDE line shed light on the decadal variability of the AMOC (Daniault et al., 2016; Lherminier et al., 2010; Mercier et al., 2013) and its relevance to climate by, for example, controlling the ocean uptake of CO_2 (Pérez et al., 2013). The GEOVIDE cruise carried out in spring 2014 covered the OVIDE line, extending further to the Labrador Sea revealing an intense AMOC over a cold and fresh SPNA (Zunino et al., 2017). The observed strong AMOC was linked to an intensified poleward transport of subtropical waters, as well as, to the increased equatorward transport of Iceland-Scotland Overflow Water (ISOW), Irminger-SPMW (IrSPMW) and Polar Intermediate Water (PIW) in 2014 relative to mean 2002 - 2010 (García-Ibáñez et al., 2018).

Anthropogenic tracers provide complementary information about the above water mass circulation changes in the SPNA. For example, chlorofluorocarbons (CFCs) and sulphur hexafluoride (SF_6) from industrial activities, or tritium (^3H) from atmospheric nuclear weapon tests conducted in the 1950s and 1960s (global fallout, GF), provide information on the ventilation of the interior Atlantic Ocean (Doney and Jenkins, 1994; Sy et al., 1997; Tanhua et al., 2005). Contrary to CFCs or ^3H, which were introduced into the surface ocean from a rather well mixed atmosphere, nuclear reprocessing plants (NRPs) represent point-like sources of artificial radionuclides. The NRPs located near La Hague and Sellafield discharge(d) liquid effluents to the English Channel and the Irish Sea, respectively, over the past 50 – 60 years, thereby tagging Atlantic Waters (AWs) passing by these locations from the 1960s on (Kershaw and Baxter, 1995). This allowed investigating AW spreading pathways and time scales downstream of these nuclear facilities (e.g. Aarkrog et al., 1983, 1987, Alfimov et al., 2004, 2013;

Núria Casacuberta 14/8/2018 9:24
Eliminado: ... [22]

Microsoft Office User 20/8/2018 11:06
Eliminado: ... [23]

Microsoft Office User 20/8/2018 10:43
Eliminado: ic

Núria Casacuberta 14/8/2018 9:25
Eliminado: are described

Microsoft Office User 24/8/2018 8:14
Eliminado: for

Microsoft Office User 24/8/2018 8:15
Eliminado: ic

Núria Casacuberta 14/8/2018 9:27
Eliminado: and

Microsoft Office User 24/8/2018 8:16
Eliminado: can

Núria Casacuberta 14/8/2018 9:29
Con formato: Subíndice

Núria Casacuberta 14/8/2018 9:29
Con formato: Superíndice

Microsoft Office User 21/8/2018 11:39
Eliminado: (global fallout, GF) carried out

Microsoft Office User 22/8/2018 11:15
Eliminado: allow understanding

Núria Casacuberta 14/8/2018 9:29
Eliminado: chlorofluorocarbons

Núria Casacuberta 14/8/2018 9:29
Con formato: Superíndice

Núria Casacuberta 14/8/2018 9:29
Eliminado: tritium

María Isabel García Ib..., 13/8/2018 18:35
Eliminado: -

María Isabel García Ib..., 13/8/2018 18:35
Eliminado: has

María Isabel García Ib..., 13/8/2018 18:36
Eliminado:

Microsoft Office User 14/7/2018 11:10
Movido (inserción) [2]

Microsoft Office User 14/7/2018 11:10
Eliminado: Artificial radionuclides from NRPs (e.g., ^{137}Cs, ^{99}Tc, ^{129}I, ^3H etc.) have been used to investigate the spreading of AW through the Nordic Seas into the Arctic Ocean, and ultimately to the western North Atlantic Ocean

Beasley et al., 1998; Casacuberta et al., 2016, 2018; Christl et al., 2015b; Dahlgaard, 1995; Edmonds et al., 2001; Holm et al., 1983; Smith et al., 1998, 2005, 2011, 2016). The schematic transport of NRP effluents and water masses in the SPNA-Artic Ocean region is displayed in Figure 1. NRP-labelled AWs are first transported by surface currents into the North Sea and then carried poleward by the Norwegian Coastal Current (NCC) into the Nordic Seas (Edmonds et al., 1998; Raisbeck and Yiou, 2002) while mixing with the Norwegian Atlantic Current (NwAC) (Gascard et al., 2004; Kershaw and Baxter, 1995). The current splits in two branches north of Norway, one branch entering the Barents Sea as Barents Sea Branch Water (BSBW) and the other branch approaching the Fram Strait west of Spitsbergen where it bifurcates again. One branch joins the East Greenland Current (EGC) and recirculates southwards as Return Atlantic Water (RAW) (Fogelqvist et al., 2003) mixing with IrSPMW and PIW (modified AW that has recirculated in the Arctic Ocean; Rudels et al., 1999b). The other branch, the West Spitsbergen Current (WSC), transports the remaining AWs at shallow to intermediate depths into the Arctic Ocean via the Fram Strait Branch Water (FSBW), where they recirculate in the Arctic Eurasian Basin before outflowing back through the Fram Strait and continuing southwards carried by the EGC (Rudels, 2015). The NRP signal also penetrates deep in the water column due to the formation of dense water north of the Greenland-Iceland and Iceland-Scotland passages, providing means of tracing the deep overflows that ventilate the deep North Atlantic Ocean (e.g. Smith et al., 2005). Thus, radionuclides discharged from European NRPs are particularly well suited for studying the water mass circulation in the SPNA (Figure 1).

Among the set of radionuclides discharged from NRPs, the ^{129}I is regarded as a robust circulation tracer for investigating water mass transport pathways, advection and mixing, and for testing the performance of ocean circulation models in the Nordic Seas, the Arctic Ocean and the Atlantic Ocean (Karcher et al., 2012; Orre et al., 2010; Smith et al., 2016). Firstly, ^{129}I can be detected at all oceanic levels far away from the source thanks to its conservative behaviour in seawater, its long half-life ($T_{1/2}$ = 15.7 Ma) and the low detection limits obtained with accelerator mass spectrometry (AMS) (e.g. Vockenhuber et al., 2015). Secondly, the presence of ^{129}I in those regions is dominated by the liquid discharge from European NRPs, which has a well-documented release history (> 5700 kg; He et al., 2013a; Raisbeck et

Eliminado:
María Isabel García Ib..., 13/8/2018 18:30
Con formato ... [24]
Marcus Christl 15/8/2018 14:05
Eliminado: are represented
Núria Casacuberta 14/8/2018 9:32
Eliminado: and explained in the following
Microsoft Office User 14/7/2018 11:10
Subido [2]: Artificial radionuclides from ... [25]
María Isabel García Ib..., 13/8/2018 18:36
Eliminado: t
María Isabel García Ib..., 13/8/2018 18:37
Eliminado: are ...arried poleward by the ... [27]
María Isabel García Ib..., 13/8/2018 18:30
Con formato ... [26]
Microsoft Office User 20/8/2018 10:50
Eliminado:)
María Isabel García Ib..., 13/8/2018 18:41
Eliminado: – ...celand and Iceland- – ... [28]
Microsoft Office User 14/7/2018 11:14
Eliminado:
Microsoft Office User 15/7/2018 12:22
Con formato ... [29]
María Isabel García Ib..., 13/8/2018 18:30
Con formato ... [30]
Microsoft Office User 24/8/2018 8:18
Eliminado: uite
Núria Casacuberta 14/8/2018 9:46
Eliminado: odine-129
María Isabel García Ib..., 13/8/2018 18:43
Eliminado: ($T_{1/2}$ = 15.7 Ma)
Núria Casacuberta 14/8/2018 9:46
Con formato ... [31]
Microsoft Office User 14/7/2018 14:29
Movido (inserción) [4] ... [32]
Microsoft Office User 14/7/2018 14:49
Eliminado: the Arctic and Atlantic Ocean ... [33]
María Isabel García Ib..., 13/8/2018 18:44
Eliminado: the
Microsoft Office User 14/7/2018 14:06
Movido (inserción) [3] ... [34]
Microsoft Office User 14/7/2018 14:38
Eliminado: ,
Microsoft Office User 15/7/2018 14:39
Con formato ... [35]
María Isabel García Ib..., 13/8/2018 18:45
Eliminado: ,
Microsoft Office User 15/7/2018 14:39
Con formato ... [36]

al., 1995), while the contribution from GF is comparably negligible (~ 90 kg worldwide release; Hou, 2004; Raisbeck and Yiou, 1999; Wagner et al., 1996). Consequently, the seawater affected by NRPs may present ^{129}I concentrations 1 – 4 orders of magnitude above the background due to GF (~ 2.5 × 10^{7} at/kg; Edmonds et al., 1998). In the western SPNA, most of the ^{129}I is nowadays present in the EGC flowing on the Greenland Shelf (Alfimov et al., 2004) and in the Denmark Strait Overflow Water (DSOW) that fills bottom depths of the Irminger and Labrador Seas (Smith et al., 2005, 2016). The other overflow water, ISOW, enters the North Atlantic through the Iceland-Scotland Sill (Hansen and Osterhus, 2000) and is present notably along the Reykjanes Ridge or overlying DSOW in the Irminger and Labrador Seas. ISOW carries comparably less ^{129}I (Edmonds et al., 2001), yet its ^{129}I concentrations at the sill have increased 900 % over the last 20 years (Alfimov et al., 2013; Edmonds et al., 2001; Vivo-Vilches et al., 2018) implying that this tracer may also provide a chronological marker for spreading pathways of such overflow water in the eastern SPNA.

Uranium-236 ($T_{1/2}$ = 23.5 Ma) is a long-lived conservative radionuclide similar to ^{129}I and a novel ocean circulation tracer investigated in the last decade (e.g. Casacuberta et al., 2014, 2016, 2018; Castrillejo et al., 2017; Christl et al., 2012; Sakaguchi et al., 2012; Winkler et al., 2012). Surface seawaters in the northern hemisphere present ^{236}U/^{238}U atom ratios of about 1000 × 10^{-12} (e.g. Christl et al., 2012) in the unique presence of GF (about 900 kg released worldwide; Sakaguchi et al., 2009). However, the ^{236}U/^{238}U ratios can be significantly higher in the Arctic and North Atlantic Oceans due to the liquid discharge of ^{236}U from European NRPs (about 100 kg, Christl et al., 2015a). This made possible tracing the waters carrying NRP-^{236}U with ^{236}U/^{238}U ratios up to 3800 × 10^{-12} in the Arctic Ocean in 2011 – 2012 (Casacuberta et al., 2016), and up to 1400 × 10^{-12} in LSW and DSOW in the western SPNA in 2010 (Casacuberta et al., 2014). In addition, both ^{236}U and ^{129}I can be combined as the dual tracer, ^{129}I/^{236}U - ^{236}U/^{238}U, to identify the radionuclide source(s) present in a given water mass (Casacuberta et al., 2016; Christl et al., 2015b). This is possible because the GF and the European NRPs introduced different amounts of ^{236}U and ^{129}I (see above) into the environment and tagged the waters with characteristic ^{129}I/^{236}U and ^{236}U/^{238}U atom ratios depending on the proximity from the source(s)

Con formato ... [37]
Núria Casacuberta 14/8/2018 9:47
Con formato ... [38]
Microsoft Office User 14/7/2018 14:13
Eliminado: regarded as a tracer particular ... [40]
Microsoft Office User 15/7/2018 14:39
Con formato ... [39]
María Isabel García Ib..., 13/8/2018 18:44
Eliminado: … … orders of magnitude ab ... [41]
Microsoft Office User 20/8/2018 10:52
Eliminado: …g^{-1}… Edmonds et al., 1998 ... [42]
Microsoft Office User 14/7/2018 14:06
Subido [3]: long half-life and the low det ... [43]
Microsoft Office User 9/8/2018 10:16
Eliminado: (Figure 1)… most of the ^{129}I i ... [44]
Microsoft Office User 15/7/2018 12:22
Con formato ... [45]
Microsoft Office User 7/8/2018 15:22
Eliminado: carrying…comparably less ^{129} ... [46]
Unknown
Código de campo cambiado ... [47]
Microsoft Office User 9/8/2018 10:18
Eliminado: ….Therefore, ^{129}I …ay also pr ... [48]
Microsoft Office User 14/7/2018 15:00
Eliminado: The East Greenland Current (E ... [49]
Microsoft Office User 15/7/2018 12:24
Con formato ... [50]
Microsoft Office User 15/7/2018 12:33
Con formato ... [51]
Microsoft Office User 15/7/2018 14:20
Eliminado:
Microsoft Office User 15/7/2018 12:35
Movido (inserción) [6] ... [52]
Unknown
Código de campo cambiado ... [53]
María Isabel García Ib..., 13/8/2018 18:30
Con formato ... [54]
Microsoft Office User 15/7/2018 14:39
Con formato ... [55]
Microsoft Office User 14/7/2018 15:35
Eliminado: Similar to ^{129}I, the presence of ... [56]
Microsoft Office User 9/8/2018 10:23
Con formato ... [57]
María Isabel García Ib..., 13/8/2018 18:46
Eliminado: ,
Microsoft Office User 9/8/2018 10:23
Con formato ... [58]
Microsoft Office User 14/7/2018 15:35
Eliminado:)
María Isabel García Ib..., 13/8/2018 18:46
Eliminado: -
Microsoft Office User 14/7/2018 16:19
Movido (inserción) [5] ... [59]
Microsoft Office User 14/7/2018 15:50
... [60]
Microsoft Office User 15/7/2018 12:35
... [61]
Microsoft Office User 14/7/2018 16:47
... [62]
Microsoft Office User 14/7/2018 16:19
Microsoft Office User 9/8/2018 11:27
... [63]
Microsoft Office User 9/8/2018 10:25
Movido (inserción) [12] ... [64]
María Isabel García Ib..., 13/8/2018 18:48
Microsoft Office User 15/7/2018 14:28
... [65]
Microsoft Office User 9/8/2018 10:25
... [66]

Consequently, this dual tracer could also help to better understand the mixing in the SPNA between AWs tagged by European NRPs and water masses carrying mainly GF (e.g. Arctic-Canadian water).

In this study, we aim at using artificial ^{129}I and ^{236}U to investigate the transport pathways and time scales of water mass circulation in the SPNA. To this end, we present the first simultaneous distribution of ^{129}I and ^{236}U along the GEOVIDE cruise track in spring 2014 (Figure 1). The study pursues three specific objectives. Firstly, we study the zonal distribution of ^{129}I and ^{236}U and their relationship with the water mass structure. Although the distribution of ^{129}I in the Irminger and Labrador Seas has been well studied in the last 30 years, there is a significant data gap east of the Reykjanes Ridge for ^{129}I, and for most of the section for ^{236}U. Secondly, we use the dual $^{129}I/^{236}U$ - $^{236}U/^{238}U$ tracer approach to distinguish the sources contribution to the presence of ^{129}I and ^{236}U in the SPNA. This information is then valuable to study the origin, mixing and spreading pathways of water masses participating in the AMOC. The combined use of ^{129}I and ^{236}U allows tracing circulation features that received significant attention in earlier modelling, tracer and physical studies, and helps to validate recent interpretations on the ventilation of the North Atlantic by overflow waters. Thirdly, tracer data from 2014 are combined with the extensive ^{129}I time series in the central Labrador Sea to further investigate the circulation time scales of AWs downstream of European NRPs.

2 Materials and methods

2.1 The cruise, study area and sample collection

The GEOVIDE cruise (Figure 1) covered the OVIDE line from Lisbon (Portugal) to the southern tip of Greenland (Cape Farewell), and from Cape Farewell to St. John's (Newfoundland, Canada) onboard the French *R/V Pourquoi pas?* between May 15th and June 30th, 2014. This cruise is part of the GEOTRACES program (section GA01: http://www.geotraces.org/cruises/cruise-summary) and contributes from a geochemical perspective to the decade-long biannual sampling (2002 to 2018) of the OVIDE line (http://www.umr-lops.fr/Projets/Projets-actifs/OVIDE).

Microsoft Office User 15/7/2018 14:33
Movido (inserción) [7]

Núria Casacuberta 14/8/2018 9:50
Eliminado: ing

Microsoft Office User 15/7/2018 14:34
Eliminado: origin and mixing of water mass

Microsoft Office User 9/8/2018 10:25
Con formato: Sin Resaltar

Microsoft Office User 9/8/2018 10:25
Con formato: Sin Resaltar

Microsoft Office User 15/7/2018 14:33
Subido [7]: better understanding the origin and mixing of water masses in the SPNA.

Microsoft Office User 9/8/2018 10:25
Con formato: Sin Resaltar

Microsoft Office User 15/7/2018 14:35
Eliminado: es in the SPNA. The information on the source is important to identify circulation features as, for example, the exchange between the Nordic Seas and the Arctic Ocean (Casacuberta et al., in prep.; Wefing et al., in prep.). Thus, new measurements of both ^{129}I and ^{236}U should help

María Isabel García Ib..., 13/8/2018 18:49
Eliminado: and

Microsoft Office User 9/8/2018 11:28
Con formato: Sin Resaltar

Microsoft Office User 9/8/2018 11:09
Eliminado: In this study, we present the distribution of ^{129}I and ^{236}U along the GEOVIDE transect (GEOTRACES GA01) from Portugal to Newfoundland in spring 2014. The ^{129}I concentrations are used alone or in combination with ^{236}U to investigate the influence from anthropogenic sources and to infer the composition, origin and spreading pathways of water masses in the SPNA. Finally, the 2014 data are compared to earlier ^{129}I observations to estimate circulation timescales of AWs tagged with reprocessing ^{129}I into the Labrador Sea.

Microsoft Office User 20/8/2018 11:07
Eliminado: 6

Microsoft Office User 7/8/2018 11:39
Eliminado: ... [67]

Microsoft Office User 14/7/2018 9:58
Bajado [1]: The water mass structure during GEOVIDE was assessed using an extended Optimum Multi-Parameter analysis (OMP) by García-Ibáñez et al. (2018). The water masses dominating the upper water column were Central Waters represented by the East North Atlantic Central Water (ENACW), and SPMW, while LSW was the most abundant water mass at intermediate depths. Deeper parts were filled, from west ... [68]

This study is based on concentrations of ^{129}I and ^{236}U, and on $^{236}U/^{238}U$ ratios determined in about 150 seawater samples collected from 14 depth profiles (Figure 1) using a rosette equipped with conductivity-temperature-depth sensors and 24 Niskin bottles of 12 L each. Sampling depths were chosen to collect water from the main water masses and circulation features at each station by considering conductivity, temperature and oxygen profiles. From east to west (Figure 1), depth profiles were located in the West European Basin (WEB: stations 1, 13, 21 and 26), the central Icelandic Basin (station 32), above the Reykjanes Ridge (station 38), the Irminger Sea (stations 44 and 60), the Labrador Sea (stations 64, 69 and 77), and on the shelf/slope of Greenland (stations 53 and 61) and Canada (station 78). Additional surface samples were obtained using a 'FISH' device that allowed the collection of seawater from about 2 m depth at 8 locations placed between depth profiles. Samples for ^{129}I of ~ 0.5 L were collected in dark plastic bottles and sealed with parafilm. The ^{236}U samples of 5 – 7 L were collected in plastic cubitainers. Bottles and cubitainers were rinsed 3 times with seawater before sample collection to avoid potential contamination.

Marcus Christl 15/8/2018 14:14
Eliminado: data

Microsoft Office User 22/8/2018 11:16
Eliminado: ,

Marcus Christl 15/8/2018 14:14
Eliminado: and

Marcus Christl 15/8/2018 14:15
Eliminado:

Microsoft Office User 20/8/2018 10:34
Con formato: Superíndice

Microsoft Office User 20/8/2018 10:34
Con formato: Superíndice

Microsoft Office User 10/8/2018 10:39
Eliminado: Niskin bottles

Núria Casacuberta 14/8/2018 10:05
Eliminado: each

María Isabel García Ib..., 13/8/2018 18:50
Eliminado: -

Núria Casacuberta 14/8/2018 10:05
Eliminado: each

2.2 Iodine-129 purification and AMS measurement

The radiochemistry of ^{129}I was done following a method described in Michel et al. (2012) at EAWAG (Switzerland). About 300 – 450 mL of sample was spiked with ~ 1.5 mg of Woodward stable iodine (^{127}I) carrier. All iodine was oxidized to iodate adding 2 % $Ca(ClO)_2$, then reduced to iodide using $Na_2S_2O_5$ and 1 M $NH_3O{\cdot}HCl$. The purification of iodine was carried out using columns filled with DOWEX® 1 × 8 ion exchange resin. The column was conditioned with deionized water and diluted KNO_3 solution before the elution of iodine with 2.25 M KNO_3 solution. The iodine was precipitated as AgI by adding $AgNO_3$, then mixed with 4 - 5 mg of Ag and pressed into AMS cathodes. The compact 0.5 MV Tandy AMS system at ETH-Zurich was used to measure the $^{129}I/^{127}I$ atom ratios (Vockenhuber et al., 2015). The $^{129}I/^{127}I$ ratios were normalized with the ETH-Zurich in-house standard D22 with a nominal $^{129}I/^{127}I$ value of $(50.35 \pm 0.16) \times 10^{-12}$ (Christl et al., 2013b). Radiochemistry blanks (n = 24) were prepared with deionized water and processed together with seawater samples following the same analytical procedures. These blanks presented $^{129}I/^{127}I$ ratios of $(0.7 – 4) \times 10^{-13}$ corresponding to (0.5 –

Marcus Christl 15/8/2018 14:15
Eliminado: the

Marcus Christl 15/8/2018 14:15
Eliminado: in the laboratory

María Isabel García Ib..., 13/8/2018 18:50
Eliminado: -

María Isabel García Ib..., 13/8/2018 18:50
Eliminado: -

3) × 10^6 atoms of ^{129}I. The ^{129}I concentrations were calculated based on measured $^{129}I/^{127}I$ ratio and the know amounts of ^{127}I carrier added to each sample. The detection limit of < 0.3 fg ^{129}I depended on the measured $^{129}I/^{127}I$ ratio of the Woodward iodine carrier which is typically at the order of ~ 10^{-13}.

María Isabel García Ib..., 13/8/2018 18:50
Eliminado: -

2.3 Uranium-236 purification and AMS measurement

Each seawater sample (5 – 7 L) was weighed, acidified to pH below 2 using concentrated suprapure HNO_3 and spiked with ~ 3 pg of ^{233}U (IRMM - 051). The uranium was co-precipitated with iron hydroxides upon addition of ~ 200 mg of U-free Fe^{2+} solution and concentrated suprapure NH_4OH by rising the pH to ~ 8. The iron precipitate was syphoned, evaporated to dryness and re-dissolved using 8 M HNO_3. The purification of uranium was carried out using UTEVA columns (Triskem). The eluate was co-precipitated with ~ 1 mg of the U-free Fe^{2+} solution and evaporated to dryness. All uranium was converted to oxide form by heating the iron precipitates to 650 ºC, then mixed with 2 – 3 mg of niobium and pressed into AMS cathodes. The compact 0.5 MV Tandy AMS system at ETH-Zurich was used to measure ^{233}U, ^{236}U and ^{238}U following Christl et al. (2013a). The measured $^{236}U/^{233}U$ and $^{236}U/^{238}U$ ratios were normalized to the ZUTRI ETH-Zurich in-house standard with nominal values of (4055 ± 200) × 10^{-12} and (33170 ± 830) × 10^{-12}, respectively (Christl et al., 2013a). Radiochemistry blanks (n = 19) were prepared onboard and in the land-based laboratory with deionized water and processed together with seawater samples following same analytical procedures. The blanks presented $^{236}U/^{233}U$ ratios < 10^{-4}, corresponding to < 40 ag of ^{236}U. The compact TANDY AMS system has an abundance mass sensitivity of ~ 10^{-12} for the mass range of actinides, corresponding to an estimated instrumental background level at the order of $^{236}U/^{238}U$ ~ 10^{-14}. Due to a mistake in the laboratory, a total of 34 samples were accidentally cross-contaminated with a very high ^{236}U standard and therefore had to be background corrected for cross talk. The uncertainty of this additional background correction led to higher errors reported for those samples (marked with '*' in Table 2).

María Isabel García Ib..., 13/8/2018 18:51
Eliminado: -

María Isabel García Ib..., 13/8/2018 18:51
Eliminado: -

3 Results and discussion

3.1 Water mass structure in 2014

The water mass structure in spring 2014 is described using the zonal sections for salinity, potential temperature and dissolved oxygen concentrations (Figure 2) to facilitate the understanding of ^{129}I and ^{236}U distributions in section 3.2. The assessment of the water mass structure from GEOVIDE was performed using an extended Optimum Multi-Parameter analysis (OMP) (further details are found in García-Ibáñez et al. 2018).

In the upper water column (< 500 m), warm and saline Central Waters dominate the eastern part of the section between the coast off Portugal and station 26 (Figures 2A and 2B). Central waters (or East North Atlantic Central Water, ENACW) are characterized by the highest potential temperatures and relatively high salinities as they have been transported from subtropical latitudes into the eastern part of the section by the northeast-flowing branches of the NAC. Part of ENACW recirculates into the Iceland Basin and the Irminger Sea, where air-sea fluxes transform them into colder and fresher SPMWs (McCartney and Talley, 1982) that occupy equivalent depths between the Subarctic Front (SAF; roughly at 22.5 °W, station 26) and Greenland (Figure 2A and 2B). The upper water column on the continental shelves and slopes of Greenland and Canada is occupied by PIW, which presents very low salinities (< 34) and potential temperatures usually < 0 ºC (Figures 2A and 2B). PIW originates from the Arctic Ocean, enters through the Fram (PIW-Atlantic) and Nares Straits (PIW-Canada), and joins the shallow western boundary transport in the EGC and LC (Figure 1).

At intermediate depths, LSW is the most abundant water mass and fills the entire section from the upper water-levels to about 2000 m depth (Figure 2). LSW is formed in the Labrador Sea and, to less extent, in the Irminger Sea by transformation of SPMWs via winter convection (e.g., Jong and Steur, 2016). Then, it flows south as part of the DBWC (e.g. Bersch et al., 2007) or east into the Irminger, Iceland and West European Basins (Figure 1). LSW is characterized by a relative minimum in salinity (< 34.9) and temperature (~ 3 ºC) at its formation region, and warmer and saltier values as it mixes with surrounding waters along its equatorward and eastward transport (Figures 2A and 2B). Station 26 is also

María Isabel García Ib…, 13/8/2018 18:52
Eliminado: helped with Figure 2 and
Microsoft Office User 7/8/2018 16:22
Con formato: Normal
Núria Casacuberta 14/8/2018 10:11
Eliminado: For a thorough
Microsoft Office User 14/7/2018 9:58
Movido (inserción) [1]
Microsoft Office User 7/8/2018 11:46
Eliminado: T…e water mass structure fro ... [69]
Microsoft Office User 7/8/2018 16:22
Con formato: Fuente: (Predeterminado) Times New Roman
Núria Casacuberta 14/8/2018 10:11
Eliminado: , please read
Microsoft Office User 7/8/2018 11:50
Eliminado: by…García-Ibáñez et al. (…(... [70]
Microsoft Office User 7/8/2018 16:22
Con formato: Fuente: (Predeterminado) Times New Roman, Negrita
Microsoft Office User 7/8/2018 16:03
Eliminado: The water masses dominating the upper water column were Central Waters represented by the East North Atlantic Central Water (ENACW), and SPMW, while LSW was the most abundant water mass at intermediate depths. Deeper parts were filled, from west to east, by DSO ... [71]
Microsoft Office User 7/8/2018 16:22
Con formato ... [72]
María Isabel García Ib…, 13/8/2018 18:53
Eliminado:
Microsoft Office User 7/8/2018 16:22
Con formato ... [73]
María Isabel García Ib…, 13/8/2018 18:54
Eliminado: s
Microsoft Office User 7/8/2018 16:22
Con formato ... [74]
María Isabel García Ib…, 13/8/2018 18:54
Eliminado: Shallow…he upper water colu ... [75]
Microsoft Office User 7/8/2018 16:22
Con formato: Inglés (británico)
María Isabel García Ib…, 13/8/2018 18:56
Eliminado: the …SW is the most abundar ... [76]
Microsoft Office User 20/8/2018 11:15
Eliminado: through …ia winter convectio ... [77]
María Isabel García Ib…, 13/8/2018 18:57
Eliminado: by winter convection …ADD ... [78]

affected by the Subarctic Intermediate Water (SAIW), which presents lower salinities (~ 34.9) and potential temperatures (4 – 7 ºC) than the other water masses surrounding it at similar depths, i.e. ENACW and SPMW from the Iceland Basin (IcSPMW), respectively (Figures 2A and 2B). SAIW forms in the western boundary of the SPNA (i.e. the LC) by mixing between LSW and subtropical waters carried by the NAC (Arhan, 1990; Read, 2000), before subducting at about 400 m depth and being advected within the northern branch of NAC (Figure 2). Depths around 1000 m in the WEB (stations 1 and 13) are also influenced by the northward-flowing Mediterranean Water (MW) (Figure 1) which is characterized by a maximum in salinity (> 36) and minimum in oxygen (~ 180 µmol/kg) (Figures 2A and 2C).

In the deep-water column (> 2000 m), the lower North East Atlantic Deep Water ($NEADW_L$) dominates the section in the WEB (east of 20 ºW), while in the western part, the most abundant water masses are the dense overflow waters. $NEADW_L$ is generally saltier, colder and older than the overlying LSW due to the major contribution of the northward flowing Antarctic Bottom Water (AABW) (Figures 2A – 2C). Dense overflow waters dominate the bottom depths on both sides of the Reykjanes Ridge and in the Irminger and Labrador Seas (Figure 1). ISOW is best identified thanks to its local salinity maximum (~ 34.92) on the flanks of the Reykjanes Ridge and between the LSW and DSOW in the Irminger and Labrador Seas (Figure 2A). This water mass is produced by mixing of old Norwegian Sea waters that overflow the Iceland–Scotland Sill and entrain SPMW and LSW in the SPNA (e.g., van Aken and De Boer, 1995). ISOW mainly flows along the eastern flank of the Reykjanes Ridge into the Irminger and Labrador Seas (Figure 1), yet increasing studies point towards the eastward return flow of this water mass through passages in the Mid Atlantic Ridge (Xu et al., 2018) or directly along the flanks of the Rockall Through into the eastern part of the GEOVIDE section (e.g. Zou et al., 2017) (Figure 1). Finally, DSOW is present between ISOW and the seafloor in the Irminger and Labrador Seas (notably stations 44 and 69). This overflow water can be distinguished from ISOW by its lower salinities (< 34.90), potential temperatures (< 2 ºC) and higher oxygen concentration (> 290 µmol/kg) (Figures 2A – 2C) due to the more recent ventilation and rapid advective flow of DSOW from the formation region north of the Denmark Strait into the GEOVIDE section (e.g. Read, 2000) (Figure 1).

Eliminado: … …ºC) than the other wate ... [79]
Microsoft Office User 20/8/2018 11:19
Eliminado:
María Isabel García Ib..., 13/8/2018 19:00
Eliminado: /
Microsoft Office User 20/8/2018 11:20
Eliminado: $^{-1}$
María Isabel García Ib..., 13/8/2018 19:00
Eliminado: a
Microsoft Office User 7/8/2018 16:22
Con formato ... [80]
María Isabel García Ib..., 13/8/2018 19:00
Eliminado: lower
Microsoft Office User 7/8/2018 16:22
Con formato ... [81]
María Isabel García Ib..., 13/8/2018 19:01
Eliminado: less well ventilated…lder than ... [82]
Microsoft Office User 7/8/2018 16:22
Con formato ... [83]
Microsoft Office User 7/8/2018 15:28
Movido (inserción) [9] ... [84]
Marcus Christl 15/8/2018 14:27
Eliminado: relative
Microsoft Office User 7/8/2018 16:22
Con formato ... [85]
Marcus Christl 15/8/2018 14:27
Eliminado: a
Microsoft Office User 7/8/2018 16:22
Con formato ... [86]
María Isabel García Ib..., 13/8/2018 19:02
Eliminado: that
Microsoft Office User 7/8/2018 16:22
Con formato ... [87]
Microsoft Office User 7/8/2018 15:34
Eliminado: which receive direct radionucl ... [88]
Microsoft Office User 7/8/2018 16:22
Con formato ... [89]
María Isabel García Ib..., 13/8/2018 19:02
Eliminado: entrain
Microsoft Office User 7/8/2018 16:22
Con formato ... [90]
Microsoft Office User 7/8/2018 15:34
Eliminado: , ISOW…flows southwest thr ... [91]
María Isabel García Ib..., 13/8/2018 19:02
Eliminado: the …SOW and the seafloorb ... [92]
Microsoft Office User 20/8/2018 11:26
Eliminado:
María Isabel García Ib..., 13/8/2018 19:03
Eliminado: /
Microsoft Office User 20/8/2018 11:26
Eliminado: $^{-1}$
María Isabel García Ib..., 13/8/2018 19:03
... [93]

3.2 The relationship of ^{129}I and ^{236}U with water masses in 2014

The concentrations of ^{129}I and ^{236}U, and atom ratios of ^{236}U/^{238}U and ^{129}I/^{236}U are reported in Table 2. Detailed depth profiles for these radionuclides are displayed along with salinity, potential temperature and dissolved oxygen concentrations in the Supporting Information (Figure S1). The ^{129}I concentrations range from (0.20 ± 0.20) × 10^{7} to (256 ± 4) × 10^{7} at/kg. The ^{236}U/^{238}U ratios range from (40 ± 20) × 10^{-12} to (2350 ± 370) × 10^{-12}. The ^{129}I/^{236}U ratios range from 0.50 ± 0.50 to 200 ± 60.

The results from this study are best described in relation to the water mass structure described in section 3.1, which has been represented with overlaid isohalines on the radionuclide distribution plots (Figure 3). The ^{129}I concentrations (Figure 3A) and ^{236}U/^{238}U ratios (Figure 3B) are generally higher west of ~ 25 °W in southward flowing waters than in northward flowing low-latitude waters dominating the eastern SPNA. This is also clear when comparing tracer values of stations 1 - 26 with those from stations 32 - 78 (Table 2). Such general radionuclide distribution is largely due to the fact that southward flowing northern waters are located downstream of Sellafield and La Hague, and therefore present additional radionuclide contributions (especially for ^{129}I) from these facilities. The highest ^{129}I concentrations (~ 250 × 10^{7} at/kg) and ^{236}U/^{238}U ratios (~ 2300 × 10^{-12}) are present in PIW and RAW carried by the EGC and LC over the shelves and slopes of Greenland and Canada. This water admixture, largely influenced by NRPs (e.g. Alfimov, 2004), can mix with DSOW precursor waters through winter convection in the Greenland Sea (e.g. Gascard et al., 2002) or directly intrude DSOW by cascading in the Labrador Sea (e.g. Falina et al., 2012). Consequently, the DSOW core, found at the lowermost 100 m in the Irminger and Labrador Seas, presents ^{129}I concentrations in the (85 – 100) × 10^{7} at/kg range and ^{236}U/^{238}U ratios of (1300 – 2300) × 10^{-12}, which is in agreement with high radionuclide levels previously reported for DSOW (Casacuberta et al., 2014; Orre et al., 2010; Smith et al., 2005, 2016). Intermediate ^{129}I concentrations ((5 – 50) × 10^{7} at/kg) and ^{236}U/^{238}U ratios ((500 – 1500) × 10^{-12}) characterize the water masses filling most of the remaining GEOVIDE section. In the upper 500 m, ENACWs record rather uniform ^{129}I concentrations (~ 10 × 10^{7} at/kg) and ^{236}U/^{238}U ratios (~ 1000 × 10^{-}

Microsoft Office User 7/8/2018 15:46
Eliminado: filling depths between LSW and DSOW (García-Ibáñez et al., 2018). ISOW may also enter the eastern SPNA entraining SPMW and LSW to form NEADW (e.g., van Aken and De Boer, 1995).

Microsoft Office User 7/8/2018 16:22
Con formato ... [94]

Microsoft Office User 14/7/2018 9:56
Eliminado: 1 Concentrations of ^{129}I, ator ... [95]

Microsoft Office User 20/8/2018 11:28
Eliminado: /kg^{-1}

Microsoft Office User 24/8/2018 8:31
Eliminado: reported

Núria Casacuberta 14/8/2018 11:07
Eliminado: .

Microsoft Office User 7/8/2018 16:47
Eliminado: by García-Ibáñez et al., (2018 ... [96]

María Isabel García Ib..., 13/8/2018 19:04
Eliminado: S…ations 1 - 26 on one hand. ... [97]

Microsoft Office User 20/8/2018 11:33
Eliminado: at /kg^{-1}… and ^{236}U/^{238}U ratios ... [98]

Microsoft Office User 7/8/2018 17:02
Con formato: Sin Resaltar

Microsoft Office User 7/8/2018 16:48
Eliminado: along the

María Isabel García Ib..., 13/8/2018 19:05
Eliminado: … ... [99]

Microsoft Office User 20/8/2018 11:34
Eliminado: at /kg^{-1}

María Isabel García Ib..., 13/8/2018 19:05
Eliminado: … …300) × 10^{-12}, which is ... [100]

Microsoft Office User 7/8/2018 17:10
Eliminado: in earlier studies

María Isabel García Ib..., 13/8/2018 19:04
Eliminado: … ... [101]

Microsoft Office User 20/8/2018 11:34
Eliminado: at/ kg^{-1}

María Isabel García Ib..., 13/8/2018 19:05
Eliminado: … ... [102]

Microsoft Office User 20/8/2018 11:34
Eliminado: at/ kg^{-1}

^{12}) in the WEB (stations 1 to 21). The ^{129}I concentrations of SPMWs located further west almost double those of ENACW (^{236}U/^{238}U ratios are similar), indicating that ENACW may be influenced by effluents from NRPs while recirculating in the northern SPNA or in the Nordic Seas. SAIW also presents relatively high ^{129}I concentrations (~ 20 × 10^7 at/kg) at stations 26 and 32, probably because of the influence of waters carried by the LC. The 500 – 2000 m layer is dominated by LSW, which displays a wide range of ^{129}I concentrations ((5 – 50) × 10^7 at/kg) and ^{236}U/^{238}U ratios ((700 – 1250) × 10^{-12}), with values decreasing downstream from its formation regions, the Labrador and Irminger Seas. Similar depths are also influenced by MW (stations 1 and 13), yet, its ^{129}I concentrations (~ 3 × 10^7 at/kg) and ^{236}U/^{238}U ratios (~ 1000 × 10^{-12}) in 2014 were significantly lower than average ^{129}I concentrations (9 × 10^7 at/kg) and ^{236}U/^{238}U ratios (1600 × 10^{-12}) reported in the outflow region of MW at the Strait of Gibraltar in 2013 (Castrillejo et al., 2017). Thus, 2014 data probably reflects the dilution of MW, which is largely affected by inputs from the Marcoule nuclear facility (Castrillejo et al., 2017), with old LSW and SPMW carrying a diluted NRP signal. The deeper parts of the section west of 20 °W and below 2000 m are influenced by ISOW, which is characterized by relatively high ^{129}I concentrations ((10 – 70) × 10^7 at/kg) and ^{236}U/^{238}U ratios ((900 – 1700) × 10^{-12}). The lowest ^{129}I concentrations ((0.2 – 2.0) × 10^7 at/kg) and ^{236}U/^{238}U ratios ((40 – 350) × 10^{-12}) are found at depths greater than 2000 m in the WEB and are associated with NEADW$_L$ (stations 1 to 13).

The distribution of ^{129}I/^{236}U (Figure 3C) is notably driven by ^{129}I concentrations, which display a greater range (3 orders of magnitude) than the ^{236}U/^{238}U ratios (2 orders of magnitude). As noted before, this is probably due to the influence of NRPs, which released about 60 times more mass of ^{129}I than of ^{236}U to the North Atlantic (further discussion in section 3.3). Thus, following the ^{129}I patterns described above, the ^{129}I/^{236}U ratios are particularly high (> 20) in the western part of the section and particularly contrasted in the Irminger and Labrador Seas as discussed in section 3.3 (Figure 3C). The highest ^{129}I/^{236}U ratios (> 100) are present in waters transported by the shallow EGC and LC. Overflow waters are also distinguished by their relatively high ^{129}I/^{236}U ratios (60 to 110 for DSOW, 15 to 40 for ISOW).

Eliminado: . ENACWs are carried by the ... [103]
María Isabel García Ib..., 13/8/2018 19:11
Eliminado: SPMWs located further west ... [104]
Microsoft Office User 21/8/2018 12:05
Eliminado: is…almost double those of I ... [105]
María Isabel García Ib..., 13/8/2018 19:13
Eliminado: … ... [106]
Microsoft Office User 7/8/2018 14:00
Eliminado: Consequently, LSW
María Isabel García Ib..., 13/8/2018 19:05
Eliminado: … ... [107]
Microsoft Office User 21/8/2018 11:12
Eliminado: at/ kg^{-1}
María Isabel García Ib..., 13/8/2018 19:05
Eliminado: … …250) × 10^{-12}), with val ... [108]
Microsoft Office User 7/8/2018 17:24
Eliminado: Mediterranean Water (…W) ... [109]
María Isabel García Ib..., 13/8/2018 19:13
Eliminado: ….yY ... [110]
Microsoft Office User 7/8/2018 17:28
Eliminado: with ^{129}I concentrations (of ... [111]
María Isabel García Ib..., 13/8/2018 19:14
Eliminado: s… which are ... [112]
Microsoft Office User 7/8/2018 17:32
Eliminado: less ^{129}I and ^{236}U than MW. ... [113]
María Isabel García Ib..., 13/8/2018 19:06
Eliminado: … ... [114]
María Isabel García Ib..., 13/8/2018 19:06
Eliminado: /
Microsoft Office User 21/8/2018 12:08
Eliminado: …t/kgkg^{-1} ... [115]
María Isabel García Ib..., 13/8/2018 19:06
Eliminado: … ... [116]
Microsoft Office User 7/8/2018 15:28
Subido [9]: ISOW is produced by mixin ... [117]
Microsoft Office User 21/8/2018 12:08
Eliminado: at
Microsoft Office User 14/7/2018 10:00
Con formato ... [118]
María Isabel García Ib..., 13/8/2018 19:06
Eliminado: -
Microsoft Office User 21/8/2018 11:12
Eliminado: at /kg^{-1}
María Isabel García Ib..., 13/8/2018 19:06
Eliminado: … ... [119]
Microsoft Office User 8/8/2018 8:53
Eliminado: distribution…is notably drive ... [120]
Microsoft Office User 24/8/2018 10:27
Con formato ... [121]
Microsoft Office User 7/8/2018 17:17
Eliminado: crontrasted…ontrasted in the ... [122]

3.3 Sources of ^{129}I and ^{236}U in the SPNA

All samples show ^{129}I concentrations and $^{236}U/^{238}U$ ratios well above the lithogenic background (LB) or the natural values (~ 0.04 × 10^7 at/kg for ^{129}I, Snyder et al., (2010); and 10^{-14} - 10^{-13} for $^{236}U/^{238}U$ atom ratios: Christl et al., (2012) and Steier et al., (2008)). This was also shown in previous studies, highlighting the influence of artificial sources on the presence of ^{129}I (e.g. Edmonds et al., 2001) and ^{236}U (Casacuberta et al., 2014; Christl et al., 2012) in the North Atlantic.

As done in earlier studies (Casacuberta et al., 2016), we can estimate the contribution to our samples from the LB, GF and NRP by combining the $^{129}I/^{236}U$ and $^{236}U/^{238}U$ in a dual tracer approach (Figure 4). This is possible because the atom ratios of $^{129}I/^{236}U$ and $^{236}U/^{238}U$ display a wide range of values due to the different input of ^{129}I and ^{236}U from the three sources. For example, the GF introduced about 10 times more ^{236}U than ^{129}I, thus this endmember is characterized by $^{129}I/^{236}U < 1$ and $^{236}U/^{238}U$ surface ratios in the (1000–2000) × 10^{-12} range. On the contrary, the total amount of ^{236}U introduced from European NRPs was much smaller than for ^{129}I. Therefore, a water mass with the additional influence of the European NRPs may present $^{129}I/^{236}U$ on the 1–350 range and $^{236}U/^{238}U$ above the GF. The natural presence of ^{129}I and ^{236}U is negligible compared to artificial sources, yet the LB can be distinguished by a very small $^{236}U/^{238}U$ (~ 10^{-13}) and a relatively large $^{129}I/^{236}U$ (~ 370). The simple mixing model (Figure 4) considers the three aforementioned endmembers constant in time, for which values were estimated by Casacuberta et al. (2016) based on the literature or on their own calculations. The mixing lines between each endmember represent all possible binary mixing scenarios, i.e. they delimit the range of $^{129}I/^{236}U$ and $^{236}U/^{238}U$ that a given water mass may show depending on the sources and on the different degrees of mixing. For instance, a sample falling in the 1 % value on the GF-NRP binary mixing line would be composed of waters carrying largely GF and about 1 % of the NRPs signal.

On top of the mixing model, we represent the results from the GEOVIDE cruise (Figure 4). Each data point represents a seawater sample collected at a certain station (Figure 4A) or assigned to a dominant water mass (Figure 4B to 4F). The results show that most of the samples fall along the GF-NRP binary mixing line with contributions from NRPs > 1 %. The largest NRP contribution, above 5 %, is observed

Microsoft Office User 7/8/2018 11:12
Eliminado: 2…Sources of ^{129}I and ^{236}U ... [123]
Microsoft Office User 8/8/2018 9:21
Con formato: Título 2
Microsoft Office User 8/8/2018 9:58
Eliminado: ir…lithogenic background (L ... [124]
Microsoft Office User 8/8/2018 8:58
Eliminado: (Casacuberta et al., 2016; Christl et al., 2015b)… we can estimate the contribution ... [125]
María Isabel García Ib..., 13/8/2018 19:16
Eliminado: … ... [126]
Microsoft Office User 21/8/2018 12:58
Eliminado: , in the last XY years and considering a steady state approach
Núria Casacuberta 14/8/2018 11:18
Con formato: Resaltar
María Isabel García Ib..., 13/8/2018 19:16
Eliminado: … ... [127]
Microsoft Office User 8/8/2018 9:05
Eliminado: ratios in a binary mixing model (Figure 3). …heThis…simple mixing mod ... [128]
María Isabel García Ib..., 13/8/2018 19:17
Eliminado: ,
Microsoft Office User 8/8/2018 8:58
Eliminado: and addresses
María Isabel García Ib..., 13/8/2018 19:17
Eliminado: –
Microsoft Office User 8/8/2018 9:02
Eliminado: . Each
María Isabel García Ib..., 13/8/2018 19:18
Eliminado: which was
Microsoft Office User 8/8/2018 9:43
Eliminado: sample is represented by one data point …ollected at a certain station (Figure ... [129]
María Isabel García Ib..., 13/8/2018 19:18
Eliminado: that was
Microsoft Office User 8/8/2018 10:20
Eliminado: for…a dominant water mass ... [130]
María Isabel García Ib..., 13/8/2018 19:18
Eliminado: … ... [131]
Microsoft Office User 24/8/2018 8:37
Eliminado: high

in the Irminger and Labrador Seas associated notably with PIW, DSOW and to lesser extent with ISOW. LSW also records NRP contributions > 1 % in the westernmost stations (e.g. 44 to 77), while LSW that has been transported further east on the section (stations 1 to 38) reflects the greater mixing or dilution with waters carrying notably GF. ENACWs are closer to the GF endmember, yet they show significant contributions (~ 1 %) from NRP. This result is unexpected, given that the transport of ENACW occurs upstream and far away from the NRPs, from subtropical latitudes into the eastern SPNA (stations 1 to 26). At least 6 samples separate from the GF-NRP mixing line and plot towards the LB endmember. These are associated with the contribution of the northward flowing AABW to $NEADW_L$ (van Aken and Becker, 1996). AABW is the oldest water mass in the SPNA and has little or no influence from nuclear activities given that it was not exposed to the surface or atmosphere for decades.

3.4 Time evolution of ^{129}I in the SPNA

In this section we compare radionuclide concentrations reported in the literature with those measured at nearby stations during GEOVIDE (Figure 5). The assessment of the temporal evolution of radionuclide distributions is important to identify the main circulation features highlighted by these tracers. The limited data on the novel ^{236}U tracer prevents from studying any temporal evolution. In the case of ^{129}I, the existing time series for the central Labrador Sea (1993–2013, Figure 5A) demonstrated that most of the tracer transport was carried by overflow waters (e.g. DSOW) and that the temporal evolution of ^{129}I concentrations in those waters could be associated with the tracer release from the European NRPs few years earlier (Edmonds et al., 2001; Orre et al., 2010; Smith et al., 2005, 2016). For instance, the literature on ^{129}I shows a rise in tracer concentrations due to the increased ^{129}I discharge rate from European NRPs in the whole water column, being more pronounced (about 10 times increase) in overflow waters (Figure 5A). The depth distribution of ^{129}I concentrations in the Labrador Sea in 2014 (station 69) displays ^{129}I concentrations in DSOW about 15 % lower (see section 3.5.4) than in 2012 – 2013 (Smith et al., 2016), yet the general shape of the depth profile is comparable (Figure 5A). The main difference between the ^{129}I depth profiles in the Irminger Sea (station 44, red squares in Figure

Núria Casacuberta 14/8/2018 11:38
Eliminado: extend

María Isabel García Ib…, 13/8/2018 19:19
Eliminado: The

Microsoft Office User 8/8/2018 9:46
Eliminado: and newly formed

María Isabel García Ib…, 13/8/2018 19:19
Eliminado: …SW also records NRP con ... [132]

Microsoft Office User 8/8/2018 9:51
Eliminado: . Samples plotting…closer to ... [133]

María Isabel García Ib…, 13/8/2018 19:19
Eliminado: … ... [134]

Microsoft Office User 22/8/2018 11:50
Eliminado: , which mixes with northward flowing Antarctic Bottom Water …ADDIN ... [135]

Microsoft Office User 7/8/2018 11:12
Eliminado: **3…Time eE** ... [136]

Microsoft Office User 22/8/2018 11:52
Eliminado: allow yet

Núria Casacuberta 14/8/2018 11:43
Eliminado: show a clear temporal trend between the ^{236}U/^{238}U ratios measured in 2014 at station 44 in the Irminger Sea and the profile reported in the Denmark Strait in 2010 (Casacuberta et al., 2014).

Microsoft Office User 8/8/2018 13:18
Eliminado: A described above, our results show that overflow waters transport significant amounts of artificial ^{129}I and ^{236}U particularly to the deep Labrador and Irminger Seas. In the case of ^{129}I, this had been documented (Figure 4) in previous studies that composed an…extensive …ime series ... [137]

María Isabel García Ib…, 13/8/2018 19:20
Eliminado: … ... [138]

Microsoft Office User 8/8/2018 13:22
Eliminado: (Edmonds et al., 2001; Orre et al., 2010; Smith et al., 2005, 2016)(Edmonds et al., 2001; Orre et al., 2010; Smith et al., 2005, 2016).

Microsoft Office User 8/8/2018 13:19
Bajado [11]: (Edmonds et al., 2001; Orr ... [139]

Microsoft Office User 8/8/2018 13:19
Movido (inserción) [11]

Núria Casacuberta 14/8/2018 11:46
Eliminado: related

Microsoft Office User 8/8/2018 13:33
Eliminado: The correspondingc^{236}U/^{238}U ... [140]

María Isabel García Ib…, 13/8/2018 19:21
Eliminado: explanation given in

Microsoft Office User 7/8/2018 10:18
Eliminado: 4…). The main difference be ... [141]

5A) and central Labrador Sea (station 69, red circles in Figure 5A) in 2014 is the surface ^{129}I peak in the latter one. Considering the 30 m deep freshwater surface layer observed between station 69 and Greenland (not shown here), we suggest that waters carried by the West Greenland Current (continuation of the EGC) may have separated from the main western boundary transport and entered the Central Labrador Sea (Cuny and Rhines, 2002). This may also explain the peak in $^{236}U/^{238}U$ ratios observed at the same location (Figure S1).

A similar assessment of ^{129}I concentrations is now possible for the water column over the Reykjanes Ridge (station 38) and the Icelandic Basin (station 32) (Figure 5B), which were first studied in 1993 (Edmonds et al., 2001). The ^{129}I concentrations in the water column are 5 - 7 times higher in 2014 than in 1993. The most pronounced increase occurs in the upper 1000 m filled by SPMWs and in the deep Icelandic Basin dominated by ISOW. This novel result shows that the ^{129}I tracer could potentially be used to trace the transformation of ENACWs into SPMWs and the evolution of ISOW. The depth profiles of ^{129}I concentration measured in the WEB in 2014 (particularly station 21) resemble the one sampled at the Porcupine Abyssal Plain (PAP) in 2012 by Vivo-Vilches et al. (2018) (Figure 5C). The ^{129}I distribution in the upper 1000 m at PAP is very similar to station 21 located 365 km to the southwest, while below that depth ^{129}I concentrations are about 2.5×10^7 at/kg higher in the PAP. These results suggest a similar water mass composition for that region, yet the offset in deep ^{129}I concentrations would support the hypothesis that effluents from the nearby Sellafield and/or La Hague NRPs may enter directly into the SPNA without previous circulation in the Nordic Seas (see section 3.5.1).

3.5 Tracing water mass circulation in the SPNA using ^{129}I and ^{236}U

We use the above information on the distribution, sources and time evolution of ^{129}I and ^{236}U to investigate the circulation of nuclear reprocessing effluents and in return, provide more insight on composition, spreading pathways and transport time scales of water masses in the SPNA.

Microsoft Office User 21/8/2018 13:04
Eliminado: squares …ircles in Figure 5A ... [142]

Microsoft Office User 8/8/2018 13:58
Eliminado: split off from the boundary currents, either the West Greenland Current or the L ... [143]

María Isabel García Ib…, 13/8/2018 19:21
Eliminado: by

Microsoft Office User 8/8/2018 14:02
Eliminado: …he depth profiles of ^{129}I ... [144]

María Isabel García Ib…, 13/8/2018 19:22
Eliminado: further discussed in

Microsoft Office User 8/8/2018 14:07
Eliminado: , although PAP might present slightly larger ^{129}I concentrations because of its proximity to Sellafield and La Hague.

Microsoft Office User 7/8/2018 11:12
Eliminado: 4

Núria Casacuberta 14/8/2018 11:50
Eliminado: s

3.5.1 Shallow water circulation in the eastern SPNA

The main transport of reprocessing effluents occurs poleward, yet the increasing observations and simulations on ^{129}I suggest that part of the NRP signal may enter directly the surface of the SPNA without previous circulation in the Nordic Seas. Such hypothesis is based on the fact that ^{129}I concentrations in surface waters of the northeastern SPNA can record values more than one order of magnitude above the GF level (2.5 × 10^7 at/kg; Edmonds et al., 1998). He et al. (2013b) proposed that the outflow through the English Channel and the Irish Sea may lead to ^{129}I concentrations in surface waters above 20 × 10^7 at/kg and modify the isotopic iodine composition in the Bay of Biscay. Modelling of ^{129}I releases from the European NRPs also shows that tracers discharged from Sellafield may expand southwards (Villa et al., 2015), which could explain ^{129}I concentrations of 77 × 10^7 at/kg measured in surface waters of the Celtic Sea (Vivo-Vilches et al., 2018). GEOVIDE data (Table 2) of ^{129}I concentrations (~ 10 × 10^7 at/kg) and ^{129}I/^{236}U ratios (7–20) in ENACWs confirms such influence from the NRPs. If that was the case, the different NAC branches could mix ENACWs with reprocessing-labeled local waters and be transported southward by surface currents (e.g. Lambelet et al., 2015; Lherminier et al., 2010; Ríos et al., 1992). Indeed, NAC branches west of station 21 recirculated anti-cyclonically into the WEB bringing waters south across the GEOVIDE section in 2014 (Zunino et al., 2017). Further, the transformation of ENACW into SPMW results in ^{129}I concentrations twice larger in the Icelandic Basin than in the WEB (Figures 5B and 5C), which suggests the near-surface transport of ^{129}I from European NRPs also occurs southward across Iceland-Scotland. Consequently, ^{129}I concentrations in shallow waters at stations 1, 13 and 21 strongly contrast with those at stations 26 and 32 located west of the SAF (Table 2). Such near surface tracer input would also explain the increase in surface ^{129}I concentrations (Figure S2) up to 10^8–10^9 at/kg in the Icelandic Basin and northwest of the British Isles by 2010–2012 (Gómez-Guzmán et al., 2013; Vivo-Vilches et al., 2018). Thus, one could potentially use ^{129}I to trace ENACWs in the upper water column of the WEB and their transformation into SPMW. This is not clearly supported by ^{236}U levels (~ 10 × 10^6 at/kg) which are close to GF in the shallow eastern SPNA, yet European NRPs introduced about 60 times less ^{236}U than ^{129}I (Christl et al., 2015b).

Microsoft Office User 7/8/2018 11:12
Eliminado: 4

Microsoft Office User 8/8/2018 14:35
Eliminado: Concentrations of ^{129}I ... [145]

María Isabel García Ib..., 13/8/2018 19:07
Eliminado: ,

María Isabel García Ib..., 13/8/2018 19:23
Comentario [1]: It is already referenced at the beginning of the sentence

Microsoft Office User 21/8/2018 11:13
Eliminado: $^{-1}$

María Isabel García Ib..., 13/8/2018 19:23
Eliminado: (He et al., 2013b)

Microsoft Office User 21/8/2018 11:13
Eliminado: $^{-1}$...easured in surface waters ... [146]

María Isabel García Ib..., 13/8/2018 19:07
Eliminado: ... ... [147]

Microsoft Office User 8/8/2018 14:38
Eliminado: have been reported in the upper eastern SPNA by earlier studies (e.g., He et al., 2013b), and in this study along with ^{129}I/^{236}U ratios > 1 for ENACWs that must have originated from the releases from Sellafield and La Hague NRPs. Thus, despite most effluents flow northward from the North Sea, it seems that part of reprocessing ^{129}I (and ^{236}U) may enter directly the SPNA without previous recirculation in the Nordic Seas. It has been suggested that the outflow through the English Channel and the Irish Sea may lead to increase the ^{129}I concentrations in surface waters to levels above 20 × 10^7 at/kg and modify the isotopic iodine composition in the Bay of Biscay (He et al. ... [148]

Núria Casacuberta 14/8/2018 11:54
Eliminado:

María Isabel García Ib..., 13/8/2018 19:26
Eliminado: higher

Núria Casacuberta 14/8/2018 11:53
Eliminado: than

Microsoft Office User 7/8/2018 10:18
Eliminado: 4... and 54...), which . This ... [149]

María Isabel García Ib..., 13/8/2018 19:08
Eliminado: ...- ... [150]

Microsoft Office User 21/8/2018 11:13
Eliminado: at/ kg^{-1} range ...n the Icelandic Basin and northwest of the British Isles by 2010–2012 (Gómez-Guzmán et al., 2013; Vivo-Vilches et al., 2018). Thus, one could potentially use ^{129}I to trace ENACWs in the upper water column of the WEB and their transformation into SPMW. This ... [151]

Microsoft Office User 8/8/2018 14:51
Con formato: Color de fuente: Automático

3.5.2 Shallow water transport and cascading in the Irminger Sea and Labrador Sea

It is well known that the eastern coast of Greenland receives RAW and PIW-Atlantic injected in the EGC (Figure 1). Similarly, the shelf of Newfoundland is bathed by the LC, which carries EGC waters and PIW-Canada, this last one being supplied through the Nares Strait (Curry et al., 2014). The tracer levels are particularly high in such waters residing on the shelves, slopes and very deep waters around Greenland and Newfoundland (Figure 3). Further, the tracer content differs between Arctic waters of Atlantic and Canadian origin enriched in ^{129}I and ^{236}U, respectively. Thus, one may use them to distinguish key circulation features such as the EGC/LC and the DWBC in the Labrador and Irminger Seas (Figure 1). For example, at shallow depths, the EGC (stations 53 to 64) presents remarkably high ^{129}I concentrations (up to ~ 250 × 10^{7} at/kg) and ^{129}I/^{236}U ratios (up to 200), while both values are significantly lower in the LC (station 78) which is characterized by comparably higher ^{236}U/^{238}U ratios (up to 2350 × 10^{-12}) (Figure 3). Such differences on the composition of ^{129}I and ^{236}U in the two shallow boundary currents are likely due to the fact that waters of Atlantic origin (PIW-Atlantic and RAW) have been largely influenced by NRP effluents (high ^{129}I). On the contrary, the LC records lower ^{129}I concentrations due to the influence of PIW-Canada waters with mainly GF signal (Ellis and Smith, 1999; Smith et al., 1998), and a large ^{236}U content (^{236}U/^{238}U ratios are likely > 2000 × 10^{-12}) from both the GF and unconstrained Arctic rivers inputs (Casacuberta et al., 2016).

Shelf waters carried by the EGC are thought to occasionally descend down the Greenland slope feeding the East Greenland Spill Jet and DSOW (von Appen et al., 2014; Falina et al., 2012; Harden et al., 2014; Koszalka and Haine, 2013; Pickart et al., 2005; Rudels et al., 1999a). The GEOVIDE section shows a rise of ^{129}I concentrations at certain depths on the Greenland slope (e.g., station 60; Figure 3 and Figure S1), and particularly in bottom waters of the Irminger Sea (station 44), which are probably related to the cascading of ^{129}I-rich waters from the Greenland Shelf. This finding would be supported by OMP analyses that estimate up to 20 % of PIW in the DSOW realm (García-Ibáñez et al., 2018). Our results also highlight that similar processes may be taking place in the Canadian shelf, but with PIW-Canada water cascading to the bottom of the Labrador Sea. This would explain the slightly higher ^{236}U/^{238}U ratios near the Newfoundland Shelf (station 77; Figure 3 and Figure S1) compared to the

Microsoft Office User 7/8/2018 11:13
Eliminado: 4

Microsoft Office User 21/8/2018 13:11
Eliminado: AW

Núria Casacuberta 14/8/2018 11:58
Eliminado: that is

Microsoft Office User 21/8/2018 13:15
Eliminado: Except for the Pacific origin ... [152]

Núria Casacuberta 14/8/2018 12:01
Eliminado: The

Microsoft Office User 10/8/2018 9:41
Eliminado: …such waters residing on th ... [153]

María Isabel García Ib…, 13/8/2018 19:27
Eliminado: depths

Núria Casacuberta 14/8/2018 12:01
Eliminado: levels… that surr ... [154]

Microsoft Office User 7/8/2018 10:19
Eliminado: 2

María Isabel García Ib…, 13/8/2018 19:27
Eliminado: , respectively

Microsoft Office User 10/8/2018 9:32
Eliminado: allowing …o identify key… ... [155]

María Isabel García Ib…, 13/8/2018 19:28
Eliminado: that carries

Microsoft Office User 10/8/2018 10:03
Eliminado: a small ^{129}I signal …ith mainly from GF signal (Ellis and Smith, 1999; Smith et al., 1998), and a large ^{236}U content (^{236}U/^{238}U ratios are likely > 2000 × 10^{-12}) , while its ^{236}U/^{238}U ratios are likely > 2000 × 10^{-12} due to ... [156]

Microsoft Office User 22/8/2018 12:02
Eliminado: descend …ccasionally descer ... [157]

offshore waters in the Labrador Sea (e.g., station 69), as well as, the higher $^{236}U/^{238}U$ ratios and lower ^{129}I concentrations in the deep Labrador Sea (influenced by PIW-Canada) compared to the Irminger Sea (influenced by PIW-Atlantic) (Figure 3 and 5A).

3.5.3 Spreading pathways of ISOW in the eastern SPNA

The ^{129}I and ^{236}U tracers may help validate current interpretations of ISOW spreading pathways in the SPNA which are largely based on model outputs or on limited observations (Fleischmann et al., 2001; LeBel et al., 2008; Xu et al., 2010; Zou et al., 2017). The ISOW is best distinguished by its relative ^{129}I concentration maxima and $^{129}I/^{236}U$ ratios of 15 – 40 due to NRPs, that are significantly higher than in surrounding waters (e.g., LSW, $NEADW_L$). This is particularly visible for ^{129}I concentrations (Figures 5B and 5C, and Table 2) in deeper parts of the Icelandic Basin (stations 32 and 38) and the WEB (stations 1 and 13), where the presence of ISOW has also been inferred from OMP analyses (García-Ibáñez et al., 2018). For ^{236}U (Figure S1), such increase is not as pronounced as for ^{129}I, probably due to the pre-existing ^{236}U from the GF. In the coming years, one can expect a stronger ^{129}I signal carried by ISOW because tracer concentrations in ISOW precursor waters have increased from 7×10^7 at/kg to 63×10^7 at/kg at the Iceland–Scotland Sill from 1993 to 2012 in response to releases from the NRPs (Alfimov et al., 2004; Edmonds et al., 2001; Vivo-Vilches et al., 2018). The overflow of ISOW through the Iceland-Scotland Sill has increasing implications for the deep ventilation of the SPNA and for the magnitude of the AMOC (García-Ibáñez et al., 2018). Thus, future time series of time-varying ^{129}I concentrations at GEOVIDE stations and further upstream may also be used to investigate timescales of ISOW ventilation in the North Atlantic Ocean.

3.5.4 Transit times and dilution factors of reprocessing-labelled Atlantic Waters

The observations of ^{129}I concentrations in DSOW filling the Central Labrador Sea between 1993 and 2013 (Figure 5A) have also been valuable to estimate transport times of Atlantic Waters carrying the NRP signal into the Arctic and the North Atlantic (Orre et al., 2010; Smith et al., 2005, 2011, 2016).

Microsoft Office User 21/8/2018 11:07
Eliminado: Pacific…anada) compared to ... [158]

Microsoft Office User 7/8/2018 11:13
Eliminado: 4

Microsoft Office User 24/8/2018 8:46
Eliminado: ing…present ... [159]

Microsoft Office User 21/8/2018 13:18
Con formato: Fuente: Sin Negrita, Superíndice

María Isabel García Ib..., 13/8/2018 18:30
Con formato: Fuente: Sin Negrita, Noruego Bokmål

Microsoft Office User 10/8/2018 10:13
Eliminado: (not observed for ^{236}U)

María Isabel García Ib..., 13/8/2018 19:09
Eliminado: -

Microsoft Office User 21/8/2018 9:54
Eliminado: s…his is particularly visible f ... [160]

María Isabel García Ib..., 13/8/2018 18:30
Con formato: Fuente: Sin Negrita, Noruego Bokmål

Microsoft Office User 8/8/2018 15:40
Eliminado:

Microsoft Office User 8/8/2018 16:02
Eliminado:

Microsoft Office User 7/8/2018 11:13
Eliminado: 4

Microsoft Office User 8/8/2018 16:02
Eliminado: The evolution of ^{129}I (and ^{236}U) in the SPNA is closely related to the effluents discharged from the two European NRPs. …In particu ... [161]

The ^{129}I time series shows two tracer pulses, one in the early 2000s and the following about 10 years later (Figure 6A, data points). Smith et al. (2005) suggested that the first sharp increase in ^{129}I concentrations in DSOW was related to the arrival of the tracer front observed in the late 1990s at 60 °N in the northern North Sea. The second peak in ^{129}I concentrations has also been related to the same cause as in the late 1990s front, but in this case, it would correspond to the return flow of AWs that were transported northwards into the Arctic Ocean before returning to the western SPNA (Smith et al., 2011). According to these authors, the 10-year gap between the two tracer fronts would be related to such 'Arctic loop', i.e. the transport of AWs by the FSBW into the Arctic Eurasian Basin, the return flow along the Lomonosov Ridge and the incorporation via the EGC into DSOW.

To test this hypothesis, we took the ^{129}I input function at 60 °N for the northern North Sea (Figure 6A, green dashed line) used in previous studies (e.g. Christl et al., 2015b; Orre et al., 2010; Smith et al., 2005). This input function is estimated assuming that the signal of both NRPs mixes in the North Sea and then is advected to 60 °N in 2 years from La Hague and in 4 years from Sellafield. Following earlier modelling studies (Smith et al., 2005), we firstly estimate a new ^{129}I input function for DSOW in the Central Labrador Sea (Figure 6A, blue line) that should match the aforementioned first tracer front shown by ^{129}I measurements between 1993 and 2001 (Edmonds et al., 2001; Smith et al., 2005). This is achieved by applying a time lag (6 years) that accounts for the transit time from 60 °N, and a dilution factor (DF = 50) that represents the mixing with waters carrying only GF signal. Secondly, we estimate a second ^{129}I input function (Figure 6A, red line) that fits the ^{129}I concentrations measured in 2012 and 2013 by Smith et al. (2016) and in 2014 by this study. We found that this is possible when the tracer input function (Figure 6A, green dashed line) is diluted 30 times and a delay-time of about 14 years is applied. Thus, 2014 data reported in this study supports the current interpretation on the 'Arctic loop' (e.g. Smith et al., 2016) and suggests that the second ^{129}I front probably peaked before the GEOVIDE cruise. Note that the latter input function (Figure 6A, red line) only provides an upper estimate for the ^{129}I transit times and the dilution factor because the observed ^{129}I concentrations in 2012 – 2014 also contains water from the shorter loop (Figure 6A, blue line). According to our results (Figure 6A), AWs follow at least two paths before arriving to the Labrador Sea: i) one short path into the Nordic Sea and

María Isabel García Ib…, 13/8/2018 19:30
Eliminado: ,…(2005) suggested that the ... [162]

Microsoft Office User 8/8/2018 16:31
Eliminado: in overflow waters in the central Labrador Sea (Figure 5A) allows investigating the time evolution of ^{129}I concentrations in relation to its discharges. For this,

María Isabel García Ib…, 13/8/2018 19:31
Eliminado: a…eu ... [163]

Microsoft Office User 8/8/2018 17:10
Eliminado: se…the ^{129}I input function es ... [164]

María Isabel García Ib…, 13/8/2018 19:31
Eliminado:

Microsoft Office User 8/8/2018 17:20
Eliminado: , primary y axis)…used in pr ... [165]

María Isabel García Ib…, 13/8/2018 18:30
Con formato ... [166]

Microsoft Office User 8/8/2018 17:19
Eliminado: (…015b) ... [167]

María Isabel García Ib…, 13/8/2018 18:30
Con formato: Noruego Bokmål

Unknown
Código de campo cambiado

Microsoft Office User 8/8/2018 17:10
Eliminado: , which mixes …he signal of ... [168]

María Isabel García Ib…, 13/8/2018 19:32
Eliminado: firstly

Microsoft Office User 8/8/2018 17:24
Eliminado: We fit the ^{129}I input function to the observations by applying…a time lag (6 ye ... [169]

María Isabel García Ib…, 13/8/2018 19:33
Eliminado: ,

Microsoft Office User 21/8/2018 9:58
Eliminado: DF=30 …elay-lag …ime ofis ... [170]

Núria Casacuberta 14/8/2018 13:38
Eliminado: delaying…about 14 years is appliedyears the ^{129}I input function at 60 °N ... [171]

María Isabel García Ib…, 13/8/2018 19:34
Eliminado: … ... [172]

then to the SPNA that takes approximately 8–10 years from the NRPs, and ii) a long path which adds approximately 8 years of circulation in the Arctic Ocean resulting in 16–18 years of transit time from the NRPs to the central Labrador Sea. A similar exercise for ^{236}U (Figure 6B) shows that the single ^{236}U measurement available for overflow waters in the central Labrador Sea (2014, this work) is above the concentrations predicted using the two fits. Although the ^{236}U data would agree with the hypothesis of a second delayed ^{129}I pulse arriving from the Arctic Ocean, there are significant inconsistencies between the simulated and measured concentrations. These might be attributed to, among other factors, the large uncertainty of the used ^{236}U data point for 2014, uncertainties on the amount released by the Sellafield NRP (Christl et al., 2015), missing information on other sources, or unaccounted features on the water mass circulation downstream the NRPs.

4 Conclusions

The distribution of artificial ^{129}I and ^{236}U in the SPNA was governed by the main water mass circulation. The highest ^{129}I concentrations and ^{236}U/^{238}U ratios are associated with water masses originating from the Nordic Seas (DSOW, ISOW and surface currents) or the Arctic Ocean (PIW). On the other end, ENACW and NEADW$_L$ transported from low latitudes north into the SPNA present ^{129}I concentrations and ^{236}U/^{238}U ratios of about 2 – 3 orders of magnitude lower. The ^{236}U/^{238}U - ^{129}I/^{236}U dual tracer approach indicates that all water masses, except NEADW$_L$, are influenced by GF and NRPs. ENACW is also influenced by effluents from NRPs (e.g. ^{129}I/^{236}U > 1), which suggests that part of the radioactive releases split off from the mainstream and enter the surface eastern SPNA either through direct exchange at the English Channel/Irish Sea or at the passage between Iceland and Scotland. Other key circulation features such as the shallow transport of PIW and RAW by the EGC and LC, or the deep North Atlantic ventilation by overflow waters (DSOW, ISOW) are particularly visible due to the presence of reprocessing ^{129}I and ^{236}U. For example, ISOW is tagged with relatively high ^{129}I and, therefore, it can be traced while spreading eastwards into the WEB among waters that have lower tracer amounts. The combined use of ^{236}U/^{238}U - ^{129}I/^{236}U allows differentiating water mass composition and origin, and serves to confirm known circulation features and validating recent interpretations on water

María Isabel García Ib..., 13/8/2018 19:34
Eliminado: -

María Isabel García Ib..., 13/8/2018 19:34
Eliminado: -

María Isabel García Ib..., 13/8/2018 19:35
Eliminado: is

María Isabel García Ib..., 13/8/2018 19:35
Eliminado: to

María Isabel García Ib..., 13/8/2018 19:35
Eliminado: t

Microsoft Office User 22/8/2018 12:05
Eliminado: missing

María Isabel García Ib..., 13/8/2018 19:35
Eliminado: that we are missing

Microsoft Office User 8/8/2018 17:41
Eliminado: front passing in 1990 – 1995 at 60 °N (green line) arrives 50 times more diluted to the central Labrador Sea about 6 years later causing a sharp increase in measured ^{129}I concentrations (Figure 5A, blue fit). Such finding was first noticed by Smith et al. (2005), who estimated a similar ^{129}I input function using a different approach (transfer factors). In their work, they also found that ^{129}I measurements were about 30 % lower than ... [173]

Microsoft Office User 8/8/2018 17:10
Con formato: Color de fuente:

Microsoft Office User 21/8/2018 13:29
Eliminado: in spr

Unknown
Eliminado: i

Microsoft Office User 21/8/2018 13:28
Eliminado: g 2014

Microsoft Office User 21/8/2018 13:30
Eliminado: , while a

Microsoft Office User 21/8/2018 13:30
Eliminado: t

María Isabel García Ib..., 13/8/2018 19:09
Eliminado:

María Isabel García Ib..., 13/8/2018 19:09
Eliminado:

Microsoft Office User 22/8/2018 12:05
Eliminado: deepest

Microsoft Office User 9/8/2018 9:39
Eliminado: .

Microsoft Office User 9/8/2018 9:49
Eliminado: combination of

Microsoft Office User 9/8/2018 9:49
Eliminado: and

mass transport pathways and time scales. For example, the LC presents mainly the GF signal and unconstrained Arctic river inputs (more ^{236}U relative to ^{129}I) indicating the contribution from PIW-Canada through the Canadian Archipelago, while the EGC, largely influenced by the NRPs (more ^{129}I relative to ^{236}U), indicates the contribution of RAW and PIW-Atlantic. The contribution of RAW/PIW-Atlantic and PIW-Canada to DSOW in the Irminger and Labrador Seas is also visible thanks to slight elevations of tracer values in near bottom depths and specific ^{236}U/^{238}U - ^{129}I/^{236}U ratios, due to cascading events. This work also contributes to extend the existing ^{129}I time series in the Labrador Sea/Irminger Sea and allows a first assessment of time-varying ^{129}I concentrations east of Reykjanes Ridge. Increasing ^{129}I concentrations are observed in the western part of the GEOVIDE section and in the Icelandic Basin. In the WEB, the short observation time (2012 – 2014) does not allow yet seeing temporal trends of ^{129}I levels. The ^{129}I data in overflow waters of the central Labrador Sea (1993 – 2014) can be fitted with reprocessing ^{129}I (and ^{236}U) input functions following earlier modelling studies to better understand the transport time scales and dilution factors of AWs tagged by the NRP signal. This study supports the current interpretations on the circulation of AWs, which apparently follow a short loop trough the Nordic Seas (8 – 10 years in this study) and a longer loop including the circulation in the Arctic Eurasian Basin (16 – 18 years in this study). Further experimental and modelling studies on ^{129}I and ^{236}U may confirm circulation features highlighted by these tracers and to shed more light on novel findings such as the transport of ISOW in to the eastern SPNA, which plays an important role on the ventilation of the deep SPNA.

Acknowledgements

We are grateful to the captain and crew of *R/V Pourquoi Pas?*, as well as the technical team for their work at sea (P. Branellec, F. Desprez de Gésincourt, M. Hamon, C. Kermabon, P. Le Bot, S. Leizour, O. Ménage, F. Pérault, and E. de Saint-Léger). A big thank to Yi Tang for help sampling and to Anita Schlatter for assistance in the laboratory. This manuscript has been notably improved thanks to the constructive comments from two anonymous reviewers. Thanks to J. -L. Menzel and the group of E. Achterberg (GEOMAR, Kiel) for providing the FISH device to collect surface seawater. The work of C.

Microsoft Office User 9/8/2018 9:50
Eliminado: appears …resents mainly the ... [174]

Núria Casacuberta 14/8/2018 13:46
Eliminado: cascading and

Microsoft Office User 21/8/2018 11:07
Eliminado: Pacific …anada appear to cas ... [175]

Núria Casacuberta 14/8/2018 13:47
Eliminado:

Microsoft Office User 9/8/2018 9:52
Eliminado: s, respectively… This work a ... [176]

María Isabel García Ib…, 13/8/2018 19:36
Eliminado: … ... [177]

Microsoft Office User 9/8/2018 9:41
Eliminado: in the WEB

María Isabel García Ib…, 13/8/2018 19:36
Eliminado: … ... [178]

Microsoft Office User 9/8/2018 9:41
Eliminado: waters

María Isabel García Ib…, 13/8/2018 19:37
Eliminado: one… short loop trough the N ... [179]

Microsoft Office User 9/8/2018 9:57
Eliminado: Results show that water circulation transit times from the NRPs to the deep Labrador Sea probably fall between the maximum of 16 – 8 years (including recirculation in the Arctic Eurasian Basin) and the shorter loop trough the Nordic Seas of 8 - 10 years. Longer time series of ^{129}I and ^{236}U will …ay allow confirm ... [180]

María Isabel García Ib…, 13/8/2018 19:37
Eliminado: P

Microsoft Office User 9/8/2018 9:59
Eliminado: ing some of these findings relevant for the understanding of the AMOC and calibrate circulation models. Thus, these tracers may provide new information on the circulation and mixing processes of waters masses involved in the changing AMOC.

Schmechtig with the LEFE-CYBER database management is also acknowledged. Some of the ^{129}I data discussed from the literature were kindly provided by V. Alfimov, H. Edmonds and J. N. Smith. Several figures were created using *Ocean Data View* (Schlitzer, 2017). We would also like to thank Natalie Dubois and Alfred Lück for providing the laboratory space and assistance at EAWAG. The GEOVIDE cruise was funded by the French National Research Agency (ANR-13-BS06-0014, ANR-12-PDOC-0025-01), the French National Center for Scientific Research (CNRS-LEFE-CYBER), the LabexMER (ANR-10-LABX-19), and Ifremer. This work was funded by the Ministerio de Economía y Competitividad of Spain (MDM2015-0552), the Generalitat de Catalunya (MERS 2017 SGR-1588) and consortium partners of the ETH-Zurich Laboratory of Ion Beam Physics (EAWAG, EMPA, and PSI). M. Castrillejo was funded by a FPU PhD studentship (AP-2012-2901) from the Ministerio de Educación, Cultura y Deporte of Spain and the ETH Zurich Postdoctoral Fellowship Program (17-2 FEL-30), co-funded by the Marie Curie Actions for People COFUND Program. N. Casacuberta's research was funded by the AMBIZIONE grant (PZ00P2_154805) from the Swiss National Science Foundation. M.I. García-Ibáñez was supported by the Spanish Ministry of Economy and Competitiveness through the BOCATS (CTM2013-41048-P) project co-funded by the Fondo Europeo de Desarrollo Regional 2014–2020 (FEDER).

References

Aarkrog, A., Boelskifte, S., Dahlgard, H., Duniec, S., Hallstadius, L., Holm, E. and Smith, J. N.: Technetium-99 and Cesium-134 as long distance tracers in Arctic Waters, Estuar. Coast. Shelf Sci., 24, 637–647, 1987.

Aarkrog, A., Dahlgaard, H., Hallstadius, L., Hansen, H. and Holm, E.: Radiocaesium from Sellafield effluents in Greenland waters, Nature, 304, 49–51, 1983.

Alfimov, V., Aldahan, A. and Possnert, G.: Water masses and ^{129}I distribution in the Nordic Seas, Nucl. Inst. Methods Phys. Res. B, 294, 542–546, doi:10.1016/j.nimb.2012.07.042, 2013.

Alfimov, V., Aldahan, A., Possnert, G. and Winsor, P.: Tracing water masses with ^{129}I in the western Nordic Seas in early Spring 2002, Geophys. Res. Lett., 31, L19305, 2004.

Microsoft Office User 24/8/2018 10:34
Con formato: Fuente: (Predeterminado) +Cuerpo de tema

Arhan, M. The North Atlantic Current and the subarctic intermediate water, J. Mar. Res., 48(1), 109–144, 1990.

Beasley, T., Cooper, L. W., Grebmeier, J. M., Aagaard, K., Kelley, J. M. and Kilius, L. R.: ^{237}Np/^{129}I Atom Ratios in the Arctic Ocean: Has ^{237}Np from Western European and Russian Fuel Reprocessing Facilities Entered the Arctic Ocean ?, J. Environ. Radioact., 39(3), 255–277, 1998.

Bersch, M., Yashayaev, I. and Koltermann, K. P.: Recent changes of the thermohaline circulation in the subpolar North Atlantic, Ocean dy, 57, 223–235, doi:10.1007/s10236-007-0104-7, 2007.

Casacuberta, N., Christl, M., Lachner, J., van der Loeff, M. R., Masqué, P. and Synal, H.-A.: A first transect of ^{236}U in the North Atlantic Ocean, Geochim. Cosmochim. Acta, 133, 34–46, doi:10.1016/j.gca.2014.02.012, 2014.

Casacuberta, N., Masqué, P., Henderson, G., Rutgers van-der-Loeff, M., Bauch, D., Vockenhuber, C., Daraoui, a., Walther, C., Synal, H. -a. and Christl, M.: First ^{236}U data from the Arctic Ocean and use of ^{236}U/^{238}U and ^{129}I/^{236}U as a new dual tracer, Earth Planet. Sci. Lett., 440, 127–134, doi:10.1016/j.epsl.2016.02.020, 2016.

Casacuberta, N., Christl, M., Vockenhuber, C., Wefing A.-M., Wacker L., Masqué P., Synal H.-A., and Rutgers van der Loeff M.: Tracing the three Atlantic branches entering the Arctic Ocean with ^{129}I and ^{236}U. J. Geophys, Res. Oceans., 2018.

Castrillejo, M., Casacuberta, N., Christl, M., Garcia - Orellana, J., Vockenhuber, C., Synal, H.-A. and Masqué, P.: Anthropogenic ^{236}U and ^{129}I in the Mediterranean Sea: First comprehensive distribution and constrain of their sources, Sci. Total Environ., 593–594, 745–759, doi:10.1016/j.scitotenv.2017.03.201, 2017.

Christl, M., Casacuberta, N., Lachner, J., Herrmann, J. and Synal, H. A.: Anthropogenic ^{236}U in the North Sea - A Closer Look into a Source Region, Env. Sci. and Tech., 2017.

Christl, M., Casacuberta, N., Lachner, J., Maxeiner, S., Vockenhuber, C., Synal, H. A., Goroncy, I., Herrmann, J., Daraoui, A., Walther, C. and Michel, R.: Status of ^{236}U analyses at ETH Zurich and the distribution of ^{236}U and ^{129}I in the North Sea in 2009, Nucl. Instruments Methods Phys. Res. Sect. B Beam Interact. with Mater. Atoms, 361, 510–516, doi:10.1016/j.nimb.2015.01.005, 2015a.

Christl, M., Casacuberta, N., Vockenhuber, C., Elsässer, C., Bailly du Bois, P., Herrmann, J. jürgen and

Microsoft Office User 10/8/2018 10:53
Eliminado: Casacuberta, N., Christl, M., Vockenhuber, C., Wefing, A.-M., Wacker, L., Masqué, P., Synal, H.-A. and Rutgers van der Loeff, M.: Tracing Atlantic Water s intro the Arctic Ocean by means of ^{129}I and ^{236}U, in prep..

Microsoft Office User 24/8/2018 10:34
Con formato: Normal

Microsoft Office User 20/8/2018 11:03
Eliminado:

Microsoft Office User 24/8/2018 10:34
Con formato: Default,Interlineado: 1,5 líneas, Control de líneas viudas y huérfanas, Adjust space between Latin and Asian text, Adjust space between Asian text and numbers

Synal, H.-A.: Reconstruction of the ^{236}U input function for the Northeast Atlantic Ocean: Implications for ^{129}I/^{236}U and ^{236}U/^{238}U-based tracer ages, J. Geophys. Res. Ocean., 1–16, doi:10.1002/2014JC010472.Received, 2015b.

Christl, M., Lachner, J., Vockenhuber, C., Goroncy, I., Herrmann, J. and Synal, H. A.: First data of Uranium-236 in the North Sea, Nucl. Instruments Methods Phys. Res. Sect. B Beam Interact. with Mater. Atoms, 294, 530–536, doi:10.1016/j.nimb.2012.07.043, 2013a.

Christl, M., Lachner, J., Vockenhuber, C., Lechtenfeld, O., Stimac, I., van der Loeff, M. R. and Synal, H.-A.: A depth profile of uranium-236 in the Atlantic Ocean, Geochim. Cosmochim. Acta, 77, 98–107, doi:10.1016/j.gca.2011.11.009, 2012.

Christl, M., Vockenhuber, C., Kubik, P. W., Wacker, L., Lachner, J., Alfimov, V. and Synal, H.: The ETH Zurich AMS facilities : Performance parameters and reference materials, Nucl. Inst. Methods Phys. Res. B, 294, 29–38, doi:10.1016/j.nimb.2012.03.004, 2013b.

Cuny, J., and Rhines, P. -B.: Labrador Sea Boundary currents and the Fate of the Irminger Sea Water, Am. Met. Soc., 32, 627-647, 2002.

Curry, B., Lee, C. M., Petrie, B., Moritz, R. E. and Kwok, R.: Multiyear Volume, Liquid Freshwater, and Sea Ice Transports through Davis Strait, 2004-10, J. Phys. Oceanogr., 44, 1244–1266, 2014.

Dahlgaard, H.: Transfer of European Coastal Pollution to the Arctic : Radioactive Tracers, Mar. Pollut. Bull., 31(95), 3–7, 1995.

Daniault, N., Mercier, H., Lherminier, P., Sarafanov, A., Falina, A., Zunino, P., Pérez, F. F., Ríos, A. F., Ferron, B., Huck, T. and Thierry, V.: The northern North Atlantic Ocean mean circulation in the early 21st century, Prog. Oceanogr., 146 (June), 142–158, doi:10.1016/j.pocean.2016.06.007, 2016.

Doney, S. C. and Jenkins, W. J.: Ventilation of the deep western boundary current and abyssal western North Atlantic: Estimates from tritium and ^{3}He distributions, J. Phys. Oceanogr., 24, 638–659, 1994.

Edmonds, H. N., Smith, J. N., Livingston, H. D., Kilius, L. R. and Edmond, J. M.: ^{129}I in archived seawater samples, Deep. Res. Part I Oceanogr. Res. Pap., 45, 1111–1125, doi:10.1016/S0967-0637(98)00007-7, 1998.

Edmonds, H. N., Zhou, Z. Q., Raisbeck, G. M., Yiou, F., Kilius, L. and Edmond, J. M.: Distribution and behavior of anthropogenic ^{129}I in water masses ventilating the North Atlantic Ocean, J. Geophys. Res.,

106, 6881–6894, 2001.

Ellis, K. M. and Smith, J. N.: The flow of radionuclides through the Canadian Archipelago, Proc. IAEA Mainre Pollut. Symp. IAEA Tech. Doc., 1094, 462–464, Monaco, 1999.

Falina, A., Sarafanov, A., Mercier, H., Lherminier, P., Sokov, A. and Daniault, N.: On the cascading of dense shelf waters in the Irminger Sea, J. Phys. Oceanogr., 42, 2254–2267, 2012.

Fleischmann, U., Hildebrandt, H., Putzka, A. and Bayer, R.: Transport of newly ventilated deep water from the Iceland Basin to the West European Basin, Deep Sea Res., 48B, 1793–1819, 2001.

Fogelqvist, E. J., Blindheim, J., Tanhua, T. T., Osterhus, S., Buch, E. and Rey, F.: Greenland-Scotland overflow studied by hydro-chemical multivariate analysis, Deep Sea Res., Part I, 50, 73–102, 2003.

García-Ibáñez, M.-I., Pérez, F. F., Lherminier, P., Zunino, P. and Tréguer, P.: Water mass distributions and transports for the 2014 GEOVIDE curise in the North Atlantic, Biogeosciences, 15, 2075-2090, 2018.

Gascard, J. C., Raisbeck, G., Sequeira, S., Yiou, F. and Mork, K. A.: The Norwegian Atlantic Current in the Lofoten Basin inferred from hydrological and tracer data (^{129}I) and its interaction with the Norwegian Coastal Current, Geophys. Res. Lett., 31, L01308, 2004.

Gascard, J., Watson, A. J., Messias, M.-J., Olsson, K. A., Johannessen, T. and Simonsen, K.: Long-lived vortices as a mode of deep ventilation in the Greenland Sea, Nature, 416(April), 525–527, 2002.

Gómez-guzmán, J. M., Villa, M., Le Moigne, F., López-gutiérrez, J. M. and García-león, M.: AMS measurements of ^{129}I in seawater around Iceland and the Irminger Sea, Nucl. Inst. Methods Phys. Res. B, 294, 547–551, doi:10.1016/j.nimb.2012.07.045, 2013.

Hansen, B. and Osterhus, S.: North Atlantic - Nordic Sea exchanges, Prog. Oceanogr., 45, 109–208, 2000.

Harden, B. E., Pickart, R. S. and Benfrew, I. A.: Offshore Transport of Dense Water from the East Greenland Shelf, J. Phys. Oceanogr., 229–245, doi:10.1175/JPO-D-12-0218.1, 2014.

He, P., Aldahan, a., Possnert, G. and Hou, X. L.: A summary of global ^{129}I in marine waters, Nucl. Instruments Methods Phys. Res. Sect. B Beam Interact. with Mater. Atoms, 294, 537–541, doi:10.1016/j.nimb.2012.08.036, 2013a.

He, P., Hou, X., Aldahan, A., Possnert, G. and Yi, P.: Iodine isotopes species fingerprinting

environmental conditions in surface water along the northeastern Atlantic Ocean., Sci. Rep., 3, 2685, doi:10.1038/srep02685, 2013b.

Holm, E., Persson, B. R. R., Hallstadius, L., Aarkrog, A. and Dahlgaard, H.: Radio-cesium and transuranium elements in the Greenland and Barents Seas, Oceanol. Acta, 6, 457–462, 1983.

Hou, X.: Application of ^{129}I as an Environmental Tracer., 262, 67–75, 2004.

Jong, M. F. and Steur, L.: Strong winter cooling over the Irminger Sea in winter 2014–2015, exceptional deep convection, and the emergence of anomalously low SST, Geophy. Res. Lett., 43, 7106–7113, doi:10.1002/2016GL069596.Received, 2016.

Karcher, M., Smith, J. N., Kauker, F., Gerdes, R. and Smethie, W. M.: Recent changes in Arctic Ocean circulation revealed by iodine-129 observations and modeling, J. Geophys. Res. Ocean., 117, 1–17, doi:10.1029/2011JC007513, 2012.

Kershaw, P. and Baxter, A.: The transfer of reprocessing wastes from north-west Europe to the Arctic, Deep Sea Res., Part II, 42(6), 1413–1448, 1995.

Koszalka, I. M. and Haine, T. W. N.: Fates and Travel Times of Denmark Strait Overflow Water in the Irminger Basin, J. Phys. Oceanogr., December, 2611–2628, doi:10.1175/JPO-D-13-023.1, 2013.

Lambelet, M., van de Flierdt, T., Crocket, K., Rehkämper, M., Kreissig, K., Coles, B., Rijkenberg, M. J. a., Gerringa, L. J. a., de Baar, H. J. W. and Steinfeldt, R.: Neodymium isotopic composition and concentration in the western North Atlantic Ocean: results from the GEOTRACES GA02 section, Geochim. Cosmochim. Acta, 177, 1–29, doi:10.1016/j.gca.2015.12.019, 2016.

LeBel, D. A., Jr., Smethie, W. M., Rhein, M., Kieke, D., Fine, R. A., Bullister, J. L., D., M., Roether, W., Weiss, R. F., Andrié, C., Smythe-Wright, D. and E, J. P.: The formation rate of North Atlantic Deep Water and eighteen Degree water calculated from CFC-11 inventories observed during WOCE, Deep Sea Res. Part I Oceanogr. Res. Pap., 55(8), 891–910, 2008.

Lherminier, P., Mercier, H., Huck, T., Gourcuff, C., Perez, F. F., Morin, P., Sarafanov, A. and Falina, A.: The Atlantic Meridional Overturning Circulation and the subpolar gyre observed at the A25-OVIDE section in June 2002 and 2004, Deep Sea Res. Part I Oceanogr. Res. Pap., 57(11), 1374–1391, doi:10.1016/j.dsr.2010.07.009, 2010.

McCartney, M. and Talley, L. D.: The Subpolar Mode Water of the North Atlantic Ocean, J. Phys.

Oceanogr., 12, 1169–1188, 1982.

Mercier, H., Lherminier, P., Sarafanov, A., Gaillard, F., Daniault, N., Desbruyères, D., Falina, A., Ferron, B., Gourcuff, C., Huck, T. and Thierry, V.: Variability of the meridional overturning circulation at the Greenland–Portugal OVIDE section from 1993 to 2010, Prog. Oceanogr., doi:10.1016/j.pocean.2013.11.001, 2013.

Michel, R., Daraoui, a., Gorny, M., Jakob, D., Sachse, R., Tosch, L., Nies, H., Goroncy, I., Herrmann, J., Synal, H. a., Stocker, M. and Alfimov, V.: Iodine-129 and iodine-127 in European seawaters and in precipitation from Northern Germany, Sci. Total Environ., 419, 151–169, doi:10.1016/j.scitotenv.2012.01.009, 2012.

Orre, S., Smith, J. N., Alfimov, V. and Bentsen, M.: Simulating transport of ^{129}I and idealized tracers in the northern North Atlantic Ocean, Environ. Fluid Mech., 10, 213–233, 2010.

Pérez, F. F., Mercier, H., Vázquez-rodríguez, M., Lherminier, P., Velo, A., Pardo, P. C., Rosón, G. and Ríos, A. F.: Atlantic Ocean CO_2 uptake reduced by weakening of the meridional overturning circulation, Nat. Geosci., 6 (February), doi:10.1038/ngeo1680, 2013.

Pickart, R. S., Torres, D. J. and Fratantoni, P. S.: The East Greenland Spill Jet, J. Phys. Oceanogr., 58 (Dietrich 1964), 1037–1053, 2005.

Raisbeck, G. M. and Yiou, F.: Use of ^{129}I as an oceanographic tracer in the Nordic Seas, Pap. Present. 5th Int. Conf. Environ. Radioact. Arct. Antarct. St. Petersburg, Russ., 127–130, 2002.

Raisbeck, G. M., Yiou, F., Zhou, Z. Q. and Kilius, L. R.: ^{129}I from nuclear fuel reprocessing facilities at Sellafield (U.K.) and La Hague (France); potential as an oceanographie tracer, J. Mar. Syst., 6(5–6), 561–570, doi:10.1016/0924-7963(95)00024-J, 1995.

Raisbeck, G.M., and Yiou, F.: ^{129}I in the oceans: origins and applications. Sci. Total Environ. 237–238, 31–41, 1999.

Read, J. F.: CONVEX-91: water masses and circulation of the Northeast Atlantic subpolar gyre, Prog. Oceanogr., 48, 461–510, https://doi.org/10.1016/S0079-6611(01)00011-8, 2000.

Ríos, A. F., Pérez, F. F. and Fraga, F.: Water masses in the upper and middle North Atlantic Ocean east of the Azores, Deep Sea Res., 39 (3/4), 645–658, 1992.

Rudels, B.: Arctic Ocean circulation, processes and water masses: A description of observations and

Microsoft Office User 24/8/2018 10:34
Con formato: Control de líneas viudas y huérfanas, Adjust space between Latin and Asian text, Adjust space between Asian text and numbers

Microsoft Office User 7/8/2018 14:53
Eliminado:

Microsoft Office User 24/8/2018 10:34
Con formato: Izquierda, Control de líneas viudas y huérfanas

ideas with focus on the period prior to the International Polar Year 2007 – 2009, Prog. Oceanogr., 132, 22–67, doi:10.1016/j.pocean.2013.11.006, 2015.

Rudels, B., Eriksson, P., Gronvall, H., Hietala, R. and Launiainen, J.: Hydrographic Observations in Denmark Strait in Fall 1997, and their Implications for the Entrainment into the Overflow Plume, Geophys. Res. Lett., 26(9), 1325–1328, 1999a.

Rudels, B., Friedrich, H. J. and Quadfasel, D.: The Arctic Circumpolar Boundary Current, Deep Sea Res., Part II, 46, 1999b.

Sakaguchi, A., Kawai, K., Steier, P., Quinto, F., Mino, K., Tomita, J., Hoshi, M.,Whitehead, N., and Yamamoto, M.: First results on ^{236}U levels in global fallout. Sci. Total Environ., 407, 4238–4242, 2009.

Sakaguchi, A., Kadokura, A., Steier, P., Takahashi, Y., Shizuma, K., Hoshi, M., Nakakuki, T., and Yamamoto, M.: Uranium-236 as a new oceanic tracer: a first depth profile in the Japan Sea and comparison with caesium-137. Earth Planet. Sci. Lett. ,333–334, 165–170, 2012.

Schlitzer, R.: Ocean Data View, http://odv.awi.de, 2017.

Smith, J. N., Ellis, K. M. and Kilius, L. R.: ^{129}I and ^{137}Cs tracer measurements in the Arctic Ocean, Deep. Res. Part I Oceanogr. Res. Pap., 45, 959–984, doi:10.1016/S0967-0637(97)00107-6, 1998.

Smith, J. N., Jones, E. P., Moran, S. B., Jr, W. M. S. and Kieser, W. E.: Iodine-129/CFC-11 transit times for Denmark Strait Overflow Water in the Labrador and Irminger Seas, J. Geophys. Res., 110, 1–16, doi:10.1029/2004JC002516, 2005.

Smith, J. N., Mclaughlin, F. A., Smethie Jr, W. M., Moran, S. B. and Lepore, K.: Iodine-129, ^{137}Cs, and CFC-11 tracer transit time distributions in the Arctic Ocean, J. Geophys. Res., 116, 1–19, doi:10.1029/2010JC006471, 2011.

Smith, J. N., Smethie Jr, W. M., Yashayev, I., Curry, R. and Aztsu-Scott, K.: Time series measurements of transient tracers and tracer-derived transport in the Deep Western Boundary Current between the Labrador Sea and the subtropical Atlantic Ocean at line W, J. Geophys. Res. Ocean., 121, 1–24, doi:10.1002/2016JC011759.Received, 2016.

Snyder, G., Aldahan, A. and Possnert, G.: Global distribution and long-term fate of anthropogenic I-129 in marine and surface water reservoirs, Geochemistry Geophys. Geosystems, 11, doi:10.1029/2009GC002910, 2010.

Microsoft Office User 24/8/2018 10:34
Con formato: Izquierda, Control de líneas viudas y huérfanas

Steier, P., Bichler, M., Keith Fifield, L., Golser, R., Kutschera, W., Priller, A., Quinto, F., Richter, S., Srncik, M., Terrasi, P., Wacker, L., Wallner, A., Wallner, G., Wilcken, K. M. and Maria Wild, E.: Natural and anthropogenic ^{236}U in environmental samples, Nucl. Instruments Methods Phys. Res. Sect. B, 266(10), 2246–2250, doi:10.1016/j.nimb.2008.03.002, 2008.

Sy, A., Rhein, M., Lazier, J., Koltermann, K., Meincke, J., Putzka, A. and Bersch, M.: Surprisingly rapid spreading of newly formed intermediate waters across the North Atlantic Ocean, Nature, 386, 675–679, 1997.

Tanhua, T., Bulsiewicz, K. and Rhein, M.: Spreading of overflow water from the Greenland to the Labrador Sea, Geophys. Res. Lett., 32, L10605, 2005.

van Aken, H. M. and Becker, G.: Hydrography and through-flow in the northeastern North Atlantic Ocean: the NANSEN project, Prog. Oceanogr., 38(4), 297–346, 1996.

van Aken, H. M. and De Boer, C. J.: On the synoptic hydrography of intermediate and deep water masses in the Iceland Basin, Deep Sea Res., Part I, 42(2), 1995.

Villa, M., López-Gutiérrez, J. M., Suh, K.-S., Min, B.-I., Periañez, R.: The behaviour of ^{129}I released from nuclear fuel reprocessing factories in the North Atlantic Ocean and transport to the Arctic assessed from numerical modelling, Mar. Poll. Bul., 90, 15-24, http://dx.doi.org/10.1016/j.marpolbul.2014.11.039, 2015.

Vivo-Vilches, C., López-Gutiérrez, J. M., Periáñez, R., Marcinko, C., Le Moigne, F., Mcginnity, P., Peruchena, J. I. and Villa-Alfageme, M.: Recent evolution of ^{129}I levels in the Nordic Seas and the North Atlantic Ocean, Sci. Total Environ., 621, 376–386, doi:10.1016/j.scitotenv.2017.11.268, 2018.

Vockenhuber, C., Casacuberta, N., Christl, M. and Synal, H. A.: Accelerator Mass Spectrometry of ^{129}I towards its lower limits, Nucl. Instruments Methods Phys. Res. Sect. B, 361, 445–449, doi:10.1016/j.nimb.2015.01.061, 2015.

von Appen, W.-J., Koszalka, I. M., Pickart, R. S., Haine, T. W. N., Mastropole, D., Magaldi, M. G., Valdimarsson, H., Girton, J., Jochumsen, K. and Krahmann, G.: The East Greenland Spill Jet as an important component of the Atlantic Meridional Overturning Circulation, Deep Sea Res. Part I, 92, 75–84, 2014.

Wagner, M.J.M., Dittrich-Hannen, B., Synal, H.A., Suter, M., and Schotterer, U.: Increase of

^{129}I in the environment. Nucl. Instrum. Methods B, 113, 490–494, 1996.

Winkler, S. R., Steier, P. and Carilli, J.: Bomb fall-out ^{236}U as a global oceanic tracer using an annually resolved coral core., Earth Planet. Sci. Lett., 359–360(1), 124–130, doi:10.1016/j.epsl.2012.10.004, 2012.

Xu, X., Schmitz Jr, W. J., Hurlburt, H. E., Hogan, P. J. and Chassignet, E. P.: Transport of Nordic Seas overflow water into and within the Irminger Sea : An eddy - resolving simulation and observations, J. Geophys. Res., 115 (September), C12048, doi:10.1029/2010JC006351, 2010.

Xu, X., Bower A., Furey, H., and Chassignet, E. -P.: Variability of the Icelans-Scotland Overflow Water Transport through the Charlie-Gibbs Fracture Zone: results from an eddying simulation and observations, Jour. Geophys. Res. Oceans., 123, 2018.

Zou, S., Lozier, S., Zenk, W., Bower, A. and Johns, W.: Observed and modeled pathways of the Iceland Scotland Over flow Water in the eastern North Atlantic, Prog. Oceanogr., 159 (April), 211–222, doi:10.1016/j.pocean.2017.10.003, 2017.

Zunino, P., Lherminier, P., Mercier, H., Daniault, N., García-Ibáñez, M.-I. and Pérez, F. F.: The GEOVIDE cruise in May - June 2014 revealed an intense MOC over a cold and fresh subpolar North Atlantic, Biogeosciences, 14, 5323-5342, https://doi.org/10.5194/bg-14-5323-2017, 2017.

Microsoft Office User 24/8/2018 10:34
Con formato: Control de líneas viudas y huérfanas, Adjust space between Latin and Asian text, Adjust space between Asian text and numbers

Microsoft Office User 9/8/2018 10:03
Eliminado: Wefing, A.-M., Casacuberta, N., Vockenhuber, C., Christl, M. and Rutgers van der Loeff, M.: Distribution of I-129 and U-236 in the Fram Strait, in prep.,

Microsoft Office User 24/8/2018 10:34
Con formato: Interlineado: 1,5 líneas

Microsoft Office User 24/8/2018 10:33
Eliminado: 14, 5323-5342, 2017.

Microsoft Office User 24/8/2018 10:34
Con formato: Fuente: (Predeterminado) +Cuerpo de tema

Microsoft Office User 15/7/2018 12:27
Eliminado:

Microsoft Office User 15/7/2018 12:28
Eliminado:

Microsoft Office User 15/7/2018 12:28
Eliminado:

5

Microsoft Office User 15/7/2018 12:34
Eliminado:

Microsoft Office User 7/8/2018 10:22
Eliminado: ... [181]

Table 1. Acronyms used to define water masses, geographic locations and radionuclide sources.

Acronym	
AABW	Antarctic Bottom Water
AMOC	Atlantic Meridional Overturning Circulation
AMS	Accelerator Mass Spectrometry
AW	Atlantic Water
BSBW	Barents Sea Branch Water
DSOW	Denmark Strait Overflow Water
DWBC	Deep Western Boundary Current
EGC	East Greenland Current
ENACW	East North Atlantic Central Water
FSBW	Fram Strait Branch Water
GF	Global Fallout
ISOW	Iceland-Scotland Overflow Water
LB	Lithogenic Background
LC	Labrador Current
LH	La Hague
LSW	Labrador Sea Water
MW	Mediterranean Water
NAC	North Atlantic Current
NCC	Norwegian Coastal Current
$NEADW_L$	North East Atlantic Deep Water lower
NRP	Nuclear Reprocessing Plant
NwAC	Norwegian Atlantic Current
OMP	Optimum Multi-Parameter analysis
PAP	Porcupine Abyssal Plain
PIW	Polar Intermediate Water
RAW	Return Atlantic Water
SAF	Sub-Arctic Front
SAIW	Sub-Arctic Intermediate Water
SF	Sellafield
SPMW	Sub-Polar Mode Water
SPNA	Sub-Polar North Atlantic
WEB	West European Basin
WSC	West Spitsbergen Current

Microsoft Office User 8/8/2018 11:08
Tabla con formato

Microsoft Office User 21/8/2018 11:28
Eliminado:

Table 2. Concentrations of ^{129}I and ^{236}U, and atom ratios of $^{236}U/^{238}U$ and $^{129}I/^{236}U$ in seawater samples collected during the GEOVIDE cruise in spring 2014. Uncertainties of radionuclide concentrations and the $^{236}U/^{238}U$ ratio are given as one sigma deviations. The uncertainty of the $^{129}I/^{236}U$ ratio was propagated from the concentration uncertainty. *^{236}U data corrected for cross talk contamination.

Station and location	ETH Code	Depth m	Dominant water mass	Salinity	Pot. Temp. °C	Oxygen µmol kg^{-1}	^{129}I $\times 10^{7}$ at kg^{-1}			^{236}U $\times 10^{6}$ at kg^{-1}			$^{236}U/^{238}U$ $\times 10^{-12}$ at at^{-1}			$^{129}I/^{236}U$ at · at^{-1}		
Station 1	TU1141-H160122	5	ENACW	35.16	16.49	250	7.2	±	0.1	9.2	±	0.4	1130	±	60	7.9	±	0.4
40º 19.99' N	TU1151-H160120	25	ENACW	35.50	15.09	262	7.4	±	0.1	10.6	±	0.8	1330	±	100	7.0	±	0.5
10º 2.16' W	TU1152-H160119	50	ENACW	35.70	13.76	254	8.2	±	0.1	9.2	±	0.5	1110	±	60	8.9	±	0.5
Bottom depth: 3536 m	TU1153-H160118	100	ENACW	35.74	13.03	239	8.3	±	0.1	8.4	±	0.4	1100	±	50	9.9	±	0.5
	TU1154-H160110	200	ENACW	35.71	12.50	228	7.5	±	0.1	8.9	±	0.5	1050	±	60	8.5	±	0.5
	TU1147-H160103	400	ENACW	35.65	11.63	212	6.6	±	0.1	8.6	±	0.5	1030	±	70	7.7	±	0.5
	TU1134-H160080	1000	MW	36.15	11.13	177	3.4	±	0.1	8.3	±	0.4	1000	±	60	4.1	±	0.2
	TU1135-H160079	1200	MW	36.11	10.42	182	3.1	±	0.1	8.4	±	0.4	990	±	60	3.7	±	0.2
	TU1136-H160078	1600	MW/LSW	35.52	6.74	220	3.1	±	0.1	10.0	±	0.6	1010	±	60	3.1	±	0.2
	TU1123-H160077	2000	LSW	35.09	4.07	248	2.1	±	0.1	7.9	±	0.4	940	±	50	2.6	±	0.1
	TU1124-H160076	2500	$NEADW_L$	35.00	3.16	246	1.0	±	0.1	2.5	±	0.6	340	±	110	4.1	±	0.9
	TU1125-H160075	3000	$NEADW_L$	34.95	2.60	244	0.2	±	0.2	2.3	±	0.3	270	±	30	0.9	±	0.9
	TU1126-H160074	3506	$NEADW_L$	34.92	2.28	243	0.2	±	0.2	4.4	±	0.3	540	±	40	0.5	±	0.5
Surface 1	TU1148-H160123	5	ENACW				7.0	±	0.1	9.3	±	0.4	1160	±	50	7.5	±	0.4
40º 19.98' N																		
9º 27.57' W																		
Station 13	TU1155-H160211	10	ENACW	35.85	15.55	259	8.5	±	0.3	8.5	±	0.4	950	±	40	10.0	±	0.5
41º 2298' N	TU1156-H160085	30	ENACW	35.83	15.00	259	7.7	±	0.3	8.6	±	0.3	980	±	40	8.9	±	0.5
13º 53.26' W	TU1158-H160061	65	ENACW	35.76	13.16	251	7.9	±	0.3	8.8	±	0.4	1010	±	50	8.9	±	0.5
Bottom depth: 5347 m	TU1159-H160084	120	ENACW	35.74	12.84	247	7.6	±	0.3	8.8	±	0.3	1030	±	40	8.6	±	0.5
	TU1160-H160083	250	ENACW	35.69	12.39	245	8.0	±	0.3	8.8	±	0.3	1030	±	40	9.1	±	0.5
	TU1149-H160082	800	IcSPMW	35.72	10.51	182	4.9	±	0.3	8.3	±	0.3	980	±	40	5.9	±	0.4
	TU1137-H160081	1150	IcSPMW	35.86	9.45	188	3.9	±	0.2	8.7	±	0.3	970	±	40	4.4	±	0.3
	TU1127-H160073	2000	LSW	35.03	3.82	258	2.6	±	0.2	6.3	±	0.3	720	±	40	4.2	±	0.4
	TU1129-H160072	3000	$NEADW_L$	34.95	2.65	249	0.2	±	0.2	1.2	±	0.2	140	±	20	2	±	2
	TU1130-H160071	4000	$NEADW_L$	34.91	2.19	243	0.2	±	0.2	0.3	±	0.2	40	±	20	6	±	7
	TU1131-H160070	4885	$NEADW_L$	34.90	2.05	243	0.5	±	0.1									
	TU1132-H160069	5334	$NEADW_L$	34.90	2.04	244	1.6	±	0.1									
Surface 2	TU1161-H160215	5	ENACW				8.9	±	0.3	8.5	±	0.4	990	±	40	10.4	±	0.6
44º 43.46' N																		
18º 10.34' W																		
Station 21	TU1162-H160124	5	ENACW	35.69	14.45	277	8.7	±	0.2	8.6	±	0.5	990	±	60	10.2	±	0.6
46º 32.65' N	TU1163-H160214	12	ENACW	35.69	14.45	277	9.1	±	0.3	8.5	±	0.4	970	±	50	10.7	±	0.6
19º 40.32' W	TU1164-H160213	50	ENACW	35.62	12.72	266	9.9	±	0.3	8.5	±	0.4	980	±	50	11.6	±	0.6
Bottom depth: 4515 m	TU1165-H160121	100	ENACW	35.66	12.52	254	8.8	±	0.2	8.1	±	0.3	940	±	40	10.9	±	0.5
	TU1166-H160212	200	ENACW	35.64	12.03	248	9.8	±	0.3	8.4	±	0.4	960	±	40	11.7	±	0.6
	TU1170-H160104	450	ENACW	35.51	11.06	252	10.3	±	0.2	9.1	±	0.5	1060	±	60	11.2	±	0.6
	TU1167-H160105	800	IcSPMW	35.31	9.03	188	8.6	±	0.2	8.6	±	0.4	980	±	40	10.0	±	0.5
	TU1168-H160096	1500	LSW	35.00	4.40	259	8.4	±	0.2	7.9	±	0.5	970	±	60	10.6	±	0.6
	TU1138-H160068	2300	LSW	34.92	3.22	273	5.5	±	0.2	7.9	±	0.3	930	±	40	7.0	±	0.4
	TU1150-H160067	2750	ISOW	34.94	2.86	267	4.4	±	0.2	6.4	±	0.3	780	±	40	6.8	±	0.5
	TU1133-H160066	4000	$NEADW_L$	34.92	2.22	242	0.6	±	0.2	0.6	±	0.2	80	±	20	9	±	4
	TU1139-H160065	4474	$NEADW_L$	34.91	2.16	240	1.1	±	0.2	0.6	±	0.2	80	±	20	17	±	6
Surface 3	TU1171-H160219	5	ENACW				10.9	±	0.4	7.9	±	0.4	920	±	50	13.9	±	0.8
47º 17.39' N																		
20º 15.71' W																		
Station 26	TU1172-H160125	5	ENACW	35.31	11.52	282	13.3	±	0.2	8.8	±	0.4	1000	±	50	15.1	±	0.7
50º 16.67' N	TU1173-H160218	25	ENACW	35.31	11.52	282	12.9	±	0.3	8.2	±	0.5	950	±	60	16	±	1
22º 36.28' W	TU1174-H160217	50	ENACW	35.19	9.85	291	16.7	±	0.3	8.1	±	0.5	970	±	60	21	±	1
Bottom depth: 4130 m	TU1205-H160117	100	ENACW	35.17	9.45	284	19.2	±	0.3	8.1	±	0.3	940	±	40	23.7	±	0.9
	TU1206-H160216	250	SAIW	35.14	8.67	265	20.4	±	0.4	9.3	±	0.4	1060	±	40	21.9	±	0.9
	TU1188-H160111	500	IcSPMW	34.99	6.69	211	15.9	±	0.3	8.3	±	0.4	970	±	50	19	±	1
	TU1183-H160106	1000	LSW	34.96	4.40	263	13.4	±	0.2	8.2	±	0.4	1020	±	50	16.3	±	0.9
Surface 4	TU1184-H160222	5	SAIW				14.9	±	0.3	7.8	±	0.4	890	±	50	19	±	1
52º 7.99' N																		
24º 3.50' W																		
Station 32	TU0971-H160126	5	SAIW	35.07	10.16	292	19.9	±	0.3	7.4	±	0.6	870	±	80	27	±	2
55º 30.336' N	TU1200-H160221	30	SAIW	35.06	10.02	292	20.5	±	0.4	8.1	±	0.3	950	±	40	25	±	1
26º 42.62' W	TU1207-H160116	60	SAIW	35.14	8.85	288	18.9	±	0.3	9.2	±	0.3	1040	±	40	20.6	±	0.7
Bottom depth: 3235 m	TU1208-H160220	150	SAIW	35.11	8.11	274	20.1	±	0.4	8.3	±	0.3	980	±	40	24.1	±	0.9
	TU1175-H160097	380	SAIW	35.04	6.70	222	15.7	±	0.3	8.0	±	0.4	970	±	50	19.5	±	0.9

Microsoft Office User 21/8/2018 11:28
Eliminado: ... [182]

Microsoft Office User 21/8/2018 11:14
Eliminado: ·

Microsoft Office User 21/8/2018 11:14
Eliminado: 1

Microsoft Office User 21/8/2018 11:14
Eliminado: ·

Microsoft Office User 21/8/2018 11:14
Eliminado: -1

Microsoft Office User 21/8/2018 11:14
Eliminado: ·

Microsoft Office User 21/8/2018 11:14
Eliminado: -1

Microsoft Office User 21/8/2018 11:14
Eliminado: ·

Microsoft Office User 21/8/2018 11:15
Eliminado: -1

	TU1201-H160098	600	IcSPMW	34.96	5.02	246	17.8	±	0.3	9.0	±	0.2	1060	±	30	19.8	±	0.6
	TU1176-H160099	850	LSW	34.93	4.32	267	15.8	±	0.3	9.1	±	0.4	1097	±	50	17.3	±	0.8
	TU1202-H160112	1200	LSW	34.91	3.84	277	18.5	±	0.3	9.7	±	0.3	1130	±	40	19.1	±	0.6
	TU1177-H160113	1700	LSW	34.93	3.55	272	12.3	±	0.2	8.8	±	0.4	1030	±	50	14.1	±	0.7
	TU1178-H160064	2250	LSW	34.93	3.11	274	10.7	±	0.3	8.1	±	0.3	960	±	40	13.2	±	0.6
	TU1179-H160063	2650	ISOW	34.96	2.84	271	10.5	±	0.2	8.0	±	0.4	920	±	50	13.2	±	0.7
	TU1180-H160062	3220	ISOW	34.96	2.53	263	13.2	±	0.3	7.0	±	0.3	820	±	40	18.8	±	0.9
Station 38	TU1189-H160230	5	IcSPMW	35.06	9.24	296	16.7	±	0.3	8.7	±	0.4	1030	±	50	19	±	1
58º 50.56' N	TU1190-H160229	20	IcSPMW	35.06	9.23	296	16.7	±	0.3	9.8	±	0.3	1170	±	50	17.0	±	0.7
31º 15.97' W	TU1193-H160228	60	IcSPMW	35.08	7.95	291	17.4	±	0.3	8.8	±	0.3	1010	±	40	19.7	±	0.8
Bottom depth: 1345 m	TU1203-H160227	110	IcSPMW	35.10	7.45	273	18.7	±	0.4	8.7	±	0.3	1010	±	40	21.4	±	0.9
	TU1204-H160226	300	IcSPMW	35.11	7.19	273	19.1	±	0.4	9.0	±	0.2	1040	±	30	21.3	±	0.7
	TU1209-H160225	650	IcSPMW	35.06	5.94	234	15.5	±	0.3	9.3	±	0.3	1050	±	40	16.6	±	0.7
	TU1210-H160224	1000	LSW	34.99	4.33	262	18.3	±	0.4	9.6	±	0.2	1070	±	30	19.1	±	0.6
	TU1213-H160223	1336	ISOW	34.99	3.90	267	21.4	±	0.5	9.3	±	0.3	1100	±	40	23	±	1
Surface 5	TU1194-H160277	5	IrSPMW				16.8	±	0.3	8.9	±	0.4	1030	±	40	19.0	±	0.8
59º 16.77' N																		
35º 33.64' W																		
Station 44	TU1217-H160276	5	IrSPMW	34.85	6.86	318	19.4	±	0.3	9.4	±	0.3	1120	±	40	20.6	±	0.8
59º 37.36' N	TU1260-	5	IrSPMW	34.85	6.86	318				9	±	3	*1040	±	330			
38º 57.234' W	TU1195-H160275	20	IrSPMW	34.85	6.85	318	17.2	±	0.3	9.9	±	0.4	1170	±	50	17.4	±	0.8
Bottom depth: 2929 m	TU1218-H160274	40	IrSPMW	34.88	4.62	306	20.9	±	0.3	9.2	±	0.3	1090	±	40	22.8	±	0.9
	TU1219-H160273	80	IrSPMW	34.90	4.30	295	19.5	±	0.3	9.1	±	0.3	1070	±	40	21.5	±	0.7
	TU1196-H160272	150	IrSPMW	34.90	4.05	298	18.4	±	0.3	9.2	±	0.3	1090	±	40	20.0	±	0.8
	TU1220-H160271	300	LSW	34.90	3.94	298	22.5	±	0.4	9.9	±	0.3	1130	±	30	22.8	±	0.7
	TU1221-H160253	850	LSW	34.87	3.62	292	24.5	±	0.4	9.6	±	0.7	1160	±	80	25	±	2
	TU1185-H160254	1400	LSW	34.93	3.57	273	10.5	±	0.2	9.2	±	0.4	1070	±	50	11.4	±	0.5
	TU1186-H160255	1800	LSW	34.93	3.26	274	14.3	±	0.2	9.5	±	0.3	1070	±	40	15.1	±	0.5
	TU1191-H160256	2250	ISOW	34.93	2.86	276	15.5	±	0.3	8.6	±	0.3	1000	±	40	18.0	±	0.7
	TU1248-H160308	2600	ISOW	34.92	2.44	282	38.7	±	0.6	10	±	1	*1180	±	130	40	±	4
	TU1261-H160307	2875	DSOW	34.88	1.17	308	98	±	2	9	±	4	*1090	±	420	110	±	40
	TU1262-H160306	2909	DSOW	34.89	1.06	309	99	±	2	11	±	3	*1280	±	310	90	±	20
Station 53	TU1265-H160285	5	PIW	31.90	-0.68	423	256	±	4	16	±	2	*2050	±	310	160	±	20
59º 53.86' N	-H160284	25	PIW	32.10	-1.18	417	247	±	5									
43º 0.33' W	TU1267-H160283	50	PIW	32.95	-1.52	364	236	±	8	12	±	4	*1570	±	510	200	±	60
Bottom depth: 193 m																		
Station 60	TU1214-H160282	5	IrSPMW	34.83	6.94	325	19.0	±	0.3	8.9	±	0.2	1040	±	30	21.4	±	0.6
59º 47.96' N	TU1197-H160281	25	IrSPMW	34.98	6.56	314	17.0	±	0.3	8.6	±	0.3	1030	±	40	19.6	±	0.7
42º 00.78' W	TU1192-H160280	50	IrSPMW	35.01	6.27	303	16.6	±	0.3	8.3	±	0.5	1020	±	60	20	±	1
Bottom depth: 1719 m	TU1198-H160279	100	IrSPMW	35.02	5.97	291	17.1	±	0.3	8.9	±	0.3	1020	±	40	19.3	±	0.7
	TU1224-H160278	200	IrSPMW	34.96	5.20	287	18.4	±	0.3	8.9	±	0.4	1030	±	50	20.8	±	0.9
	TU1215-H160268	500	IrSPMW	34.94	4.45	280	22.8	±	0.5	9.5	±	0.4	1140	±	50	24	±	1
	TU1216-H160257	750	IrSPMW	34.90	3.85	286	21.3	±	0.4	9.3	±	0.3	1120	±	40	22.8	±	0.8
	TU1225-H160258	1000	LSW	34.92	3.77	278	23.1	±	0.5	13	±	2	*1600	±	210	18	±	2
	TU1229-H160259	1190	LSW/ISOW	34.93	3.61	277	25.6	±	0.4	9.5	±	0.9	*1210	±	120	27	±	3
	-H160260	1500	LSW/ISOW	34.92	3.16	281	30.3	±	0.5									
	TU1242-H160305	1672	LSW/ISOW	34.92	3.00	281	36.1	±	0.6	9	±	1	*1100	±	180	40	±	6
	TU1243-H160304	1712	LSW/ISOW	34.91	2.94	284	37.4	±	0.6	8.7	±	0.9	*1080	±	120	43	±	5
Station 61	TU1263-H160296	5	SAIW	32.40	0.07	412	219	±	4	15	±	3	1940	±	340	140	±	30
59º 45.21' N	H160290	25	SAIW	32.63	-0.41	402	244	±	4									
45º 6.74' W	TU1269-H160289	50	SAIW	32.81	-0.65	383	251	±	4									
Bottom depth: 144 m																		
Station 64	TU1236-H160288	5	IrSPMW	34.81	6.71	317	24.7	±	0.4	9	±	1	*1060	±	160	29	±	4
59º 4.30' N	TU1226-H160287	25	IrSPMW	34.81	6.68	317	21.5	±	0.4	12	±	1	*1370	±	140	19	±	2
46º 5.29' W	TU1227-H160286	50	IrSPMW	34.86	6.13	319	18.4	±	0.3	11	±	1	*1480	±	180	16	±	2
Bottom depth: 2473 m	TU1230-H160261	100	IrSPMW	34.95	5.37	294	22.2	±	0.4	11	±	1	*1390	±	140	20	±	2
	-H160262	200	IrSPMW	34.94	4.79	289	29.2	±	0.5									
	TU1231-H160267	450	LSW	34.92	4.22	288	26.8	±	0.5	9	±	1	*1080	±	140	30	±	4
	TU1232-H160100	900	LSW	34.87	3.60	295	24.7	±	0.4	7.9	±	0.8	*970	±	100	31	±	3
	H160088	1150	LSW	34.91	3.71	281	23.7	±	0.4									
	TU1222-H160089	1400	LSW	34.93	3.55	274	21.0	±	0.3	9.8	±	0.3	1130	±	40	21.3	±	0.7
	TU1238-H160090	1800	LSW	34.92	3.05	278	27.7	±	0.4	9	±	1	*1070	±	120	31	±	4
	TU1228-H160303	2150	ISOW	34.93	2.70	278	20.9	±	0.3	11	±	1	*1300	±	150	19	±	2
	TU1249-H160302	2462	DSOW	34.90	2.15	291	56.2	±	0.9	9.5	±	0.9	*1160	±	110	60	±	6
Surface 6	TU1239-H160231	5	LSW				30.9	±	0.5									
56º 44.79' N																		
47º 31.31' W																		
Station 69	H160232	5	LSW	34.62	6.24	326	48.8	±	0.8									
55º 50.50' N	TU1254-H160233	25	LSW	34.67	3.72	324	49.9	±	0.8	9	±	3	1060	±	350	60	±	20
48º 5.59' W	TU1264-H160234	50	LSW	34.79	3.78	297	41.8	±	0.7	5	±	3	*640	±	320	80	±	40
Bottom depth: 3678 m	-H160239	100	LSW	34.83	3.81	296	32.9	±	0.6									
	TU1240-H160	200	LSW	34.84	3.62	298	29.8	±	0.5	9	±	2	*1080	±	190	32	±	6
	TU1272101-H160	500	LSW	34.86	3.49	296	29.3	±	0.5	7	±	2	*820	±	290	40	±	20
	TU1273-H109160	1000	LSW	34.85	3.39	296	26.0	±	0.4									
	TU1274-H160092	1800	LSW	34.92	3.57	274	17.6	±	0.3	5	±	2	*620	±	300	30	±	20
	TU1275-H160241	2200	LSW	34.92	3.22	275	20.0	±	0.4	8	±	3	*940	±	330	26	±	9
	TU1233-H160093	2800	ISOW	34.92	2.70	279	24.5	±	0.4	8.9	±	0.9	*1070	±	110	28	±	3
	TU1251-H160301	3500	ISOW	34.91	1.75	294	72	±	1	15	±	2	*1770	±	270	49	±	8

Microsoft Office User 9/8/2018 12:50
Eliminado: TU1268

Microsoft Office User 9/8/2018 12:49
Eliminado: TU1244

Microsoft Office User 9/8/2018 12:50
Eliminado: TU1250

	TU1255-H160300	3659	DSOW	34.90	1.47	299	85	±	1	19	±	3	*2230	±	340	44	±	7
Surface 7 53º 40.18' N 49º 29.49' W	TU1277-H160269	5	LSW				31.6	±	0.5	10.2	±	0.5	1220	±	70	31	±	2
Surface 8 52º 46.17' N 51º 48.26' W	TU1278-H160270	5	SAIW/PIW				71	±	1	15.7	±	0.9	2090	±	140	45	±	3
Station 77 52º 59.98' N 51º 6.01' W Bottom depth: 2522 m	TU1245-H160242	5	LSW	34.47	7.28	324	37.9	±	0.6	9	±	1	*1040	±	170	45	±	7
	-H160243	25	LSW	34.63	5.30	334	32.2	±	0.6									
	TU1279-H160244	50	LSW	34.74	3.57	312	32.3	±	0.6	10.4	±	0.4	1230	±	50	31	±	1
	TU1246-H160245	100	LSW	34.79	3.42	304	32.4	±	0.6	9	±	1	*1040	±	170	38	±	6
	TU1280-H160246	200	LSW	34.83	3.46	299	30.9	±	0.5	10.4	±	0.4	1210	±	50	30	±	1
	TU1281-H160102	650	LSW	34.86	3.46	294	27.0	±	0.4	10.3	±	0.4	1190	±	50	26	±	1
	TU1284-H160247	950	LSW	34.87	3.41	294	24.1	±	0.4	10.6	±	0.3	1240	±	50	22.7	±	0.8
	TU1234-H160094	1250	LSW	34.91	3.54	279	22.8	±	0.4	9.5	±	0.9	*1130	±	100	24	±	2
	TU1282-H160299	1700	LSW	34.92	3.12	276	21.7	±	0.4	9.8	±	0.5	1140	±	70	22	±	1
	TU1285-H160095	2200	ISOW	34.92	2.60	280	35.5	±	0.6	10.6	±	0.3	1270	±	50	34	±	1
	TU1252-H160298	2477	ISOW	34.91	2.18	285	48.7	±	0.8	8	±	3	*1030	±	310	60	±	20
	TU1286-H160297	2500	ISOW	34.91	2.09	287	47.0	±	0.8	12.1	±	0.6	1400	±	70	39	±	2
Station 78 51º 59.33' N 53º 40.01' W Bottom depth: 377 m	TU1256-H160248	5	PIW	31.79	5.17	342	75	±	1	16	±	4	*2110	±	500	50	±	10
	TU1257-H160249	25	PIW	32.86	-0.57	452	77	±	1	19	±	3	*2350	±	370	41	±	6
	TU1270-H160250	50	PIW	33.06	-1.46	340	74	±	1	12	±	4				60	±	20
	TU1258-H160251	200	PIW	34.08	0.77	308	64	±	1	11	±	2	*1380	±	280	60	±	10
	TU1287-H160252	367	PIW	34.62	2.92	283	44.2	±	0.8	11.2	±	0.5	1350	±	70	40	±	2

Microsoft Office User 21/8/2018 11:28
Eliminado:

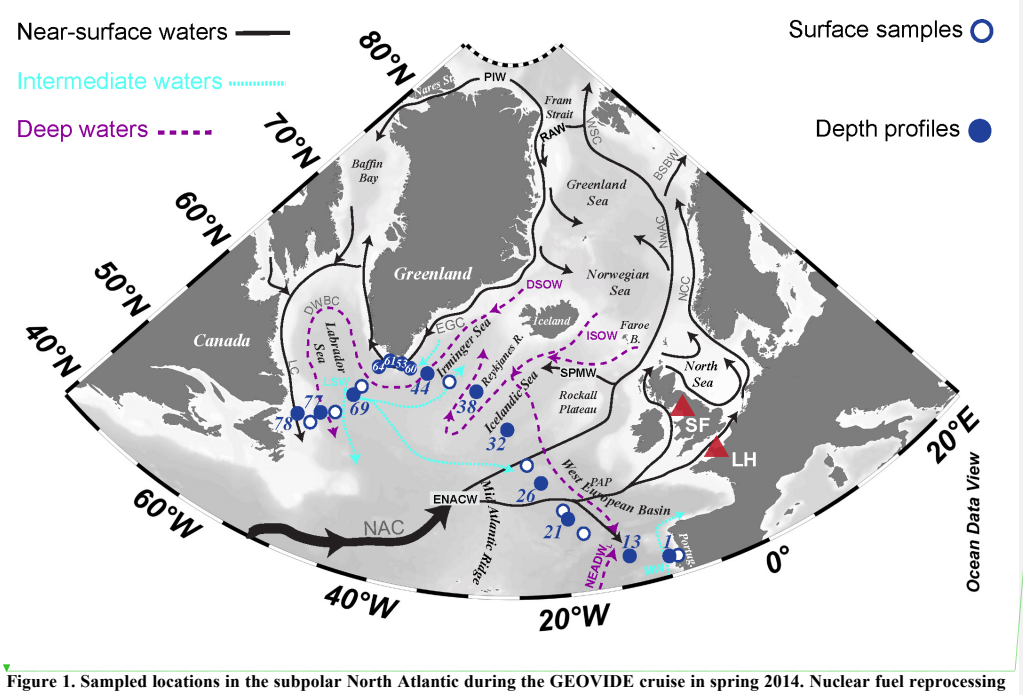

Figure 1. Sampled locations in the subpolar North Atlantic during the GEOVIDE cruise in spring 2014. Nuclear fuel reprocessing plants of La Hague (LH) and Sellafield (SF) are represented along with main water masses and their schematic spreading pathways adapted from Daniault et al., (2016) and Smith et al., (2005). Acronyms are defined in Table 1.

Microsoft Office User 21/8/2018 11:28
Eliminado: ... [183]

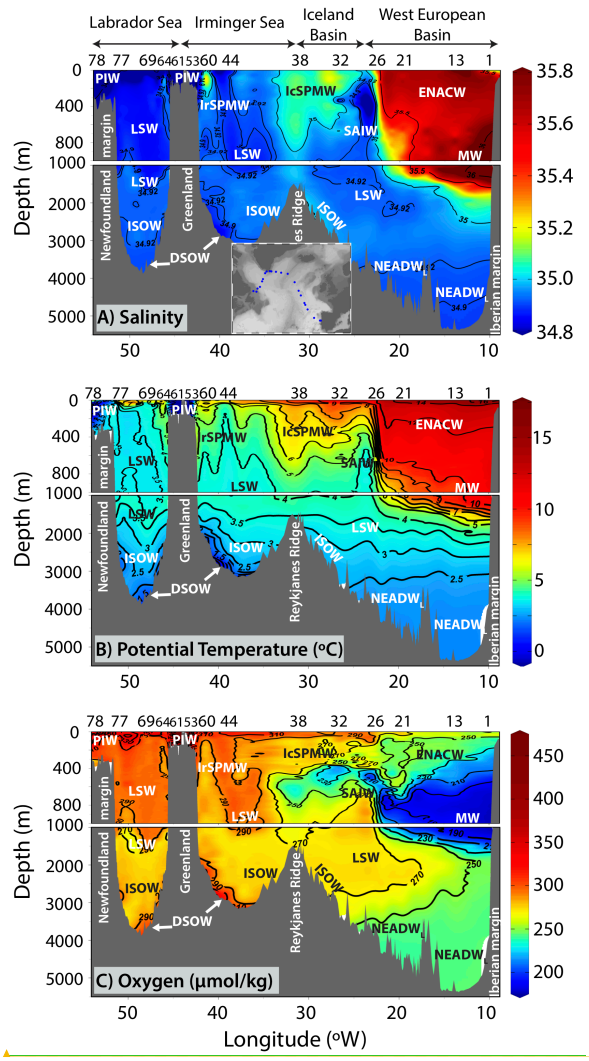

Figure 2. Vertical distribution of (A) salinity, (B) potential temperature and (C) dissolved oxygen along the GEOVIDE section in spring 2014. Water mass acronyms are defined in Table 1.

Unknown
Con formato: Fuente: 9 pt, Negrita

Microsoft Office User 8/8/2018 11:18
Con formato: Sin Resaltar

Microsoft Office User 8/8/2018 11:18
Con formato: Sin Resaltar

Microsoft Office User 8/8/2018 11:18
Con formato: Sin Resaltar

Microsoft Office User 8/8/2018 11:18
Con formato: Sin Resaltar

María Isabel García Ib..., 13/8/2018 19:38
Eliminado: A

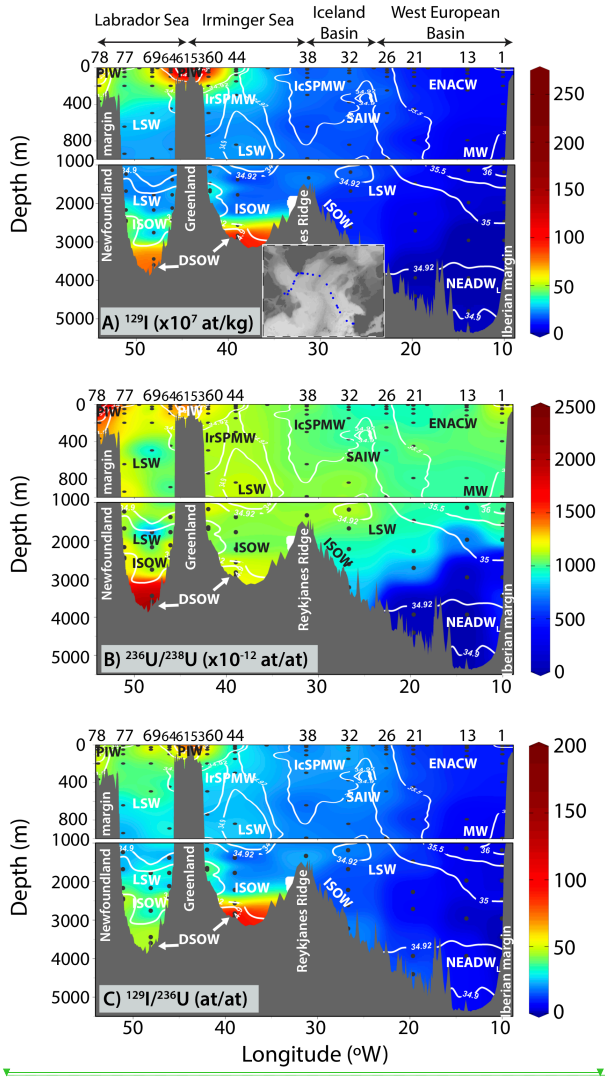

Figure 3. Vertical distribution of (A) ^{129}I concentrations, and atom ratios of (B) ^{236}U/^{238}U and (C) ^{129}I/^{236}U during the GEOVIDE cruise in spring 2014. Isohalines are overlaid to represent the water mass distribution. Acronyms are defined in Table 1.

Microsoft Office User 21/8/2018 11:28
Eliminado:

Microsoft Office User 7/8/2018 10:31

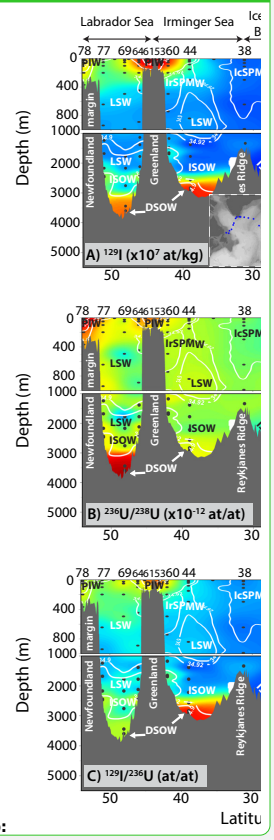

Eliminado:

Microsoft Office User 7/8/2018 10:16
Eliminado: 2

Microsoft Office User 7/8/2018 10:58
Eliminado: structure reported by García-Ibáñez et al., (2018).

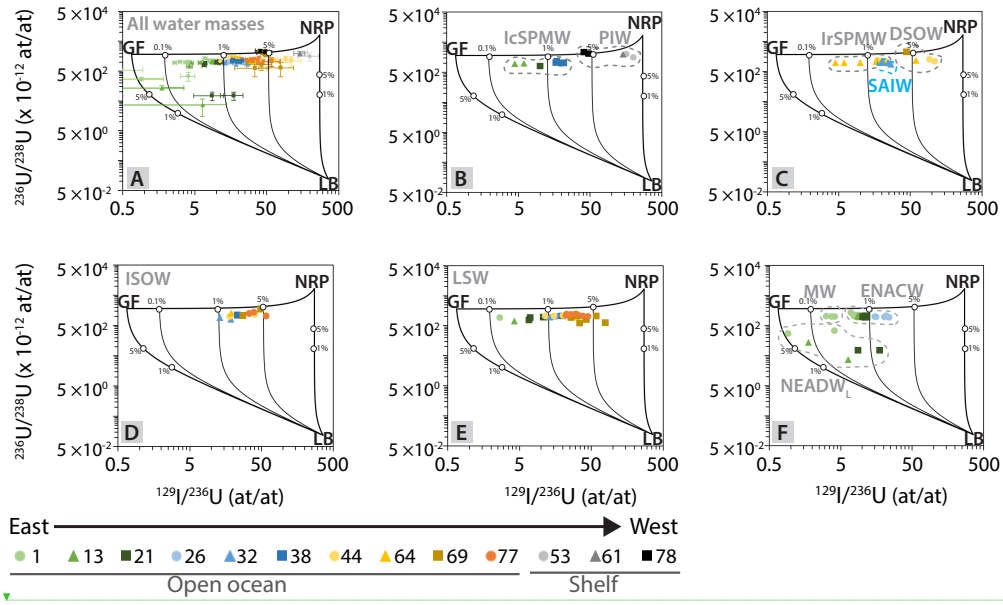

Figure 4. $^{129}I/^{236}U$ and $^{236}U/^{238}U$ atom ratios obtained during the GEOVIDE cruise in spring 2014 plotted on top of a binary mixing model (details in section 3.3) to estimate the contribution from the three sources to the subpolar North Atlantic (global fallout, GF; European nuclear fuel reprocessing plants, NRP; and the natural or lithogenic background, LB). Data are plotted for (A) each station, and (B to F) for the main water masses described in section 3.1. Diagram (A) also shows the data uncertainties. Explanation on how to interpret the results is provided in section 3.3. Further detail about the binary mixing model can be found in the original study (Casacuberta et al., 2016). Water mass acronyms are defined in Table 1.

Microsoft Office User 7/8/2018 10:31
Eliminado: ... [184]

Microsoft Office User 7/8/2018 11:01
Bajado [8]: Further description on the binary mixing model is provided elsewhere (Casacuberta et al., 2016; Christl et al., 2015b).

Microsoft Office User 7/8/2018 10:16
Eliminado: 3

Microsoft Office User 7/8/2018 11:01
Eliminado: Binary mixing lines between global fallout (GF), European nuclear fuels reprocessing plants (NRP) and the lithogenic background (LB) allow estimating the contribution from these three sources to the presence of ^{129}I and ^{236}U in the subpolar North Atlantic.

María Isabel García Ib..., 13/8/2018 19:39
Eliminado: The

María Isabel García Ib..., 13/8/2018 19:39
Eliminado: are

Microsoft Office User 8/8/2018 11:18
Eliminado: (B to F)

María Isabel García Ib..., 13/8/2018 19:39
Eliminado: '

María Isabel García Ib..., 13/8/2018 19:40
Eliminado: '

Microsoft Office User 7/8/2018 11:13
Eliminado: A

Microsoft Office User 7/8/2018 11:01
Movido (inserción) [8]

Microsoft Office User 8/8/2018 11:17
Eliminado: Further description on the binary mixing model is provided elsewhere (Casacuberta et al., 2016; Christl et al., 2015b).

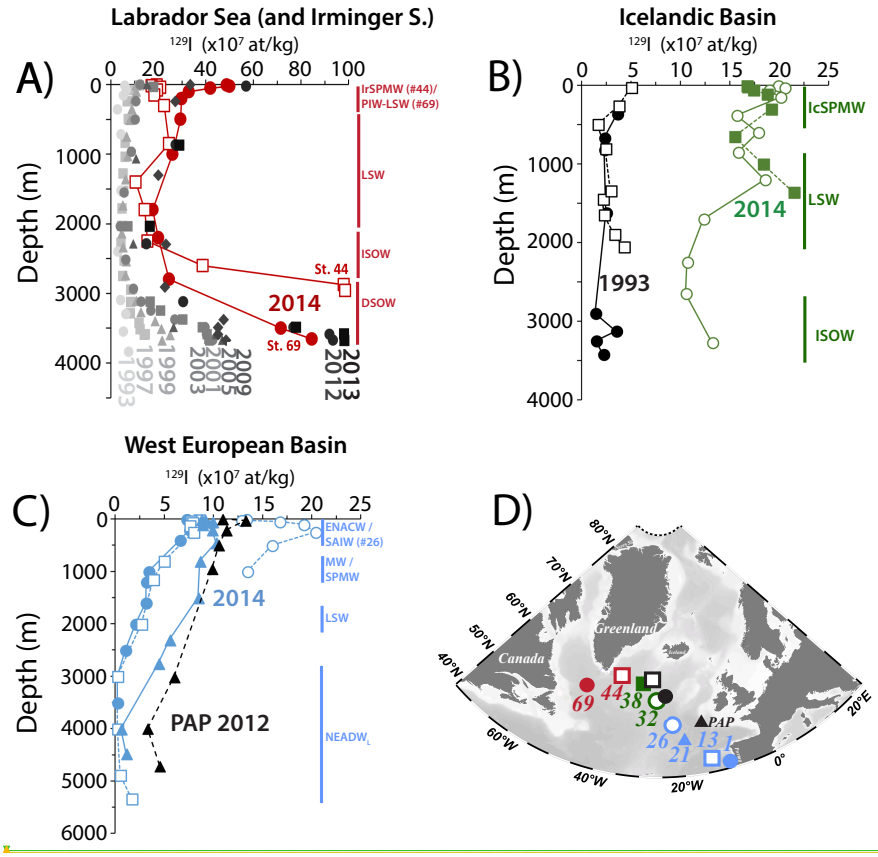

Figure 5. Vertical profiles of ^{129}I concentrations at locations shown in (D) of selected GEOVIDE stations and of those reported in nearby locations by earlier studies. (A) ^{129}I in the Labrador and Irminger Seas, red profiles represent data from this work (2014). Data from 1993 was reported southwest of GEOVIDE station 69 by Edmonds et al. (2001). Data from 1997 to 2013 were reported at Station 17 of the AR7W line: for 1997, 1999 and 2001 by Smith et al. (2005); for 2003, 2005 and 2009 by Orre et al. (2010); and for 2012 and 2013 by Smith et al. (2016). (B) In the Icelandic Basin, green profiles show data from GEOVIDE stations 32 and 38 in 2014, while black profiles represent data from 1993 reported by Edmonds et al. (2001). (C) In the West European Basin, blue profiles represent data from GEOVIDE stations 1 to 26, while data from 2012 in the Porcupine Abyssal Plain (PAP) was reported by Vivo-Vilches et al. (2018). Water masses found during GEOVIDE cruise have been summarized and represented in same colour as the ^{129}I concentration profiles. Acronyms are defined in Table 1.

Microsoft Office User 21/8/2018 11:29
Eliminado: ... [185]

Unknown
Con formato: Fuente: 9 pt, Negrita

Unknown
Con formato: Fuente: 9 pt, Negrita

Microsoft Office User 7/8/2018 10:16
Eliminado: 4

Microsoft Office User 8/8/2018 11:21
Eliminado: ^{129}I concentrations i

María Isabel García Ib..., 13/8/2018 19:40
Eliminado: ,

Microsoft Office User 8/8/2018 11:29
Eliminado: (this work (red) and Edmonds et al., 2001; Orre et al., 2010; Smith et al., 2005, 2016), (B) the

Microsoft Office User 8/8/2018 11:30
Eliminado: (this work (green) and

María Isabel García Ib..., 13/8/2018 19:41
Eliminado: ,

Microsoft Office User 8/8/2018 11:30
Eliminado: (black)

Microsoft Office User 8/8/2018 11:30
Eliminado: ,

Microsoft Office User 8/8/2018 11:31
Eliminado: (this work (blue) and

María Isabel García Ib..., 13/8/2018 19:41
Eliminado: ,

Microsoft Office User 8/8/2018 11:31
Eliminado: (black)

Microsoft Office User 8/8/2018 11:32
Eliminado: , and (D) map with locations for each station.

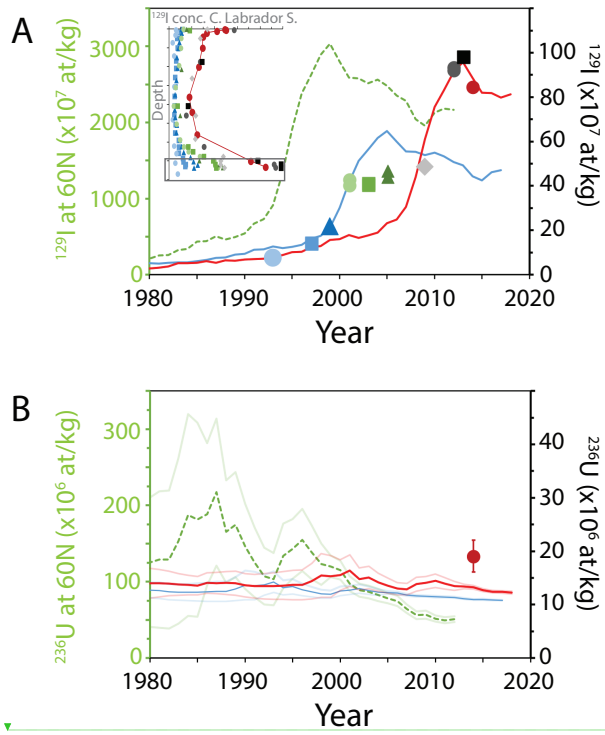

Figure 6. Comparison between measured (data points) and simulated (lines) radionuclide concentrations in bottom waters (DSOW) at the central Labrador Sea for (A) ^{129}I and (B) ^{236}U. The green y-axis on the left represents radionuclide concentrations over time (or the radionuclide input functions, also in green) at 60 ºN due to releases from the European Nuclear Reprocessing Plants and which were reported by Christl et al. (2015b). Note that for ^{236}U, the average input function is accompanied with a lower and upper bound estimate to acknowledge the current uncertainties on the ^{236}U releases from Sellafield and La Hague (Christl et al., 2015b). The black y-axis on the right represents radionuclide concentrations, measured or simulated, in bottom waters of the central Labrador Sea. Represented on these axes are the blue and red lines that represent two versions of the radionuclide input function at 60 ºN after dilution (DF=50 and 30 respectively) and application of a time delay (6 and 14 years respectively) that corresponds to the transport from 60 ºN to central Labrador Sea. The blue and red simulations include background concentrations for ^{129}I (2.5 × 10^7 at/kg; Edmonds et al., 2001) and ^{236}U (10 × 10^6 at/kg; e.g. Christl et al., 2012) due to the global fallout. In the black y-axis are also represented the radionuclide concentrations measured in 2014 that correspond to the bottom sample collected in GEOVIDE station 69. Earlier data on ^{129}I concentrations at similar locations were reported for 1993 by

Microsoft Office User 21/8/2018 10:37
Eliminado: ... [186]

Microsoft Office User 7/8/2018 10:16
Eliminado: 5

Microsoft Office User 8/8/2018 11:40
Eliminado: Concentrations of

Microsoft Office User 8/8/2018 11:43
Movido (inserción) [10]

María Isabel García Ib..., 13/8/2018 19:42
Eliminado: which

Microsoft Office User 21/8/2018 11:15
Con formato: Fuente: 9 pt, Negrita

Microsoft Office User 21/8/2018 11:15
Eliminado: -1

María Isabel García Ib..., 13/8/2018 19:42
Eliminado: ,

Microsoft Office User 21/8/2018 11:15
Con formato: Fuente: 9 pt, Negrita

Microsoft Office User 21/8/2018 11:16
Eliminado: -1

María Isabel García Ib..., 13/8/2018 19:42
Eliminado: ,

Microsoft Office User 21/8/2018 11:15
Con formato: Fuente: 9 pt, Negrita

Microsoft Office User 21/8/2018 11:16
Con formato: Fuente: 9 pt, Negrita

Edmonds et al. (2001); for 1997, 1999 and 2001 by Smith et al. (2005); for 2003, 2005 and 2009 by Orre et al. (2010); and for 2012 and 2013 by Smith et al. (2016).

María Isabel García Ib…, 13/8/2018 19:42
Eliminado: ,

Microsoft Office User 8/8/2018 11:40
Eliminado: in the bottom of the central Labrador Sea. Measurements are from this work (red dots, 2014); Edmonds et al. (2001) for 1993; Smith et al. (2005, 2016) for 1997, 1999, 2001, 2012 and 2013; and Orre et al. (2010) for 2003, 2005 and 2009. The ^{129}I input function from reprocessing plants was calculated for 60 ºN in Christl et al. (2015b). The blue and red lines correspond to the same input function that has been diluted and delayed in time to fit the measurements. B) Same as (A) but for ^{236}U. The uncertainties of the ^{236}U input functions are also shown with corresponding, more clear colours. The ^{236}U measurement is from this study.

Microsoft Office User 8/8/2018 11:43
Subido [10]: Christl et al. (2015b). The blue correspond to the same input function that has been diluted and delayed in time to fit the measurements. B) Same as (A) but for ^{236}U. The uncertainties of the ^{236}U input functions are also shown with corresponding, more clear colours. The ^{236}U measurement is from this study.